NUREG/CR-3874

Near-Ground Tornado Wind Fields

Prepared by J. R. McDonald

Texas Tech University

Prepared for
U.S. Nuclear Regulatory
Commission

GPO Printed copy price: $5.50

NUREG/CR-3874
RB

Near-Ground Tornado Wind Fields

Manuscript Completed: May 1984
Date Published: July 1984

Prepared by
J. R. McDonald

Institute for Disaster Research
Texas Tech University
Lubbock, TX 79409

Prepared for
Division of Radiation Programs and Earth Sciences
Office of Nuclear Regulatory Research
U.S. Nuclear Regulatory Commission
Washington, D.C. 20555
NRC FIN B8099
Under Contract No. NRC-04-82-002

FOREWORD

This final project report summarizes efforts and results that have been accomplished during the performance period of NRC Contract No. NRC 04-82-002, which began on September 27, 1982. Project Officer until his resignation from NRC on September 16, 1983 was Robert F. Abbey, Jr. He was replaced by Robert Kornasiewicz, Hydraulic Section Leader of the Earth Sciences Branch. The assistance of these two gentlemen in administering this contract is acknowledged and appreciated.

Principal Investigator for Texas Tech University is Dr. James R. McDonald. The research effort is coordinated through the Institute for Disaster Research at Texas Tech University. Dr. Joseph E. Minor is Director of the Institute.

Two papers, which represent the substantive work of this project, are referenced in this final report. Copies of the two papers are included in the Appendix for convenience.

TABLE OF CONTENTS

LIST OF ILLUSTRATIONS

LIST OF TABLES

I. INTRODUCTION

The major objective of this project is to systematically study damage caused by major tornado events that occurred during the performance period in an effort to estimate wind speed, to observe tornado missile behavior and to document the methodology for performing engineering oriented damage surveys. From information gained from the specific studies and other damage documentation experiences, appropriate concludions are drawn regarding the characteristics of near-ground tornado wind fields.

The criteria for making a decision to perform a damage documentation survey following a tornado event was an indication that the damage intensity was F4 or greater on the Fujita Scale (F-Scale). The Institute for Disaster Research (IDR) has an extensive network of colleagues who can provide information on extent of damage in almost any area of the country. Other factors considered are number of deaths and injuries, damage to engineered structures, and reports of tornado-generated missiles.

Other types of windstorm events such as hurricanes also were documented, when the opportunity presented itself. Although not directly related to near-ground tornado wind fields, the possibility of measuring wind speeds are greater in hurricanes than in tornadoes. Correlations of measured wind speed and appearance of damage from other types of storms are very useful in calibrating the wind speed ranges of F-Scale (Mehta, et al., 1981).

During the contract performance period the number of intense storms was minimal. For this reason several no-cost extensions to the contract were requested in order to obtain more time for damage investigation efforts. After one and one-half years there were opportunities to study only two significant events:

(1) Hurricane Alicia (1983)

(2) Tornado Outbreak in North and South Carolina (1984)

During the contract performance period, one or two tornadoes turned out to be rated F4, but the designation was not made until several weeks later. At the time the event took place the indications did not justify a damage investigation effort. One tornado in Oklahoma received a very questionable F4 rating after the fact.

Without any new data, it was necessary to rely upon the data collected previously for analysis of near-ground wind fields. In particular, the data collected from the Altus Oklahoma tornado of May 11, 1982 was used to develop a new approach to tornado wind speed estimates.

In the design of nuclear power plant structures and other critical facilities, information is needed on both the probability of a tornado occurrence and the characteristics of near-ground wind fields. The

Institute for Disaster Research, under a previous contract with NRC (Contract No. NRC-04-76-345) developed a methodology for regionalization of tornado hazard probability for the contiguous United States. The methodology has been published as a NUREG report (McDonald, 1983). A topical report on the regionalization of tornado hazard probability was submitted as part of the scope of the previous NRC contract.

This report is written as a general treatise on near-ground tornado wind fields. In Section II an engineering perspective on tornadoes is stated. Section III describes the data available for the study of near-ground tornado wind fields. Section IV discusses tornado wind speeds and briefly describes a new method for making more rational estimates of tornado wind speeds from damaged structures. Section V describes the damage indicators that are present in the wake of a tornado event and discusses other factors that affect the appearance of damage. A perspective on tornado-generated missiles is presented in Section VI. Conclusions and recommendations for further study are contained in the last section of the report.

II. ENGINEERING PERSPECTIVE ON TORNADOES

It is important to distinguish between the meteorologist's and engineer's perspective in the tornado, because this difference in perspective affects the manner in which each professional pursues evaluations of the phenomenon. The meteorologist's motivations for study emphasize scientific understanding of the tornado phenomenon and the need for being able to accurately forecast the conditions which spawn tornadoes. The engineer's needs are different; his needs emphasize understandings of tornadoes in designing new and evaluating existing structures to withstand the effects of tornado induced loads.

Engineering-oriented studies and evaluations of tornado induced damage to buildings and other structures are conducted for two principal reasons:

(1) To enhance understandings of structural response to wind-induced loads.

(2) To improve understandings of near-ground tornado wind fields.

This second objective is specifically a part of this study. It involves the calculation of near-ground wind speeds, the characterization of air flow near ground and the contributions of other pertinent facts observed during investigations.

III. AVAILABLE TORNADO DATA

The nuclear power industry recognized the need to design nuclear power plants to resist tornadoes approximately 15 years ago (1970). At that time very little was known about tornadoes, especially about their near-ground wind fields. In fact there were many misconceptions about tornado phenomena that had been perpetuated in the news media for years. It was in response to the need for design information that engineers rather than meteorologists became involved in studying tornado phenomena. Early pioneers included George Reynolds, Jack Cermak, Nathan Newmark and others. The Lubbock Tornado of 1970 presented an opportunity to study the effects of a devastating tornado on engineered structures (Mehta, et al., 1971).

A subcommittee of the American Nuclear Society ANS 2.3 began work on an industry standard for the siting of nuclear power plants in 1973. The subcommittee looked specifically at the problem of tornadoes and other extreme winds. This committee immediately recognized the lack of both knowledge and information on the subject of tornadoes and identified areas of needed research. The two main areas were in tornado climatology and near-ground tornado wind fields. The standard was published in 1983 (ANS, 1983).

A. Tornado Climatology

Tornado records have been maintained more or less systematically since 1916 by various agencies of the government. The collected information consisted primarily of date, location, deaths, injuries, and in some cases a brief description of the damage. Only the more intense tornadoes that produced visible damage were likely to get into the record books. The type of data needed for engineering applications were not available. The engineer needed information on tornado climatology, intensity, path length, path width and direction of travel. The Fujita-Scale (Fujita, 1971) was a significant development in establishing a means of describing tornado intensity. While the Fujita-Scale has been criticized for its somewhat arbitrary classifications, it has been accepted by both the meteorological and engineering communities as the standard for rating tornado intensity.

Two tornado data sets were compiled more or less independently from existing records by personnel at the National Severe Storms Forecast Center (NSSFC, 1979) and the University of Chicago (Tecson, et al., 1979). Word descriptions of tornadoes were used to systematically assign Fujita-Scale intensity ratings to the tornadoes in the records. In addition, NSSFC personnel used accounts of tornado damage in newspapers and other publications to rate the intensity of tornadoes. These two efforts resulted in improvement of the tornado record quality, but later studies (McDonald and Abbey, 1979) showed that there were many inconsistencies in the two data sets. A further concern about the tornado records in some people's mind is the use of the Fujita-Scale to classify tornado intensity.

The Fujita-Scale essentially defines six categories of tornado intensity as shown in Table 1. Associated with each intensity category is a wind speed range and word descriptions of damage produced by wind speeds in the range. A tornado incident then is classified by looking at the most intense damage and comparing it with the damage descriptions of each category. The Fujita-Scale classification then is assigned on the basis of appearance of damage.

There are several drawbacks to the system. In the first place a tornado must affect one of several damage indicators, such as buildings, trees or crops or must produce windborne missiles. If a tornado occurs over open country, it is difficult to make an accurate assessment of its intensity using the Fujita-Scale. The scheme does not take into account to any extent the relative strength of construction. If applied according to fundamental concept, a house blown off its foundation is rated F4, regardless of the age, state of repair or type of construction. A third difficulty with the F-Scale is the wind speed ranges associated with each F-Scale classification. In developing the classification Dr. Fujita used his best judgment in selecting word descriptions and photographs of typical damage for each wind speed range. However, there has never been a systematic study of the correlation of appearance of damage to wind speed. Thus, the study of near-ground tornado wind fields should include correlations between appearance of damage and wind speeds in tornadoes. Because actual measurements of wind speed in tornadoes are virtually impossible, indirect methods must be utilized. A new approach to an indirect method of wind speed estimation is subsequently described in this report.

B. Tornado Damage Documentation

Since 1970, personnel at Texas Tech University, through the Institute for Disaster Research, has documented damage in more than 56 separate windstorms, including tornadoes, hurricanes and other extreme winds. Figure 1 shows the locations of the damage documentation efforts on a U.S. map.

Data on windstorm damage is archived in the documentation files that are maintained by IDR. Photographs, photo logs, tape recorded word descriptions, maps, drawings, and newspaper accounts of the windstorm event are kept on file. Individual reports are published on the more significant events.

C. Tornado Event Survey

In order to provide a systematic way for tornado researchers to locate documented tornado events, a data retrieval system was developed at Texas Tech University called TORNADO EVENT SURVEY (TES) (Peterson, et al., 1980). A file of information and data on specific tornado events for which credible scientific documentations are available has been compiled. The file was developed to support a program of research into the character of near-ground tornado windfields. To facilitate the location and extraction of data and information from this file, a computer-based information retrieval system was developed.

TABLE 1

F-SCALE CLASSIFICATION OF TORNADOES BASED ON APPEARANCE OF DAMAGE (Fujita, 1971)

(F0) LIGHT DAMAGE 40 - 72 mph

This speed range corresponds to Beaufort 9 through 11. Some damage to chimneys or TV antennae; breaks branches off trees; pushes over shallow-rooted trees; old trees with hollow insides break or fall; sign boards damaged.

(F1) MODERATE DAMAGE 73 - 112 mph

73 mph is the beginning of hurricane wind speed or Beaufort 12. Peels surfaces off roofs, windows break; trailer houses pushed or overturned; trees on soft ground uprooted; some trees snapped; moving autos pushed off the road.

(F2) CONSIDERABLE DAMAGE 113 - 157 mph

Roof torn off frames houses leaving strong upright walls standing; weak structures or outbuildings demolished; trailer houses demolished; railroad boxcars pushed over; large trees snapped or uprooted; light-object missiles generated; cars blown off highway; block structures and walls badly damaged.

(F3) SEVERE DAMAGE 158 - 206 mph

Roofs and some walls torn off well-constructed frame houses; some rural buildings completely demolished or flattened; trains overturned; steel framed hangar-warehouse type structures torn; cars lifted off the ground and may roll some distance; most trees in a forest uprooted, snapped or leveled; block structures often leveled.

(F4) DEVASTATING DAMAGE 207 - 260 mph

Well-constructed frame houses leveled, leaving piles of debris; structures with weak foundations lifted, torn and blown off some distance; trees debarked by small flying debris; sandy soil eroded and gravel flown in high winds; cars thrown some distance or rolled considerable distance finally to disintegrate; large missiles generated.

(F5) INCREDIBLE DAMAGE 261 - 318 mph

Strong frame houses lifted clear off foundation and carried considerable distance to disintegrate; steel-reinforced concrete structures badly damaged; automobile-sized missiles fly distances of 100 yards or more; trees debarked completely; incredible phenomena can occur.

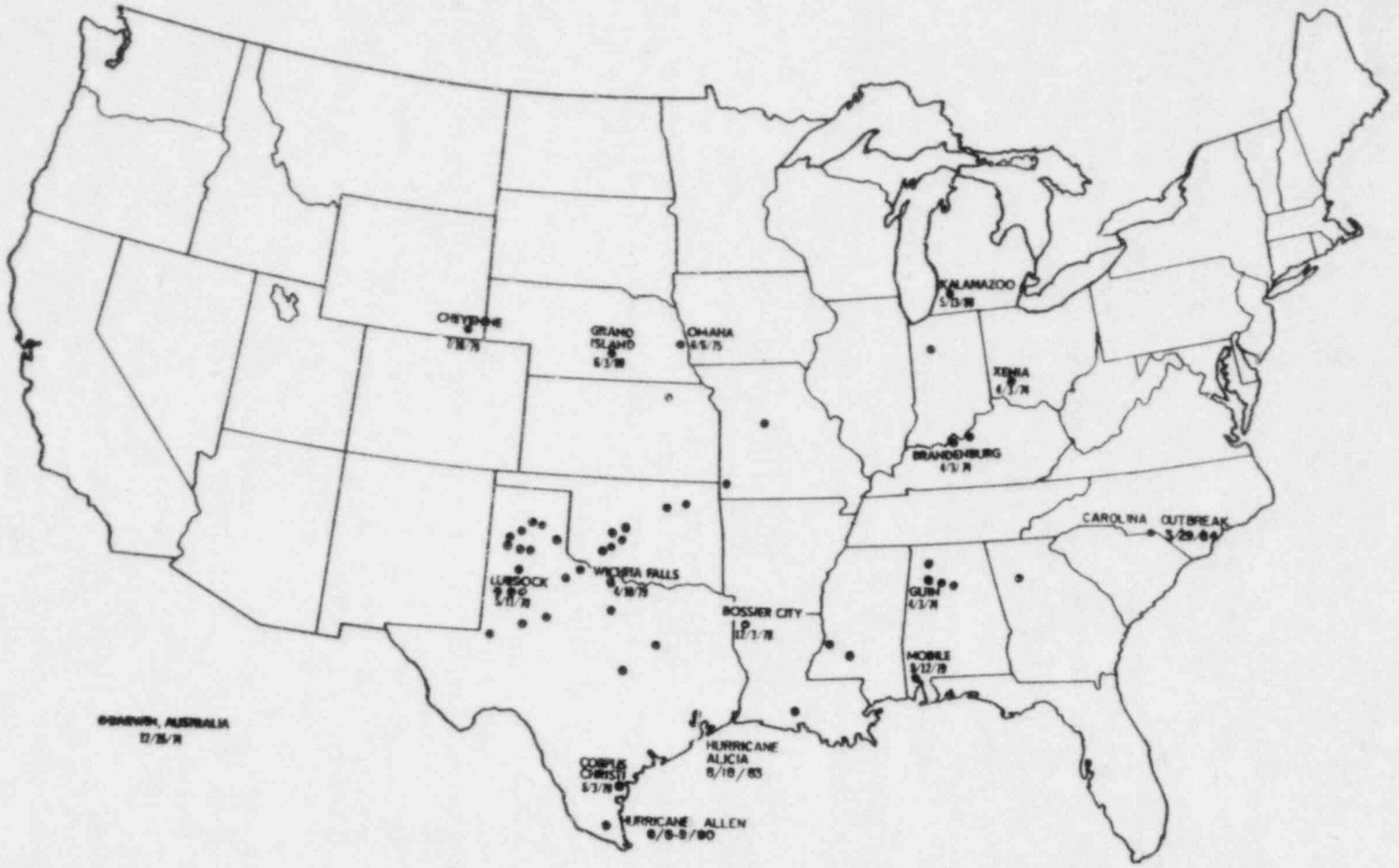

FIGURE 1. LOCATIONS OF WINDSTORM DAMAGE INVESTIGATIONS BY INSTITUTE FOR DISASTER RESEARCH, TEXAS TECH UNIVERSITY

The system consists of a Central File and an Information Retrieval System. The Central File was developed by systematically reviewing tornado event records in selected publications and subsequently, obtaining through library research copies of available scientific publications pertaining to the event. The basic criterion used to establish an event file is the availability of a journal quality article on the event.

Once an individual tornado event file has been established, a standard data sheet is compiled. This data sheet serves both as a work sheet for the event file and as an input form to facilitate keypunching of selected data for insertion into a computer data base. Thus, data available in each individual tornado event file is summarized for use in the information retrieval system. Data recorded on this form and inserted into computer storage are intended to facilitate information searches and to provide the researcher with pertinent information regarding the events, as well as regarding the contents of the file. When called from storage, these data are printed in readable rather than codified form. Currently the Central File has more than 200 tornado events listed for which there is published data on a particular event.

D. A Methodology for Tornado Damage Documentation

In the course of performing tornado damage documentation over a period of years, a methodology has evolved that assures accurate and complete collection of the data. This methodology is described in a separate document and will not be repeated here. An additional feature of the documentation methodology is that it provides guidelines for judging the quality of data gathered following a windstorm event. This feature is important when judging the quality of data collected by a group of inexperienced personnel.

Damage documentation must be done with great care. The experience of the personnel doing the documentation is critical to the quality of data collected. Rescue operations and cleanup following any storm quickly destroys evidence of near-ground wind field behavior. Clearing streets, moving pieces of debris for access, or toppling broken walls change the appearance of the damage and can give the study team a totally wrong impression. Members of the team must be able to recognize when the debris has been moved or modified.

The investigation must be meticulous, not unlike an autopsy. In the Omaha tornado of 1975, a Chevrolet van was reported to have been picked up by the wind and carried over a five story hospital building. The physical evidence was that the van was parked on one side of the hospital building before the tornado occurred and was found on the opposite side of the building afterward. The Texas Tech study team was skeptical of the report. After a couple of hours of searching, pieces of the van were found along a large diameter arc around the building. Ground marks along the path indicated that the van had rolled and tumbled the entire way and had not been airborne at all.

IV. TORNADO WIND SPEEDS

A. Maximum Wind Speeds

Prior to 1970 the literature contained many references to tornado wind speeds of 400-800 mph (e.g., Flora, 1954). By 1976 scientific and engineering studies had progressed to the point that at the Symposium on Tornadoes held at Texas Tech University the group of more than 150 tornado researchers from all parts of the U.S. agreed in principle that maximum tornado wind speeds fall in the range of 225-275 mph (Golden, 1976). The wind speed range of F5 tornadoes is 260-318 mph. Thus, only the very worst tornadoes ever observed or expected should fall into this category.

B. Wind Speed Estimates

Since direct measurements of tornadoes are virtually impossible, only indirect means can be utilized. The two most popular methods that have been used are:

(1) Photogrammetric analyses of tornado movies

(2) Engineering analyses of damaged structures

Photogrammetric analyses of movies have been attempted by several researchers (Golden, 1975; Forbes and Fujita, 1976; Zipser, 1976). One disadvantage of this method is that the films rarely show the lower 100 ft of the tornado funnel, which is of most interest as it affects ordinary structures. However, the method does give a good indication of the visible circulation that can be seen in the film. It does not give clues to the circulation inside the core that is hidden by dust or moisture condensation.

Wind speed estimates have been made from time to time by a number of researchers. Segner (1960) presented wind speed estimates from an engineering analysis of structures damaged by the Dallas tornado of 1957. More recently, wind speed estimates have been derived from engineering analyses of damage caused by the Lubbock tornado (Mehta, et al., 1971) and the Xenia, Ohio tornado (Mehta, et al., 1974). If analyses are based on a damaged structure, then the wind speed estimate is a lower bound. On the other hand, if a structure experienced tornado wind effects and was not damaged, then analyses give an upper bound on the wind speed. Not all structures are amenable to wind speed calculations. Mehta (1976) established a Credence Level which can be used to judge how reliable a wind speed estimate might be. The Credence Level is a qualitative evaluation.

As a part of this study Marshall, McDonald and Mehta (1983) applied the principles of load and resistance factor design (LRFD) to make wind speed estimates and to compute confidence limits on the estimates. In the three cases cited above, wind speeds were calculated based on average characteristics of the structure. Several different variables are involved in a wind speed analysis, including material strength

properties, construction practice, orientation of structure with respect to wind direction, and pressure coefficients used to convert wind speed to wind pressure. Each of these variables may contribute to deviations from the true value of wind speed to produce damage. These variables may lead to an overestimate or underestimate of the actual wind speed to cause damage. In order to quantify the degree of error in a wind speed estimate, statistical properties of the load and resistance behavior of the structure must be known. LRFD treats the load and resistance properties of structures in terms of continuous probability distributions (Ellingwood, et al., 1980). In contrast, nominal strengths or loads are treated as discrete values.

The LRFD method was applied to structures damaged by a tornado at Altus Air Force Base near Altus, Oklahoma on May 11, 1982 (McDonald and Marshall, 1983). Table 2 summarizes wind speed calculations for four damaged buildings. The failure wind speed along with 95 percent confidence limits are shown in the table. The parachute drying tower had the smallest confidence band. This structure, which is about 28.5 ft by 15.5 ft in plan and sixty-two feet high is the most amenable of the four buildings to wind speed calculations (See Figures 2 and 3). It is interesting to note that if Mehta's Credence Level criteria (Mehta, 1976) is applied to these wind speed calculations, a high degree of confidence in the wind speed values would be implied.

TABLE 2

SUMMARY OF WIND SPEED ESTIMATES IN THE
ALTUS, OKLAHOMA TORNADO OF MAY 11, 1982

Building	Failure Origin	Estimated Failure Wind Speed (mph)
Parachute Drying Tower	Tension in Anchor Bolts	116 ± 19
Dining Hall	Toenailed Roof Anchorage	121 ± 27
Recreation Building	Toenailed Roof Anchorage	120 ± 29
Communication Building	Twisted Wire Loops	108 ± 26

See Appendix for details.

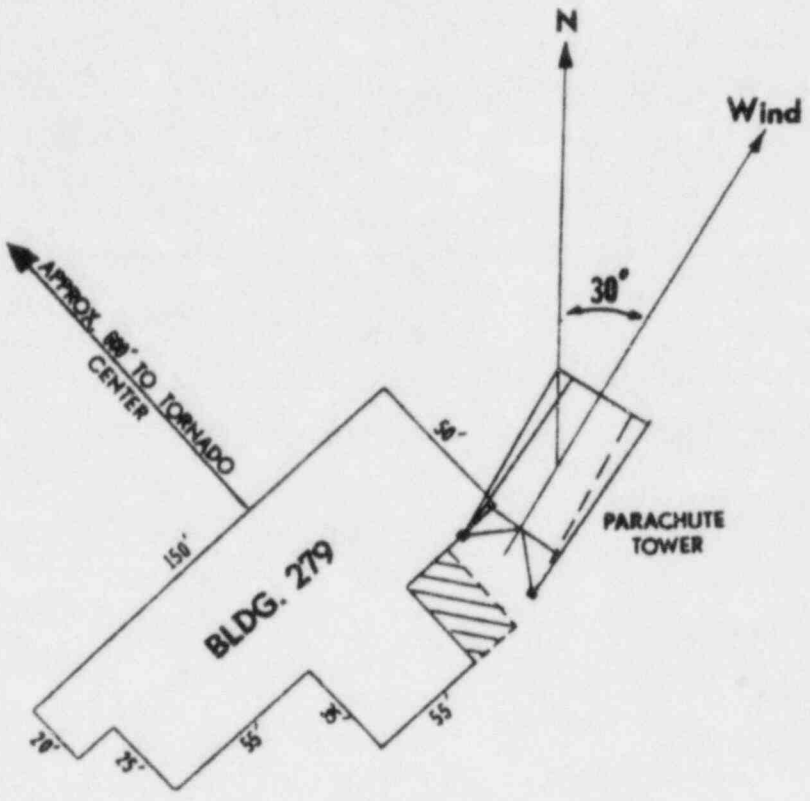

FIGURE 2. PLAN VIEW OF THE PARACHUTE TOWER AT BUILDING 279

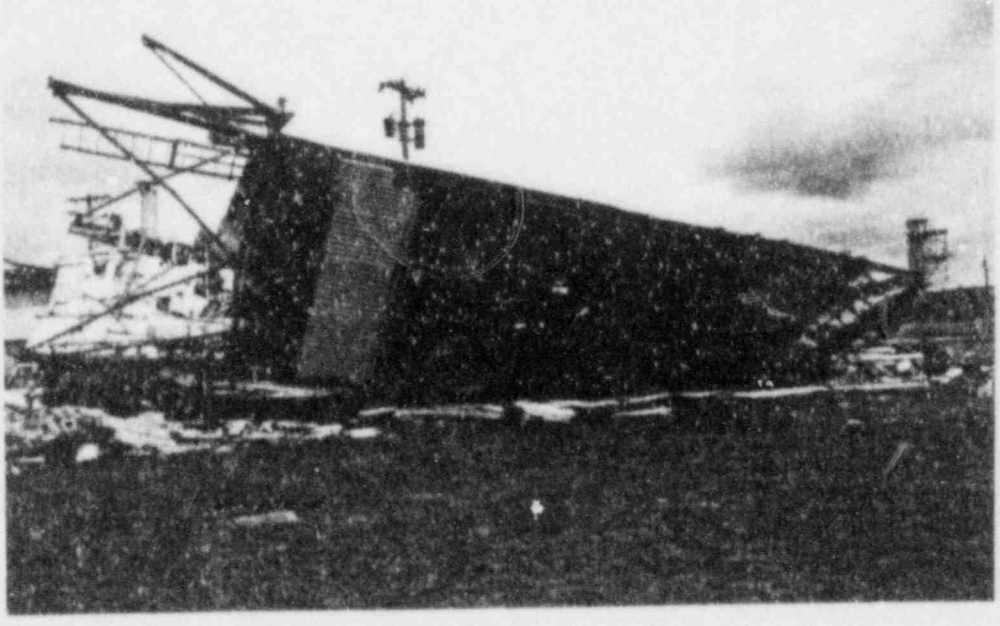

FIGURE 3. OVERTURNED PARACHUTE DRYING TOWER (failure initiated when anchor bolts in two of the corner columns failed in tension)

V. CHARACTERISTICS OF NEAR-GROUND WIND FIELDS

The damage and debris patterns left in the wake of a tornado event are the indicators of the nature of near-ground tornado wind fields. If the path of a tornado passes over open country, the indicators are not so obvious. However, if the path is studied, it may be possible to learn something of the nature of the tornado from marks on the ground or the disturbance of crops in the field. Forests which have a fairly uniform distribution of trees also gives a good indication of wind directions at the point in time when the tree was uprooted or broke. Damage in cities gives the most information about near ground wind fields. Wind speeds can be estimated from some structures. Debris patterns also give indications of directions of flow. Other factors that affect the type of damage and debris patterns left by a tornado include suction vortices, translational speed, wind direction, and path width of the tornado. Each of these factors is discussed separately below.

A. Ground Marks

The pioneering work on ground marks was done by Dr. T.T. Fujita at the University of Chicago (Fujita, et al., 1967; Fujita, 1975). He was the first to discover swirl marks in corn and potato fields that were associated with secondary vortices which he called suction vortices. These marks, as well as visual or photographic observations provide concrete evidence of the presence of suction vortices in the main tornado circulation under certain circumstances. Suction vortices are short lived and very unstable. They appear and disappear as they rotate around the parent tornado funnel. As many as five or six suction vortices have been seen rotating around a tornado core at one time.

The evidence of suction vortices in fields and relatively open country is indisputable. Questions asked by engineers who are concerned with design of structures to resist tornadoes are: What effectd do these suction vortices have on structures? Do the rotating winds of the suction vortex create additional forces that must be added vectorily to the wind forces produced by the parent tornado circulation? Is the suction vortex the primary damaging mechanism? These are very tough questions to answer. The evidence to back up the answers presented herein are somewhat circumstantial.

Tornado damage surveys on the ground have not found overwhelming evidence of damage produced by suction vortices in areas of relatively high terrain roughness as in a residential or suburban area. Virtually all evidence of the presence of suction vortices has been found in flat, open terrain such as grain fields or pastures.

The lack of suction vortex presence in rough terrain is explained by the fact that suction vortices are short lived and unstable. In rough terrain, mechanical turbulence and interference of flow by structures tends to break up and dispurse the suction vortices.

Aerial photographs of residential damage such as the one shown in Figure 4 show swaths of debris on the ground that proponents of the suction vortex damage theory would say suggest the presence of suction vortices. Two alternate explanations are offered for the presence of the swaths:

(1) The swaths of debris result from the interference of flow produced by another building or structure. As the air moves around the obstruction, some of the debris collects at the obstruction, while the rest of it flows in a swath around the building (see Figure 5).

(2) Debris falls out of the moving air stream when the velocity decreases. As long as the suction vortex is rotating, the debris should not fall out in a swath.

Thus, from what has been observed of ground marks in both smooth and rough terrain, the suction vortex does not appear to be a viable force-producing mechanism on structures, where the terrain surrounding the structure is relatively rough and is producing mechanical turbulence.

B. Damage to Forests

Tree damage in uniformly distributed forests gives good indication of tornado wind field circulation (see Figures 6 and 7). The patterns of fallen trees clearly indicate that the winds are circulating around a central core. However, to date no one has come up with a correlation between observed tree damage and wind speeds. The indicators of tree damage in the Fujita-Scale damage descriptions (Table 1) are subjective and have no quantifiable basis.

The number of variables in a forest make it very difficult to generalize, even on a qualitative basis. A few of the major factors that affect tree damage are:

(1) Soil conditions - wet, dry, stiff or soft, sandy or clay.

(2) Root types - deep or shallow.

(3) Type of wood - hardwood, softwood, flexible or stiff, ductile or brittle.

(4) Season - leafy or bare.

Tree fall is a good indicator of cyclonic or anticyclonic circulation of the tornado winds. In the case of cyclonic winds, the direction of tree fall on the right hand side of the tornado (looking in the direction of travel) is toward the center of the path. If the circulation is anticyclonic, the opposite will be true.

FIGURE 4. DAMAGE TO RESIDENCES IN XENIA, OHIO

FIGURE 5. DEBRIS HAS COLLECTED AGAINST ARROW WOOD SCHOOL (when a structure interferes with flow of debris, it gives appearance of a swath)

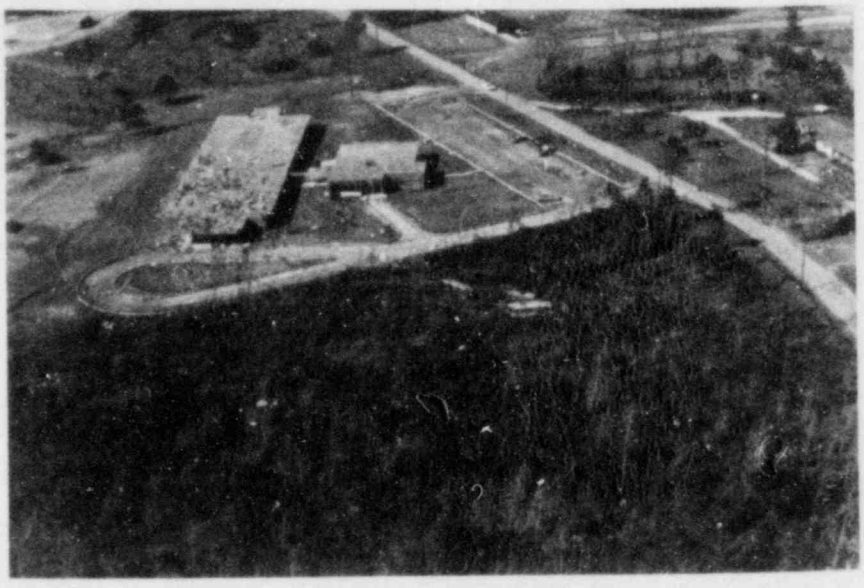

FIGURE 6. TREE DAMAGE GIVES INDICATION OF WIND FIELD CIRCULATION (Note: Buses were rolled and tumbled from circular drive)

FIGURE 7. TREE DAMAGE NEAR NORTH PIKE ELEMENTARY SCHOOL NEAR McCOMB, MISSISSIPPI

C. Translational Speed of Tornado

The appearance of tornado damage is much affected by the translational speed of the tornado. If a tornado affects power lines or other occupied structures, at two different points along the path, the translational speed can be determined with perhaps better accuracy than any other wind speed component.

Translational wind speeds vary from as low as five miles per hour to a maximum of about 70 mph. The tornadoes that struck Grand Island, Nebraska on June 3, 1980 traveled very slow. Examples of fast translating tornadoes were the ones in the Super Outbreak of April 3, 1974, where the typical translational speed was approximately 60 mph.

The damage paths have different appearances, depending on whether the translational speed is slow (85-20 mph), medium (20-40 mph) or fast (40-70 mph). If the translational speed is slow, the tornado winds affect a particular point in the damage path for a greater length of time. As a result, the debris patterns are very mixed up. The indicators of circulation are not as distinctive. Damage is usually worse, because the winds had longer to act on a structure. The appearance of damage will be much worse than the actual wind speeds would suggest. Debris will tend to be scattered in all directions, rather than in a particular direction. If the translational speed is in the medium range, the damage pattern will give a good indication of circulation. Objects or tree falls on the right hand side of the path will be moved in the direction of tornado travel and toward the center of the path. Objects and tree fall on the left side of the path centerline will be in the opposite direction of tornado travel. If the tornado is translating very rapidly, objects and tree fall on the right hand side tend to be forward with very little inward movement. On the left hand side of the path, the translational speed and the circulation component are essentially acting in opposite directions and tend to cancel each other. The effect is that the centerline of the tornado core is very near the left hand side of the tornado damage path.

Thus, the translational speed of the tornado has a very definite effect on the appearance of damage in a tornado damage path. The translational speed should be determined early in any damage investigation effort, because it has a definite influence on appearance of damage.

D. Wind Direction

To say that a tornado wind velocity can come from any direction seems to be stating the obvious. However, in talking with the general public at the scene of a tornado event, people tend to believe that the wind velocities are in the direction of the tornado path. As pointed out above, this tends to be true if the translational speed of the tornado is fast. However, the direction of wind at any particular point on the ground depends on the tornado path relative to the point in question. Minor, et al. (1977) concluded, "...directions of large wind speeds occurring at the selected points indicate that the laregest wind speeds within the tornado were following the large cyclonic

circulation attendant to the Lubbock Tornado." Similar conclusions were drawn from studies of the Xenia, Ohio tornado and the Omaha, Nebraska tornado.

E. Path Width

Correlations between path width and tornado intensity have been published in the literature (Schaefer, 1980). The purpose of this discussion is not to elaborate on those correlations. Rather, the effects of the near-ground wind field as a function of path width are presented in this section.

Tornado path widths have been reported as narrow as five yards or as wide as one and one-half miles. Path width trends seem to indicate that path width is directly related to intensity. The most intense tornadoes such as the Xenia, Ohio tornado, the Lubbock, Texas and Wichita Falls, Texas tornadoes tend to follow the trend. Each one was more than three-quarters of a mile wide and each was rated F4 or F5. Other high intensity tornadoes were not so wide. The Bossier City, Louisiana tornado and the Birmingham, Alabama tornadoes were relatively narrow, but were very intense. The Birmingham tornado was rated F5, while the Bossier storm was rated F4. Thus, path width is not necessarily an indicator of intensity. Intense tornadoes can be both wide or narrow.

VI. TORNADO-GENERATED MISSILES

Much as been written in the technical literature on tornado-generated missiles. Despite a lot of studies, the three important questions remain:

1. What kinds of missiles are picked up and transported by tornado winds?

2. How fast do they travel?

3. How far and how high do they travel?

Various types of missiles that are picked up and transported by tornadoes as well as those that were not picked up by a particular storm have been documented in the technical literature (McDonald, 1976). Under previous contract with NRC, personnel from Texas Tech University discovered and analyzed some of the most awesome missiles ever observed (McDonald, 1981). Six steel wide flange beams weighing as much as 720 lbs each were picked up and transported by the Bossier City, Louisiana tornado of December 3, 1979 (see Fig. 8). One of these beams was carried in the air a distance of 1000 ft and then impacted through the roof of a house. Another one of the beams traveled 450 ft. and penetrated eight ft. into the ground. As a result the ANSI Task Committee adopted the wide flange beam as the controlling design missile in the Standard (ANS, 1983). This missile incident provided a unique opportunity to study the effectiveness of computer simulation codes for tornado missiles. In this case the point of origin of the missile was known; its type of anchorage and the final impact point were also known. A very good representation of the tornado wind field in the vicinity of the school from where the missile originated was obtained from ground and aerial surveys of the damage by TTU personnel and Dr. Fujita from the University of Chicago. Malaeb (1980) studied this problem using the tornado missile simulation code developed at Texas Tech University (McDonald, 1975). The two parameters thought to be most significant (missile release velocity and flight parameters) were varied over probable ranges until a combination was obtained that produced trajectories that matched the initial location and final impact point of each beam. The results of the study were very encouraging. They showed that the computer code could simulate the effects of the observed missile using reasonable values of the parameters involved. This was just one incident, and conditions were ideal for the type of study performed. However, other studies are needed of this type to further confirm the results. A part of the scope of work on this current contract was to identify missile incidents that could be studied in a similar manner. No new missile events of significance were identified in the documentation performed during this contract period.

The impact effects of large postulated tornado missiles, such as utility poles and large diameter pipes have been tested and are fairly well understood (Vassallo, 1975; Rotz, 1976; Stephenson, 1977). The wide flange beams, which could be found on any construction site at a nuclear power plant appears to be the most significant missile at this

FIGURE 8. STEEL WIDE FLANGE BEAM TRANSPORTED BY BOSSIER CITY, LOUISIANA TORNADO

point. There has not, to our knowledge, been a documented case of a utility pole or large diameter pipe being picked up and transported as have the wide flange beams. Further studies on both the flight characteristics and impact effects need to be conducted for the wide flange missiles.

VII. CONCLUSION

A. Summary

A study of near-ground tornado wind fields has been conducted by inspecting damage and debris patterns found in tornado damage paths. Because there were no significant tornado events (F4 or greater) during the contract performance period, data from the literature and the files of the Institute for Disaster Research were used to perform the analyses. Additional data from field studies are still needed to reinforce the conclusions presented in this report.

Based on this study and other information found in the technical literature, the following statements can be made regarding near-ground tornado wind fields:

1. Maximum tornado wind speed ever experienced or expected is in the range of 250-300 mph.

2. Appearance of damage, taken by itself, is a misleading parameter of tornado intensity. Type of construction, age of construction, materials and other construction features significantly affect structural performance of a building subjected to wind loads and should be taken into account in assigning Fujita-Scale ratings.

3. Damage to forests gives a good indication of tornado wind field flow patterns, but do not give verifiable values of wind speed.

4. Factors such as translational speed, wind direction and path width affect appearance of damage of a tornado.

5. Even the most awesome appearing missiles do not require incredible wind speeds to explain them. Some progress in computer simulation of tornado missiles have been made.

B. Need for Continued Research

The need for additional information on tornado behavior and characteristics remains. Over the past six years, a great amount of new information has been gained from systematic study of all significant tornado events. This effort needs to be continued by agencies such as NRC in order to have the data needed to design critical facilities for nuclear power plants and other nuclear materials handling facilities. If this systematic investigation is not continued, a serious gap in the information base will exist that can never be completely overcome.

LIST OF REFERENCES

ANS, 1983: "Standard for Estimating Tornado and Extreme Wind Characteristics at Nuclear Power Sites," ANSI/ANS 1.3-1983, American Nuclear Society, La Grange Park, IL.

Ellingwood, B., Galambos, T.V., MacGregor, J.G., and Cornell, C.A., 1980: "Development of A Probability Based Load Criterion for the American National Standard A58," NBS Special Publication 577, National Bureau of Standards, Washington, DC.

Flora, S.D., 1954: Tornadoes of the United States, University of Oklahoma Press, Norman, Oklahoma, pp. 79, 80.

Forbes, G.S. and Fujita, T.T., 1976: "Photogrammetric Characteristics of the Parker Tornado of April 3, 1974," Proceedings, Symposium on Tornadoes: Assessment of Knowledge and Implications for Man, Texas Tech University, Lubbock, Texas.

Fujita, T.T., 1975: "New Evidence from April 3-4, 1974 Tornadoes," Preprints, Ninth Conference on Severe Local Storms, pp. 248-254, American Meteorological Society, Boston, MA.

Fujita, T.T., 1971: "Proposed Characterization of Tornadoes and Hurricanes by Area and Intensity," SMRP No. 91, Satellite and Mesometeorology Research Project, The University of Chicago, Chicago, IL.

Fujita, T.T., 1970: "The Lubbock Tornadoes: A Study of Suction Spots," Weatherwise, Vol. 23, No. 4.

Fujita, T.A., Bradbury, D.L. and Black, P.G., 1967: "Estimation of Tornado Wind Speed for Characteristic Ground Marks," Chicago University, Department of Geophysical Sciences, Satellite and Mesometeorology Research Project, Research Paper No. 69, October.

Golden, J.H., 1976: "An Assessment of Windspeeds in Tornadoes," Proceedings, Symposium on Tornadoes: Assessment of Knowledge and Implications for Man, Texas Tech University, Lubbock, TX.

Golden, J.H. and Davies-Jones, R.P., 1975: "Photogrammetric Wind Speed Analysis and Damage Interpretation of the Union City, Oklahoma Tornado May 24, 1973, Preprints, Second U.S. National Conference on Wind Engineering, Colorado State University, Ft. Collins, CO.

Malaeb, D.A., 1980: "Simulation of Tornado-Generated Missiles," Thesis submitted in partial fulfillment of the requirements for the degree of Master of Science in Civil Engineering, Texas Tech University, Lubbock, TX.

Marshall, T.P., McDonald, J.R. and Mehta, K.C., 1983: "Utilization of Load and Resistance Statistics in a Wind Speed Assessment," IDR 62D, Institute for Disaster Research, Texas Tech University, Lubbock, TX.

McDonald, J.R., 1983: "A Methodology for Tornado Hazard Probability Assessment," NUREG/CR-3058, U.S. Nuclear Regulatory Commission, Washington, DC.

McDonald, J.R., 1981: "Incredible Tornado-Generated Missiles," Preprints, Fourth U.S. National Conference on Wind Engineering Research, University of Washington, Seattle, WA, pp. 29-36.

McDonald, J.R., 1976: "Tornado-Generated Missiles and Their Effects," Proceedings, Symposium on Tornadoes: Assessment of Knowledge and Implications for Man, Texas Tech University, Lubbock, TX..

McDonald, J.R., 1975: "Flight Characteristics of Tornado-Generated Missiles," Institute for Disaster Research, Texas Tech University, Lubbock, TX.

McDonald, J.R. and Abbey, R.F., Jr., 1979: "Comparison of the NSSFC and DAPPLE Tornado Data Tapes," Preprints, Eleventh Conference on Severe Local Storms, American Meteorological Society, Boston, MA.

McDonald, J.R. and Marshall, T.P., 1983: "Damage Survey of the Tornadoes Near Altus, Oklahoma on May 11, 1982," IDR 68D, Institute for Disaster Research, Texas Tech University, Lubbock, TX.

Mehta, K.C., 1976: "Windspeed Estimates: Engineering Analysis," Proceedings, Symposium on Tornadoes: Assessment of Knowledge and Implications for Man, Texas Tech University, Lubbock, TX.

Mehta, K.C., McDonald, J.R. and Minor, J.E., 1976: "Windspeed Analysis of the April 3-4, 1974 Tornadoes," Journal of the Structural Division, ASCE, Vol. 102, No. ST9, Proc. Paper 12429, pp. 1709-24.

Mehta, K.C., McDonald, J.R., Minor, J.E. and Sanger, A.J., 1971: "Response of Structural Systems to the Lubbock Storm," SRR 03, Texas Tech University, Lubbock, TX (NTIS Accession No. PB-204-938).

Mehta, K.C., Minor, J.E., McDonald, J.R. and Reinhold, T.A., 1981: "Valuable Information from Wind-Caused Damage in Hurricane Frederic," Preprints, Fourth U.S. National Conference on Wind Engineering Research, University of Washington, Seattle, WA.

Minor, J.E., Mehta, K.C. and McDonald, J.R., 1977: "The Tornado: An Engineering-Oriented Perspective," NOAA Technical Memorandum ERL NSSL-82, National Severe Storms Laboratory, Norman, OK.

National Severe Storms Forecast Center, 1979: Tornado Data Set 1950-79, NOAA, U.S. Dept. of Commerce, Kansas City, MO.

Peterson, R.E., Wagner, F.B. and Minor, J.E., 1980: "Tornado Event Survey (TES), IDR 70D, Institute for Disaster Research, Texas Tech University, Lubbock, TX.

Schaefer, J.T. and Kelly, D.L., 1980: "Tornado Track Characteristics and Hazard Probabilities," U.S. Nuclear Regulatory Commission, Washington, DC.

Segner, E.P., 1960: "Estimates of Minimum Wind Forces Causing Structural Damage in the Tornadoes at Dallas, Texas, April 2, 1957," U.S. Weather Bureau Research Paper No. 41, pp. 169-175.

Stephenson, A.E., 1977: "Full-Scale Tornado-Missile Impact Tests," EPRI NP-440, Final Report, Electric Power Research Institute, Palo Alto, CA.

Tecson, J.J., Fujita, T.T. and Abbey, R.F., Jr., 1979: "Statistics of U.S. Tornadoes Based on the DAPPLE Tornado Tape," Preprints, Eleventh Conference on Severe Local Storms, American Meteorological Society, Boston, MA.

Vassallo, F.A., 1975: "Missile Impact Testing of Reinforced Concrete Panels, Calspan Corporation, Report No. HC-5609-D-1, Buffalo, NY.

Zipser, R.A., 1976: "Photogrammetric Studies of a Kansas Tornado and a Hawaiian Tornadic-Waterspout," M.S. Thesis, Dept. of Meteorology, University of Oklahoma, Norman, OK.

APPENDIXES

APPENDIX A — DAMAGE SURVEY OF THE TORNADOES NEAR ALTUS, OKLAHOMA ON MAY 11, 1982

APPENDIX B — THE UTILIZATION OF LOAD AND RESISTANCE STATISTICS IN A WIND SPEED ASSESSMENT

DAMAGE SURVEY OF THE TORNADOES NEAR ALTUS, OKLAHOMA ON MAY 11, 1982

by

James R. McDonald, P.E.
Timothy P. Marshall

Institute for Disaster Research
Texas Tech University
Lubbock, Texas

July 1983

FOREWORD

The Institute for Disaster Research has studied tornado damage for 13 years. From damage and debris patterns much can be learned about near-ground tornado wind fields. The two tornadoes that struck near Altus, Oklahoma provided still another opportunity to study the effects of tornadoes on structures. Initial reports of damage suggested that there was only one tornado path at Altus. After corroborating with the National Severe Storms Laboratory Chase Team and after examining the damage paths, the two separate tornadoes were identified. The tornado that passed through the Altus Air Force Base was of particular interest, because it affected buildings that had received significant degrees of engineering attention in their design.

The cooperation of personnel at Altus Air Force Base, Altus, Oklahoma, in coordinating this damage survey is gratefully acknowledged. The assistance of the disaster team on the base helped our storm study team acquire the necessary information for this study. Also, the assistance of Captain A.R. Walker of the Airforce Base Weather Station and Captain Walter L. Garner of the Civil Engineering Department is appreciated.

Funds for this tornado damage documentation effort were provided by the U.S. Nuclear Regulatory Commission Contract No. NRC-04-76-345. Robert F. Abbey, Jr., serves as contract monitor on the project.

TABLE OF CONTENTS

LIST OF ILLUSTRATIONS

LIST OF TABLES

INTRODUCTION

On the afternoon of May 11, 1982, several tornadoes touched down in southwestern Oklahoma. One of the tornadoes struck the east side of the city of Altus and traveled three miles in a northeasterly direction through the Altus Air Force Base, causing extensive damage (Figure 1). A second tornado touched down northeast of the Air Base just west of the Friendship community and traveled in a northerly direction at least twelve miles (Figure 2).

The next day, a windstorm damage investigation team from the Institute for Disaster Research at Texas Tech University traveled to Altus, Oklahoma to document and evaluate the damage.

The objectives of the damage documentation effort were:

1) To collect and evaluate data on the performance of buildings damaged by the tornado.

2) To define the damage path and identify gradations of damage within the path using the F-scale rating system.

3) To document tornado-generated missiles.

The investigation team spent two days inspecting the damage. Members of the team included an engineer, a meteorologist, and an undergraduate student in civil engineering. The purpose of this report is to present preliminary findings based on data gathered from the damage.

METEOROLOGICAL SUMMARY

On the morning of May 11, 1982 there was a surface low-pressure system in western Kansas and another located in northeastern New Mexico. As the day progressed, the low-pressure systems remained relatively

FIGURE 1. VIEW LOOKING WEST OF THE TORNADO WHICH STRUCK THE ALTUS AIR FORCE BASE (photograph courtesy of Dr. Howard Bluestein, OU-NSSL Severe Storm Intercept Project).

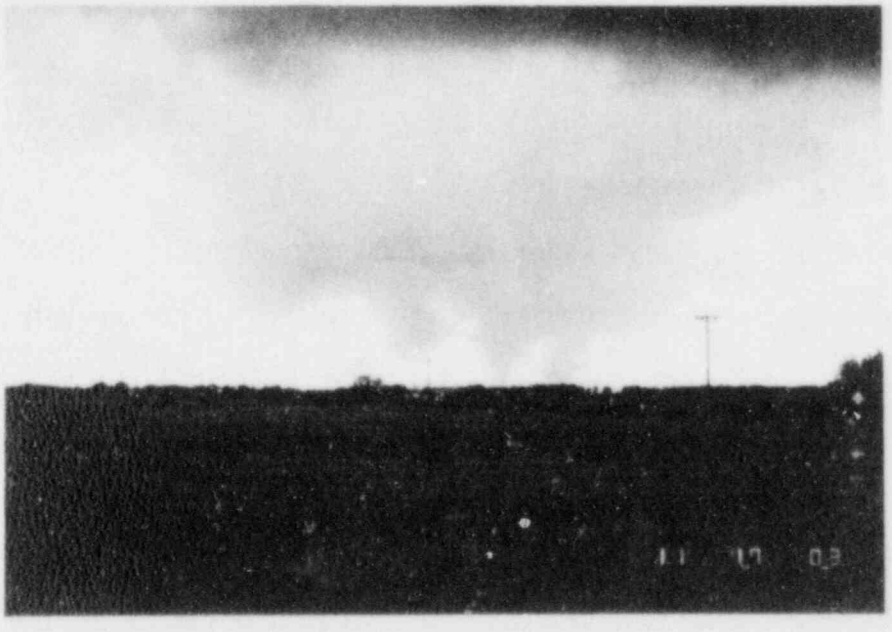

FIGURE 2. VIEW LOOKING NORTHWEST OF A MULTI-VORTEX TORNADO NEAR FRIENDSHIP, OKLAHOMA (photograph courtesy of Dr. Howard Bluestein, OU-NSSL Severe Storm Intercept Project).

stationary and a dryline developed in eastern New Mexico. The dryline demarcated dry, stable air to the west from moist, unstable air to the east. By mid-afternoon, the leading edge of the dryline had moved eastward into West Texas and several thunderstorms developed in the moist air along and to the east of the boundary. By 6:00 p.m., the most severe thunderstorms were located in the vicinity of the dryline bulge and extended northeastward into southwestern Oklahoma (Figure 3). Within the next few hours, a total of twenty-seven tornadoes were reported in this area (Storm Data, 1982). Most of the tornadoes occurred in open country and damage was minimal. However, the two tornadoes near Altus, Oklahoma caused extensive damage. A sequence of significant severe weather events in western Oklahoma leading through the tornadoes near Altus is shown in Table 1.

CHARACTERISTICS OF THE TORNADO PATHS

The first tornado touched down on the east side of Altus (Figure 4). There was only minor damage to trees, fences, and street lights until the storm entered the Air Force Base. The tornado intensified and traveled northeastward from the main gate, across the center of the base and lifted just east of the main runway.

Within a few minutes after the first tornado, a larger tornado touched down northeast of the Air Force Base near the community of Friendship. The tornado traveled northward for twelve miles through the countryside damaging rural homes and trees. Two people were killed by flying debris two miles west of Friendship as they were heading for

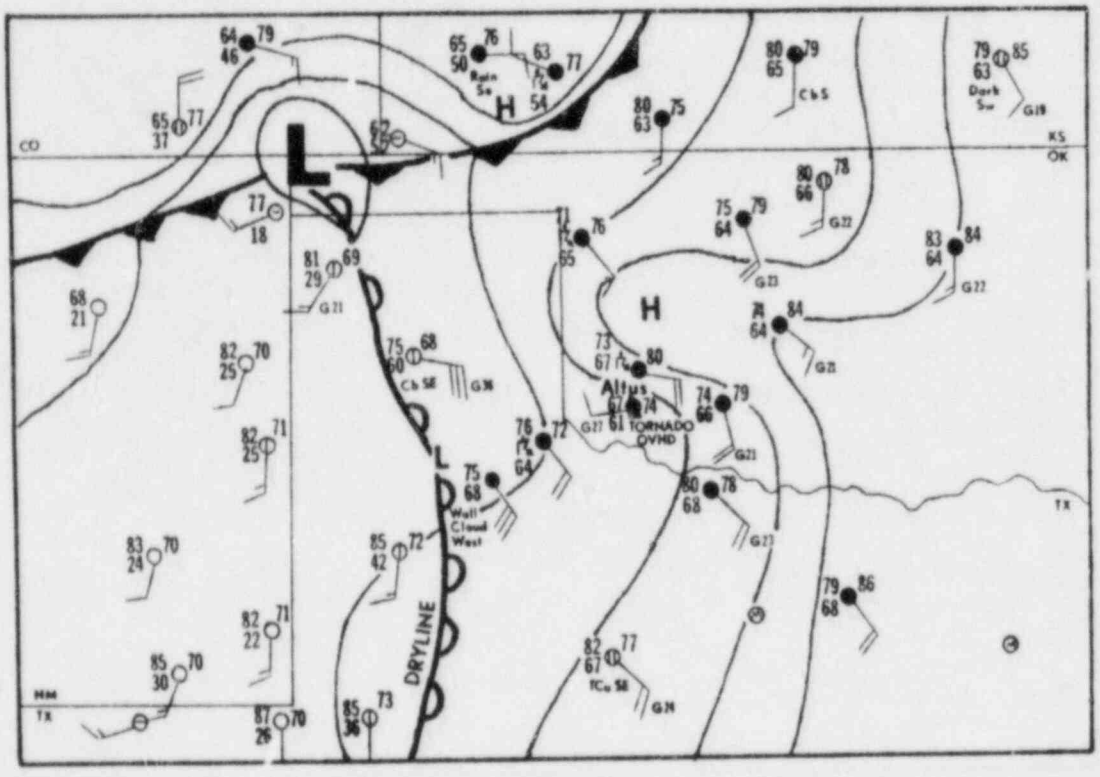

FIGURE 3. SURFACE ANALYSIS AT 6:00 P.M. (CDT) ON MAY 11, 1982. For each station model, the temperature (°F) is the upper left number, dewpoint (°F) is lower left, altimeter (in.) is upper right and wind speed is 10 miles per hour for each full barb.

TABLE 1

OKLAHOMA CITY SEVERE STORM SUMMARY, MAY 11, 1982

Severe weather report listings received by National Weather Service
Oklahoma City, CDT

4:00p.m.	Baseball sized hail at Eldorado in southwest Jackson County, Oklahoma.
4:17	Tornado watch issued for western Oklahoma.
4:49	Jackson county sherrif reported funnel cloud 10 miles southwest of Altus.
5:00	Tornado watch valid.
5:03	Oklahoma Highway Patrol at Altus reported tornadoes on the ground west of Altus and near Creta.
5:18	Oklahoma Highway Patrol at Altus reported tornado on the ground seven miles west of Altus.
5:14	NSSL Chase Team reported tornado on the ground eight miles south of Blair in Jackson County.
5:35	Oklahoma Highway Patrol at Altus reported tennis ball sized hail in Altus and a tornado six miles west of Blair in Jackson County.
5:38	Oklahoma Highway Patrol at Altus reported tornado on the ground one and a half miles south of Altus city limits.
5:59	Oklahoma Highway Patrol at Clinton reported unconfirmed tornado 11 miles southwest of Cheyenne.
6:00	Oklahoma Highway Patrol at Altus reported a tornado at Altus Air Force Base. Later report gave estimated damage of one million dollars easily with seven buildings extensively damaged or destroyed.
6:10	Oklahoma Highway Patrol at Clinton reported confirmed tornado five miles west of Cheyenne moving northeast.
6:58	Oklahoma Highway Patrol at Clinton reported numerous funnel clouds mainly in Roger Mills County.
6:59	Oklahoma Highway Patrol at Altus reported tornado on the ground one and one half miles south of Lone Wolf in Kiowa County.
7:31	Amateur radio reported a tornado four miles west-southwest of Arnett in Ellis County.
7:46	Oklahoma Highway Patrol at Altus reported tornado on the ground two miles north of Sentinel in Southern Washita County.
8:18	Sayre Police Department reported tornado on the ground seven miles southeast of Sayre in Beckham County.
8:42	Oklahoma Highway Patrol at Clinton reported tornado ten miles west of Clinton.
10:55	Madill Police Department reported golf ball sized hail had occurred at Texoma Lake. Estimated time around 10:15 p.m.

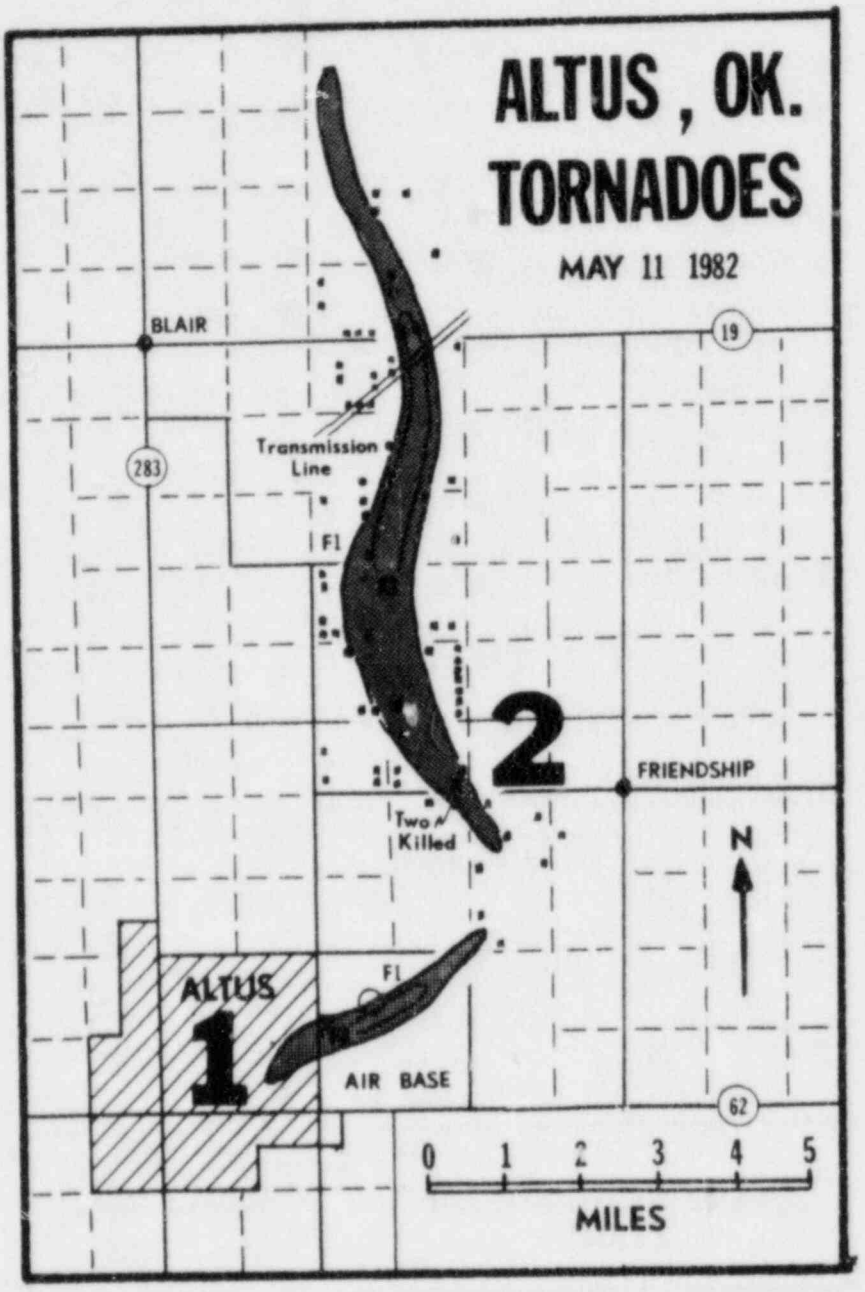

FIGURE 4. DAMAGE PATH OF THE ALTUS AND FRIENDSHIP TORNADOES

an outdoor storm cellar. A 138 KV transmission line owned by Public Service of Oklahoma was downed as the tornado crossed Route 19, 3.5 miles east of Blair. F-scale classifications were assigned to rural building damage. Since no engineered structures were in the path of the Friendship tornado, wind speed estimates were not attempted. The characteristics of both tornadoes are listed in Table 2.

ALTUS AIR FORCE BASE

The initial survey revealed that the damage path extended from the main gate across the center of the base and ended just east of the main (north-south) runway (Figure 5). The damage produced by this tornado was of great interest to the storm study team because it provided an opportunity to study the effects of tornadic winds on buildings that had received various degrees of engineering attention in their design. The storm also presented a unique opportunity to compare wind speed estimates from appearance of damage with wind speeds obtained from structural analysis of damaged building components.

F-scale ratings (Fujita, 1971) were assigned to each building examined by the storm study team based on appearance of damage and the word description associated with each F-scale classification. Care was taken not to be influenced by structural features or degrees of engineering attention. Later after all F-scale assignments had been made, independent wind speed calculations were made based on structural analysis using load and resistance statistics (Ref. Marshall, et al. 1983).

The damage path through the Altus Air Force Base shown in Figure 5 was assembled using F-scale criteria. Buildings which sustained F1

TABLE 2

CHARACTERISTICS OF THE ALTUS AND FRIENDSHIP TORNADOES

TORNADO SEQUENCE (CST)	Altus	Friendship
Observed funnel touchdown	5:48 p.m.	6:02 p.m.
Tornado entered the Air Base	5:51 p.m.	--
Tornado over Weather Station	5:55 p.m.	--
Tornado dissipated	6:00 p.m.	6:22 p.m.
PATH LENGTH		
Touchdown to lift up	3.5 mi	12.0 mi
Damage to F-3 intensity	.5 mi	3.5 mi
Damage of F-2 intensity	1.0 mi	6.0 mi
Damage of F-1 intensity	2.0 mi	10.0 mi
PATH WIDTH		
Average F-1 intensity	0.29 mi	0.75 mi
Average F-2 intensity	0.17 mi	0.50 mi
Average F-3 intensity	0.06 mi	0.33 mi
SENSE OF ROTATION	counterclockwise	counterclockwise
DIRECTION OF TRAVEL	east-northeast	north
AVERAGE TRANSLATIONAL SPEED	5-10 mph	25 mph
TORNADO CIRCULATION	single-vortex	multiple-vortex

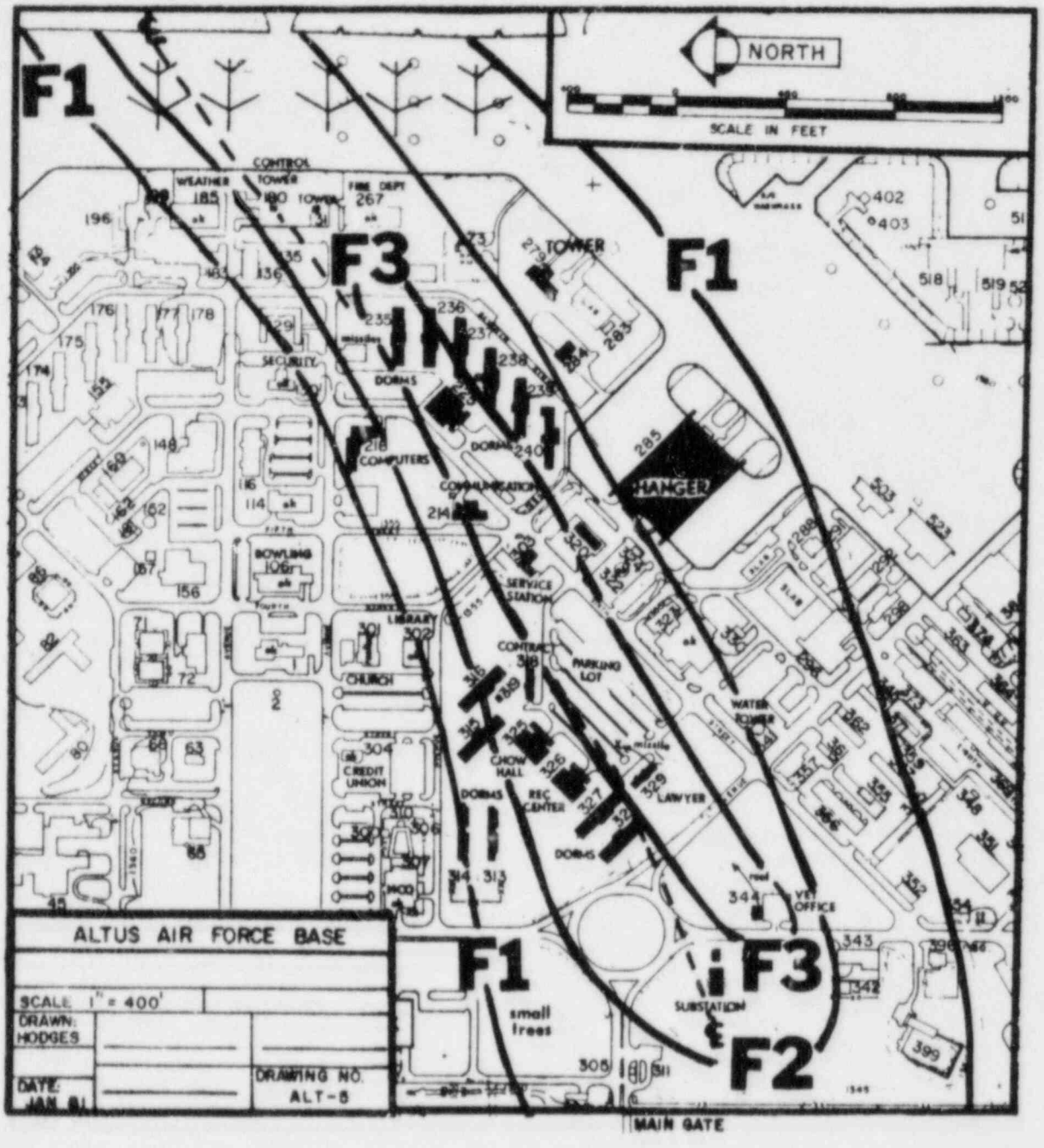

FIGURE 5. TORNADO DAMAGE PATH THROUGH ALTUS AIR FORCE BASE. (Gradations of damage are shown by F-scale.)

intensity damage or greater are shaded in Figure 5. Six buildings were heavily damaged (F3), eleven had moderate damage (F2), seven had light damage (F1). From analysis of fallen trees and debris trajectories, the center line of the tornado appeared to be parallel to the northern periphery of the F3 intensity damage track. The individual performances of buildings which sustained the heaviest damage are discussed below. A rational for the assignment of the F-scale rating also is given.

Veterinary Clinic (Building 344)

The veterinary clinic is a reinforced concrete masonry building with a flat timber roof (Figure 6). It was located about 200 feet to the right of the tornado center. As the tornado passed, portions of the roof on the windward (south) side were uplifted and transported as far as a hundred feet toward the east. The roof joists were toenailed to a 2x8 plate anchored to a bond beam at the top of the wall. The bond beam was reinforced with two #5 bars. As the roof lifted, horizontal cracks formed in the mortar joint just below the bond beam. These cracks were observed around the perimeter of the building. Based on the loss of roof and minimal damage to the reinforced concrete block walls, damage to the building appears to be upper F2 or lower F3.

Dormitories (Buildings 315, 316, 327 and 328)

These three-story dormitories have reinforced concrete frames with nonloadbearing brick walls (Figure 7). Each building is oriented in a northwest to southeast direction and is located just left of the tornado center line. The longest side of each building was normal to the strongest tornadic winds.

FIGURE 6. VIEW OF SOUTHEAST CORNER OF VETERINARY CLINIC (the cracks in the mortar joint below the bond beam occurred as the roof lifted).

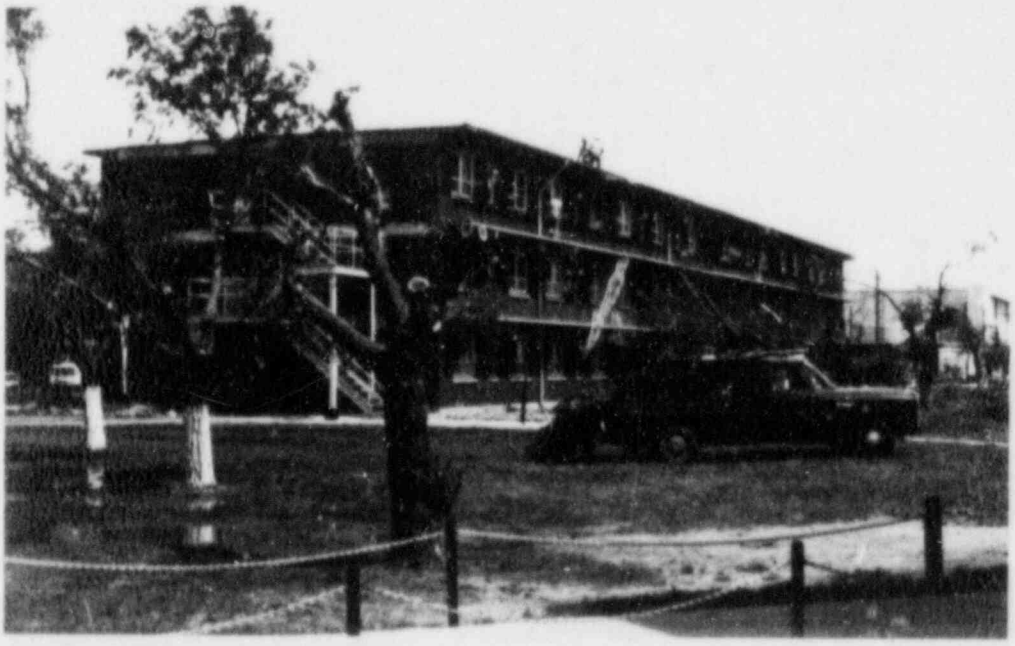

FIGURE 7. VIEW OF THE WINDWARD SIDE OF DORMITORY BUILDING #315 (the reinforced concrete structure has nonloadbearing masonry walls).

Most of the damage caused by the tornado was superficial with some broken windows and loss of roofing material. Based on superficial damage to the buildings, the damage was estimated to be F2.

Base Lawyer's Office (Building 329)

The base lawyer's office is a single story concrete masonry building and was 100 feet to the right of the tornado centerline. As the tornado passed, the window panels on the back wall failed inward, the timber roof was uplifted, and the front wall fell outward (Figure 8). The top course of each wall was a bond beam. Each bond beam was reinforced with two #5 bars. The bond beam, located on the back wall, traveled in a northeasterly direction nearly 200 feet before striking a pickup and a car (Figure 9). Also, a 12 foot long timber missile sliced through four CMU blocks on the back wall.

Based on the roof damage and missile present, the damage was estimated at upper F2 to lower F3.

Dining Hall (Building 325)

The dining hall is a single story masonry building with a timber roof. The center of the tornado passed 200 feet to the south of the building. Roof damage was observed along the entire length of the windward (north) wall (Figure 10).

A closer view of the damage to the cafeteria roof is shown in Figure 11. The roof consisted of 2x10 wooden joists spaced at 12 inches on center. The joists were secured with 10d nails which were toenailed to a wooden plate at the top of the wall. As the tornado passed, part of

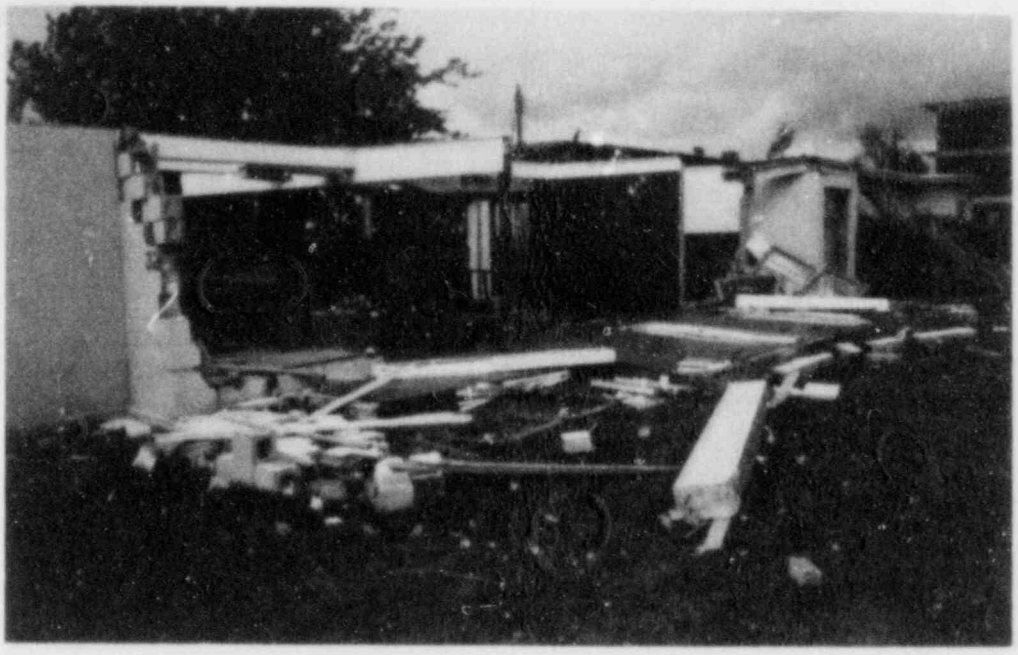

FIGURE 8. FRONT WALL OF THE BASE LAWYER'S OFFICE.

FIGURE 9. CONCRETE MASONRY BOND BEAM MISSILE (missile traveled from the base lawyer's office northeastward approximately 200 feet before striking the vehicles).

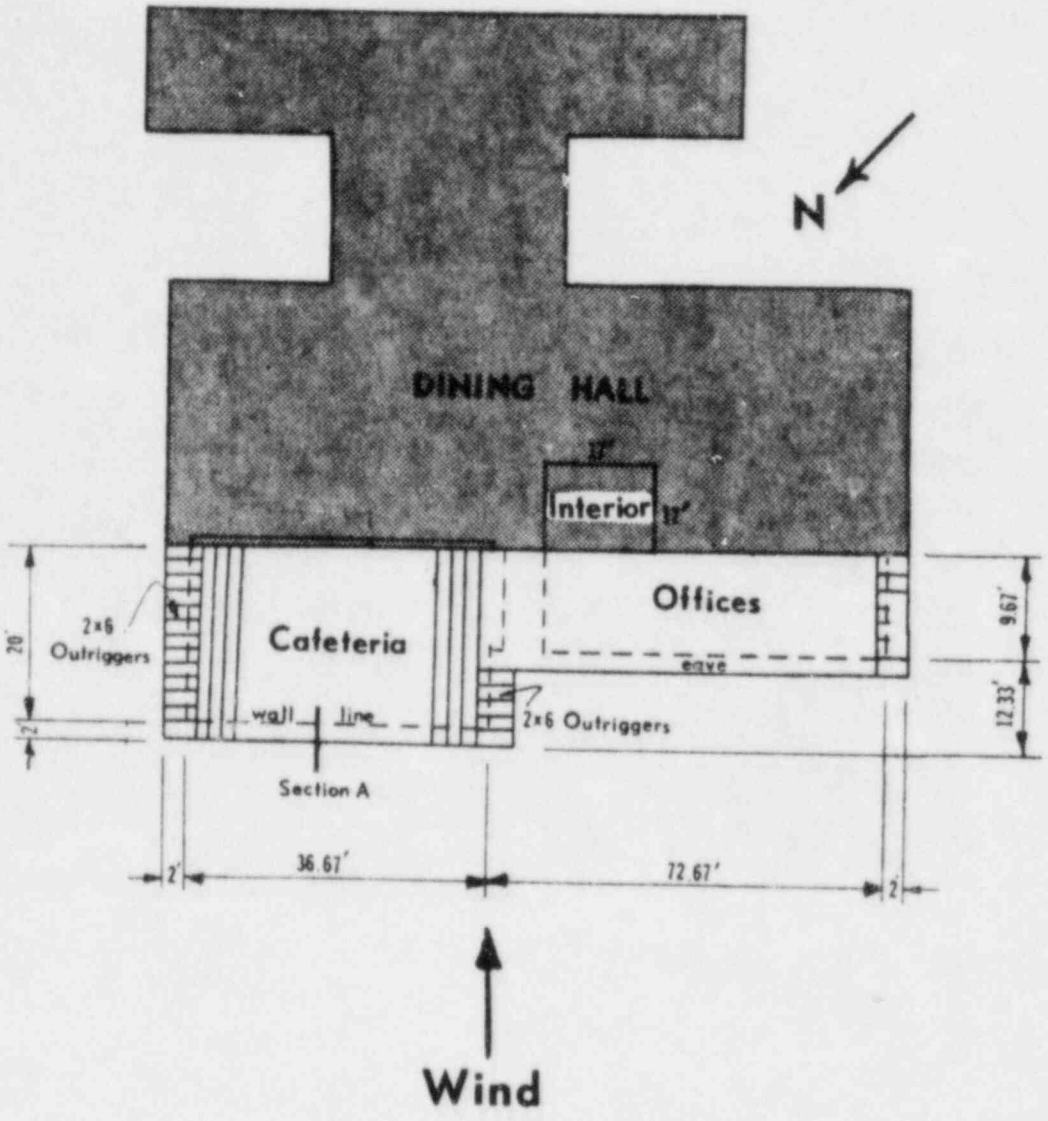

FIGURE 10. ROOF PLAN OF DINING HALL (damage to roof is unshaded).

FIGURE 11. DAMAGE TO THE DINING HALL CAFETERIA ROOF.

the roof, including the roof joists, was removed and one precast concrete bond beam was lifted up and slightly displaced.

Based on the damage to the roof, the damage intensity was estimated to be F2.

Recreation (Building 326)

The Recreation Building is adjacent to the Dining Hall and similarly constructed. It is a single story masonry structure with a flat timber roof (Figure 12). Most of the damage occurred at the northwest corner of the building next to the windward side. A portion of the roof was uplifted and window glass was blown inward (Figure 13). The roof joists remained in place but the wood decking was removed. An exterior metal door in the windward wall was damaged by an impact of several timber missiles. Based on the damage to the roof corner and the presence of the missile, the damage intensity was rated F2.

Trees in the area sustained light damage and some utility poles were snapped near the ground. However, none of the utility poles were transported by the winds.

Contracts Office (Building 318)

The Contracts Office has precast tilt-up wall panels and a mansard-type timber roof (Figure 14). It was located just left of the tornado centerline. Damage to the building was superficial with broken windows and damage to its fascia from impact of small timber missiles.

Several cars in a nearby parking lot were damaged by flying roof gravel, other small missiles and hail. Windows broke in some cars and

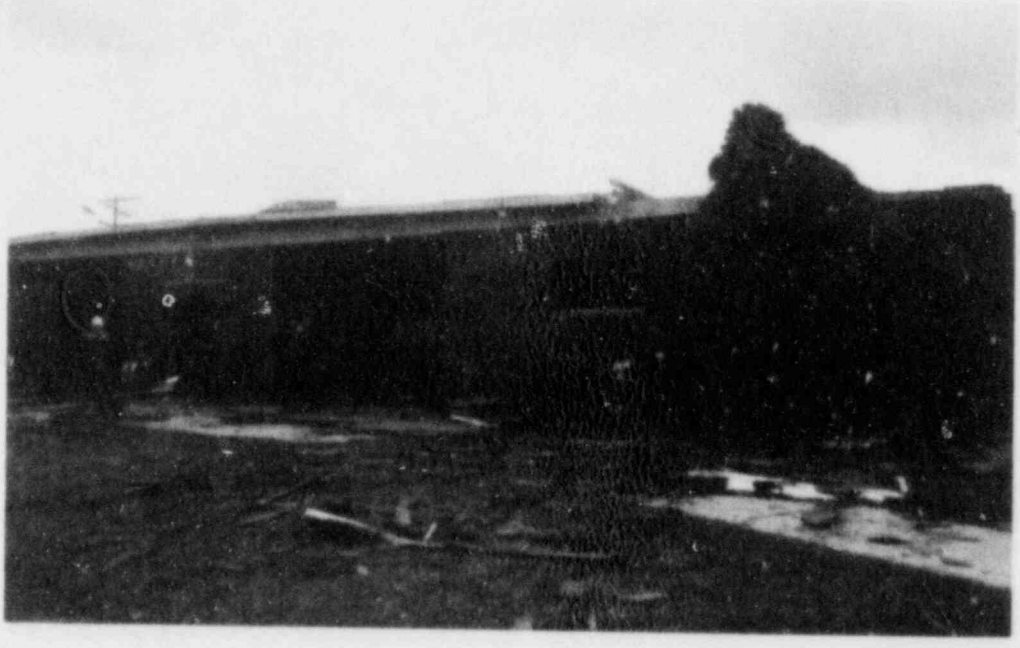

FIGURE 12. ROOF DAMAGE TO RECREATION BUILDING (damage was confined to roof fascia and roof corner).

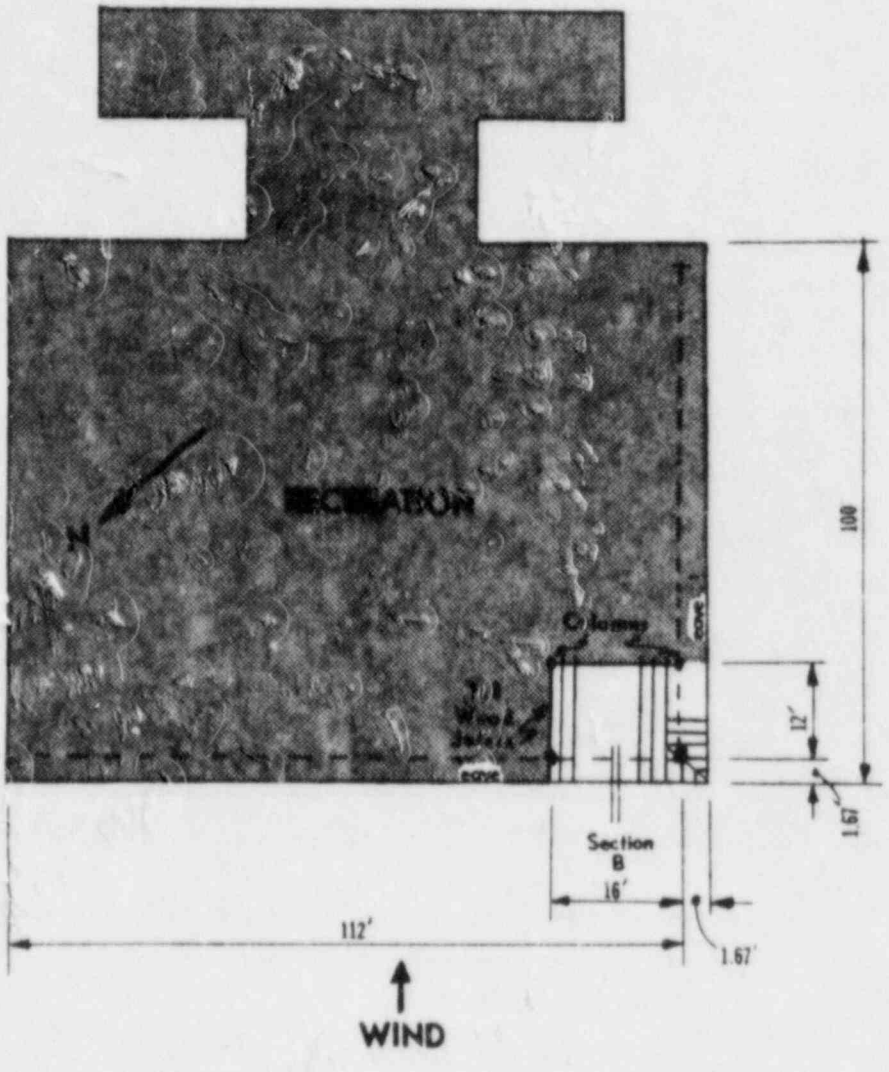

FIGURE 13. ROOF PLAN OF RECREATION BUILDING
(damage at roof corner is unshaded).

FIGURE 14. FRONT VIEW OF CONTRACTS OFFICE (damage was superficial).

allowed roof gravel and mud to collect inside. Two compact vehicles overturned but most of the cars remained in place. Based on superficial damage to the building, overturned cars in the parking lot and the observed missiles, the damage intensity was rated F2.

Aircraft Hangar (Building 285)

A large hangar 500 feet wide by 600 feet long and 80 feet tall was damaged by the tornado. The damage was confined to the siding, doors and roof on the windward (southwest) side. As the tornado passed, the hangar doors were blown inward (Figure 15). Each door section is 65 feet high and 20 feet wide. The doors are suspended from the top of the hangar and are guided on tracks at the bottom. A closer view of the hangar doors revealed that the lower edge of the center door was pushed about four feet inward. The hangar was approximately 600 feet to the right of the tornado centerline, on the periphery of the tornadic winds.

The roof is constructed with 30 in. wide by 8 ft long sheets of 18 gage metal deck. The deck is 1.5 in. deep and has ribs spaced 6 in. apart. One-quarter inch diameter spot welds at the ends of each rib attached the deck to the roof framing system. Several of the sheets were uplifted and then fell back into the building.

Asbestos siding was removed from portions of the walls at the corners. The siding was removed after it cracked and allowed the anchor bolt to slip through the crack. Based on damage to the hangar doors, the partial roof uplift and loss of siding at wall corners, the damage intensity was rated F1.

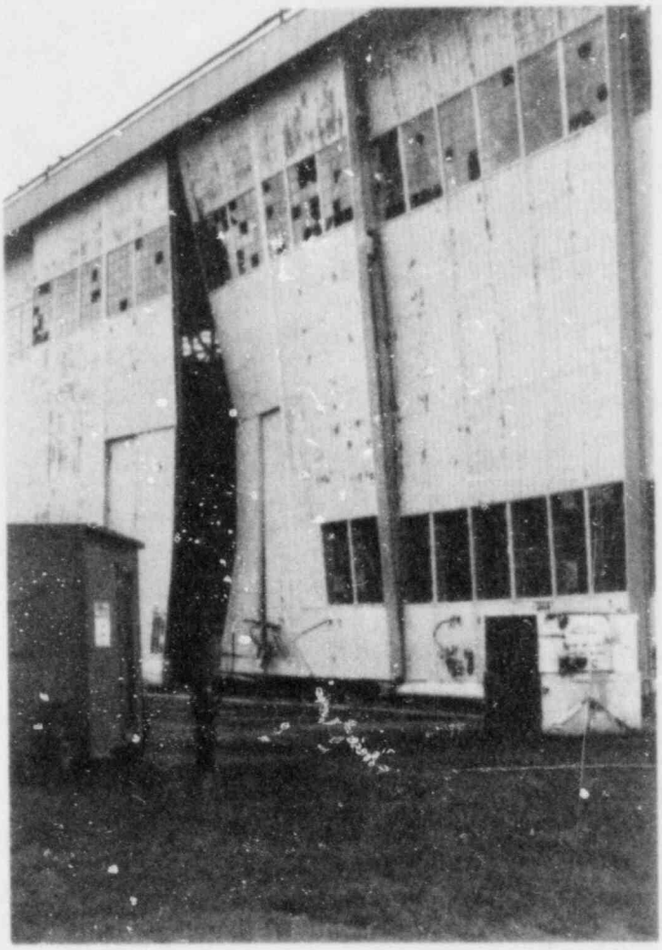

FIGURE 15. DOORS OF AIRCRAFT HANGAR (force of wind bent doors inward).

Communications Building (Building 214)

The Communications Building is a single story concrete block building with a lightweight concrete roof. The building has a long, rectangular shape and is oriented in a north-south direction (Figure 16). As the tornado passed by, roof sections on the south half of the building were uplifted whereas the northernmost half of the roof remained in place. This observation supports the contention that the center of the tornado passed directly over the building.

The roof consists of a 2-in. thick perlite (lightweight) concrete slab poured over a fabric-backed wire mesh. The mesh is laid in 8-ft wide strips. It is secured to the steel joists with twisted galvanized wire. The open web steel joists are spaced 30 in. on center and are anchored to a bond beam with two half inch diameter bolts. The somewhat unusual construction of the roof is the result of the building being designed to resist blast. As the tornado passed by, the twisted galvanized wires failed and the perlite slabs were lifted and rolled off the roof (Figure 17), but the steel joists remained in place. Based on damage to the roof and the surroundings, the damage intensity was assigned a rating of F-3.

Barracks (Buildings 235-240)

A series of five two-story wooden barracks were heavily damaged by the tornado. Sections of the roofs were removed and second story walls collapsed (Figure 18). Not all the roofs failed in the same manner. Some of the roof failures were attributed to anchorage of the roof to the

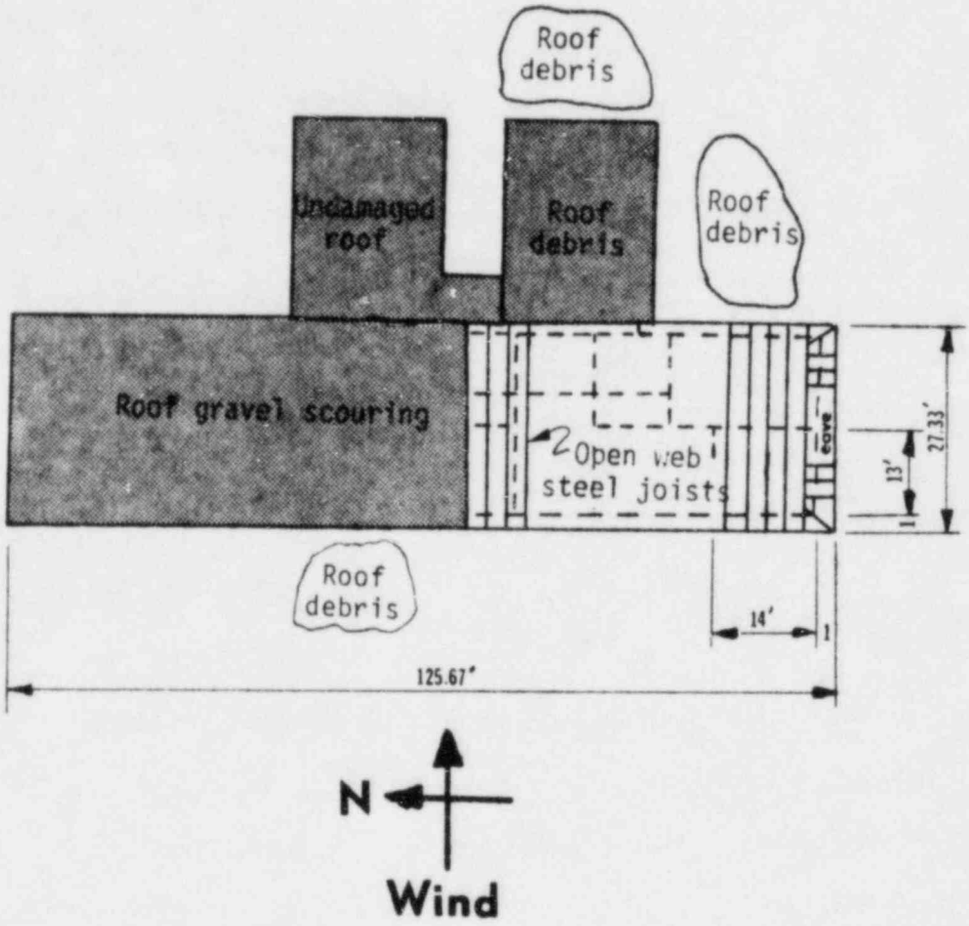

FIGURE 16. ROOF PLAN OF COMMUNICATIONS BUILDING (damaged area is unshaded).

FIGURE 17. DAMAGE TO COMMUNICATIONS BUILDING (eight ft wide sections of lightweight roof slab were lifted).

FIGURE 18. SEVERE-LOOKING DAMAGE TO WOODEN BARRACKS (most barracks lost their roofs and parts of second-story walls).

wide. Roof joists that were toenailed to plates on top of the walls pulled loose. In other cases, the wood joists split horizontally along their entire length. When the roof joists were removed the top of the walls were left unsupported and in many cases the walls collapsed. The damage intensity was estimated to be F2 or F3 based on damage to the wooden roof system.

C-5 Galaxy Aircraft

Two C-5 Galaxy aircraft and one C-141 sustained major damage while four C-5s had minor damage. The aircraft were parked in a north-south row facing west before the tornado (Ref. Fig. 5). As the tornado passed over the aircraft, one C-5 Galaxy pivoted 90 degrees toward the south (Figure 19). The nose of the aircraft came in contact with the wing of another. The aircraft that pivoted was located on the northern (left) periphery of the tornado. Specifications of the C-5 Galaxy aircraft are listed in Table 3.

Parachute Drying Tower (Building 279)

The Parachute Drying Tower was located on the right side of the tornado path approximately 650 feet from the tornado center (Figure 20). The rectangular tower measured 28'-6"x15'-6" in plan and was 62'-4" high. It was anchored to concrete footings with four 5/8" diameter A307 anchor bolts at each corner. As the tornado passed, the tower pivoted about a line through the two corner columns on the leeward (northeast) side of the tower (Figure 21) and fell toward the northeast. The anchor bolts failed in tension. Based on the collapse of the tall, rather fragile tower, the damage was rated F1.

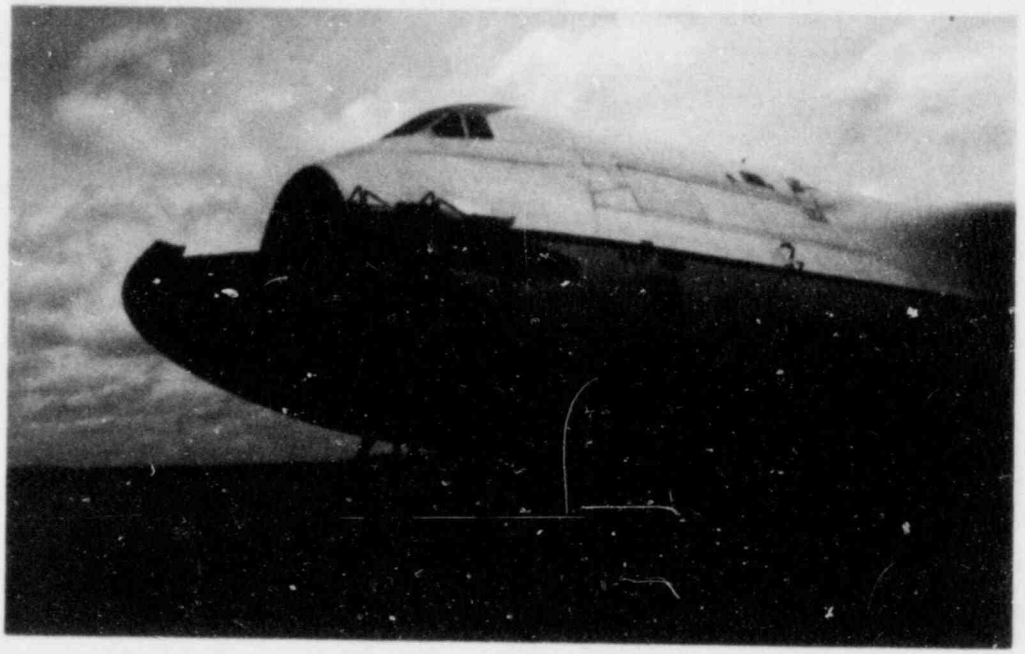

FIGURE 19. DAMAGE TO THE NOSE OF A C-5 AIRCRAFT (aircraft pivoted 90 degrees and struck wing of another C-5 as the tornado passed).

TABLE 3

C-5 AIRCRAFT SPECIFICATIONS

WEIGHT	
without cargo and fuel	335,000 lbs
without carge, fully fueled	635,500 lbs
normal weight, cargo and fuel	635,850 lbs
maximum gross weight	769,000 lbs
DIMENSIONS	
wing span	223 feet
length	248 feet
stabilizer height	65 feet
stabilizer span	69 feet
FUEL CAPACITY	49,000 gallons = 318,500 lbs
PERFORMANCE	
take off speed at 712,500 lbs	160 mph
landing speed at 400,000 lbs	131 mph

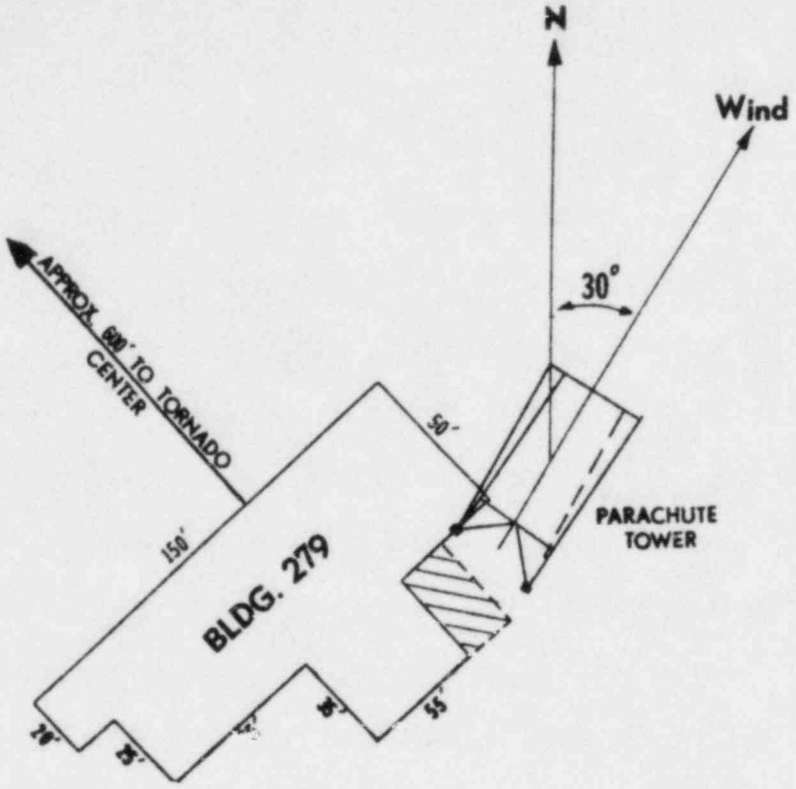

FIGURE 20. PLAN VIEW OF THE PARACHUTE TOWER AT BUILDING 279.

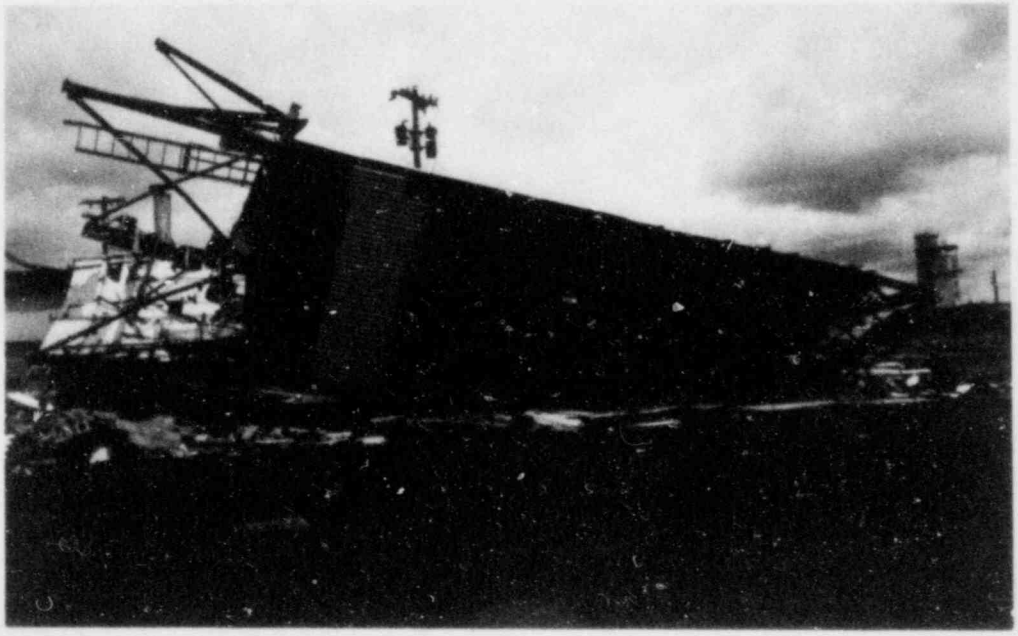

FIGURE 21. OVERTURNED PARACHUTE DRYING TOWER (failure initiated when anchor bolts in two of the corner columns failed in tension).

WIND SPEED CALCULATIONS

The maximum intensity of the damage at Altus Air Force Base, based on appearance of damage (F-scale) was rated F3. Later, Marshall (1983) calculated wind speeds based on structural analysis of damaged structural components. Construction plans were obtained for the Parachute Drying Tower, Dining Hall, Recreation Building and Communications Building. From these plans, Marshall calculated expected wind speeds to produce the observed damage and confidence limits using load and resistance statistics. A comparison of wind speeds estimated from F-scale descriptions and wind speeds based on structural analysis is shown in Table 4. Results from the Communication Building are not included in Table 4 because the exact spacing of the wire ties that anchor the roof slab to the joists is unknown.

The failure modes for the structural analyses were primarily due to connection and anchorage failures. The Parachute Tower overturned when anchor bolts in two of the corner columns failed in tension. Roof failure at the Dining Hall and Recreation buildings occurred when the wood joists, which were toenailed to the plate at the top of the wall, uplifted. Uncertainties in the pullout strength of toenailed connections are reflected in the rather wide confidence bands.

In the case of the Parachute Tower, structural calculations predict an expected value that is 25 percent greater than the mean F1 wind speed value. In the case of the Dining Hall and Recreation buildings the wind speed based on the structural calculations are less than the mean F-scale

TABLE 4

SUMMARY OF WIND SPEED ESTIMATES IN THE ALTUS TORNADO
(after Marshall, et al. 1983)

Building	Failure Origin	Distance from Tornado Center
Parachute Drying Tower	Anchor Bolt Connection	650 ft to right
Dining Hall	Toenailed Roof Connection	100 ft to left
Recreation Building	Toenailed Roof Connection	100 ft to left

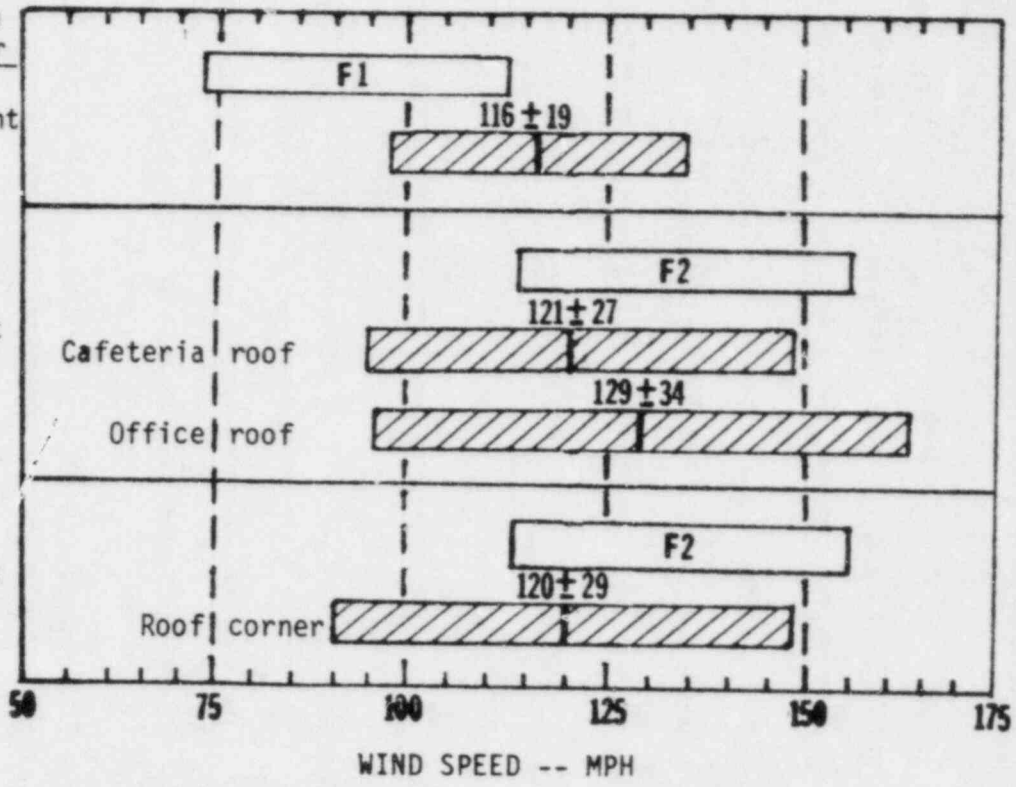

*Three second gust with 95% confidence limits

wind speeds by, at most, 13 percent. Thus, in these cases the differences in calculated wind speeds and wind speeds based on F-scale ratings is not significant. Other cases, expecially at higher wind speeds may show more significant differences.

Based on a combination of F-scale ratings and strucutral calculations, it appears that wind speeds in the Altus tornado were less than 150 mph.

CONCLUSIONS

The following conclusions were made from assessing damage at Altus Air Force Base:

1. Based on both appearance of damage and structural calculations, estimated wind speeds probably did not exceed 150 mph at roof height.

2. Engineered structures performed well in the tornadic winds.

3. The Parachute Tower provided an ideal case for making wind speed calculations since it was a clean, free-standing structure.

4. Correlation between wind speeds estimated from assignment of an F-scale rating and structural calculations did not agree, but the differences are not large.

REFERENCES

Fujita, T.T., 1971: "Proposed Characterization of Tornadoes and Hurricanes by Area and Intensity," SMRP Research Report 91, University of Chicago, 15 p.

Marshall, T.P., J.R. McDonald and K.C. Mehta, 1983: "Utilization of Load and Resistance Statistics in a Wind Speed Assessment," Institute for Disaster Research, Texas Tech University, Lubbock, Texas, 91 p.

National Oceanic and Atmospheric Administration (NOAA), 1981: Storm Data, May 1982.

THE UTILIZATION OF LOAD AND RESISTANCE STATISTICS IN A WIND SPEED ASSESSMENT

by

Timothy P. Marshall
James R. McDonald, P.E.
Kishor C. Mehta, P.E.

INSTITUTE FOR DISASTER RESEARCH
Texas Tech University
Lubbock, Texas 79409

May 1983

FOREWORD

The Institute for Disaster Research has promoted the concept of tornado wind speed estimates from analysis of damage to structures for many years. Up to this point, these wind speed estimates have been based on nominal values of material strengths and fluid dynamic parameters such as pressure coefficients. The validity of wind speed estimates was judged by a qualitative method. The study reported herein is a first attempt to use the concept of Load and Resistance Factor Design (LRFD) to quantify the uncertainties in the wind speed estimates. The methodology is applied to selected buildings that were damaged by a tornado that hit Altus Air Force Base, Altus, Oklahoma on May 11, 1982.

The report is essentially a reproduction of the thesis submitted by Timothy P. Marshall in partial fulfillment of the requirements for the degree of Master of Science in Civil Engineering.

Financial support for this study was furnished in part by the U.S. Nuclear Regulatory Commission (Contract Nos. NRC-04-76-345 and NRC-04-82-002). Robert F. Abbey, Jr. is contract monitor for the Nuclear Regulatory Commission.

TABLE OF CONTENTS

LIST OF TABLES

LIST OF FIGURES

CHAPTER I
INTRODUCTION

1.1 Background

A significant natural disaster in terms of a wind event provides an opportunity for engineers and meteorologists to conduct a damage survey and assess the performance of structures in the path of the storm. The knowledge gained in estimating wind speeds responsible for causing the damage can be used to better design structures to resist the wind.

Before 1950, few studies appeared in the literature on wind speed estimates derived from damaged structures. Most notably, the Dallas tornado in 1957 provided the first significant opportunity to study the damage caused to many structures with different types of construction. Segner (1960) presented wind speed estimates from an engineering analysis of the damaged structures. More recently, wind speed estimates have been derived from engineering analyses of damage caused by the Lubbock tornado (Minor et al., 1971) and the Xenia, Ohio tornado (Mehta et al., 1974). In all the above cases, a wind speed was calculated based on average characteristics of the structure.

A problem arises in that several variables may be responsible for deviations from the calculated wind speed. Material strength properties, construction practices, orientation of the structure and pressure coefficients are a few of the variables which are subject to uncertainties. These variables may, in turn, lead to an overestimate or underestimate of the calculated wind speed to cause the damage. In order to quantify the degree of error in a wind speed estimate, statistical properties of the load and resistance behavior of the structure must be known.

Within the past several years, a new concept has emerged in the design of engineered structures which enables engineers to account for the variations in the strength and types of loading on structures. The concept is termed Load and Resistance Factor Design (LRFD). LRFD treats the load and resistance properties of structures in terms of continuous probability distributions. In contrast, nominal strengths or loads are discrete values.

1.2 Purpose

The purpose of this study is to utilize recently published load and resistance data in conjunction with statistical methods to place a degree of confidence in a calculated wind speed.

1.3 Outline

The theory of variability applicable to load and resistance equations is discussed in Chapter II. Structural resistance statistics are presented in Chapter III along with a brief discussion of the major uncertainties. Chapter IV contains wind load statistics. The methodology for handling highly fluctuating pressure coefficients in a turbulent wind flow is addressed. Examples are presented in Chapter V which illustrate the use of load and resistance statistics to establish a degree of confidence in the calculated wind speed. Conclusions are presented in Chapter VI.

CHAPTER II
THE CONCEPT OF VARIABILITY

2.1 Factor of Safety

Engineers have long recognized the inherent uncertainties in applied loads and structural resistance. As a result, they have developed code specified design criteria which allow for a safety factor between the nominal strength of the material and the nominally applied loads. This safety factor can be expressed as

$$SF = \frac{R_n}{L_n} \tag{2.1}$$

where R_n is the nominal code-specified resistance and L_n is the nominally applied load. The safety factor is greater than one and is a deterministic value which describes the safety of the structure. However, structural resistance and applied loads are random variables which truly represent continuous probability distributions (Figure 1). Here, $\overline{L}$ and $\overline{R}$ describe the central tendency or mean value of the applied load and structural resistance, respectively. Areas under each curve represent the probability of safety whereas the area under the intersecting curves represents the probability of failure. The probability of safety, as shown by Ghiocel et al.(1975), can be represented by

$$P_s = P(L \leq R) = P(R \geq L) = \int_o^\infty F_L(x) f_R(x)\, dx \tag{2.2}$$

where P represents probability, $F_L(x)$ is the cumulative distribution function for the applied load and $f_R(x)$ is the probability density function of the structural resistance. Similarly, the probability of failure can be represented by

$$P_f = P(R \leq L) = P(L \geq R) = \int_o^\infty F_R(x) f_L(x)\, dx \tag{2.3}$$

Failure implies partial or total collapse of the structure.

Since structural resistance and applied loads are continuous prob-

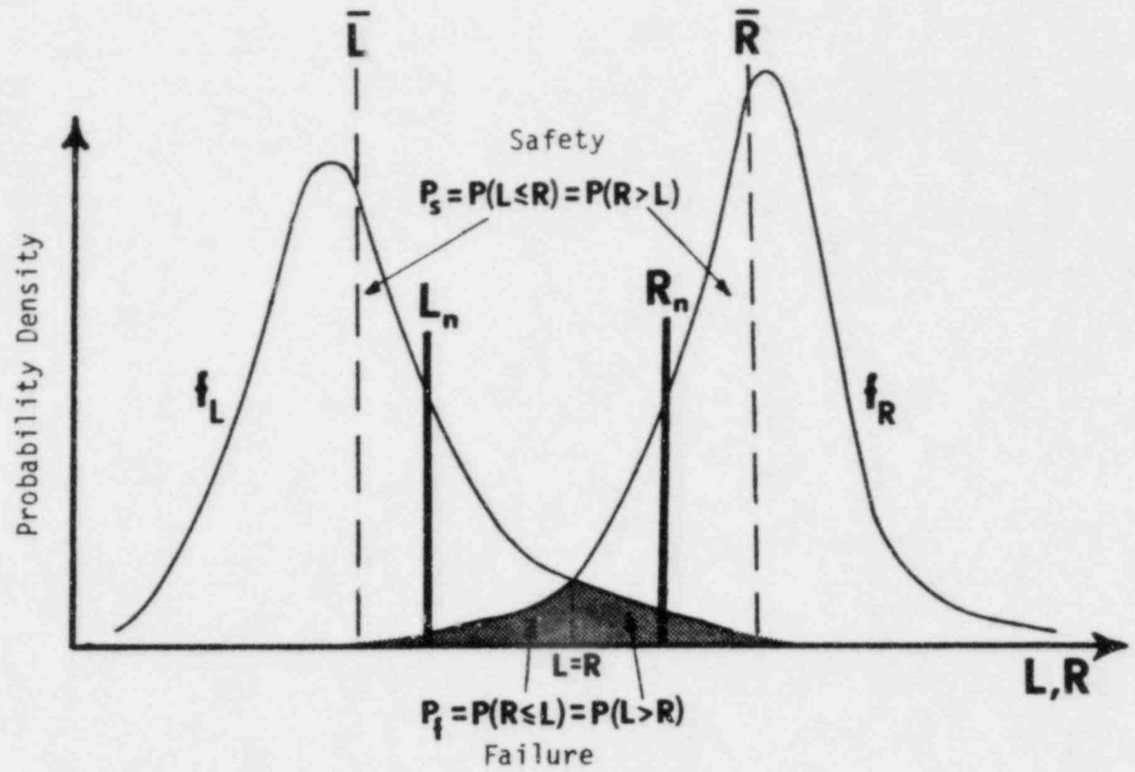

Figure 1 A typical Load and Resistance probability distribution. The shaded region indicates the probability of failure.

ability distributions, the safety factor is non-deterministic and depends on the degree of confidence chosen. For Normal probability distributions, a conventional factor of safety can be described as

$$SF_c = \frac{\bar{R} - K\sigma_R}{\bar{L} + K\sigma_L} \qquad (2.4)$$

where K represents the chosen number of standard deviations from the mean and σ_R and σ_L represent the standard deviations of the structural resistance and the applied load respectively.

2.2 Load and Resistance Equations

Ellingwood et al. (1980) recognized that the randomness in the resistance of a structural element arises from uncertainties in the material properties, fabrication, and underlying design assumptions of member strength. They expressed the structural resistance as a function of these three variables

$$R = R_n M F P \qquad (2.5)$$

where R_n is the nominal code-specified resistance and the terms M, F, and P represent ratios of actual values to nominal code-specified values.

The random variable M represents the variation in the material strength of the member and can be obtained by dividing the actual static strength by the code-specified strength. The random variable F represents the uncertainties in the fabrication of the member. This term is the ratio of the actual geometric properties of the member divided by the code-specified geometric properties. In the case of hot-rolled steel beams, variations in geometric properties are introduced by the rolling process, welding tolerances and initial distortions of the member. The random variable P represents the uncertainties between the idealized design assumption and the actual behavior of the member. These uncertainties arise as the result of using non-exact equations which contain assumptions such as perfectly elastic, homogeneous and isotropic properties. This term can also include the uncertainties in the sample size and the assumed statistical distribution.

The expression for computing the wind pressure can be written as

$$q = c\ GC_p\ V^2 \tag{2.6}$$

where q is the wind pressure in pounds per square foot (psf), c is the air density term, usually 0.00256, G is the gust response factor, C_p is the pressure coefficient and V is the wind speed in miles per hour. The values for the pressure coefficient and gust response factor can be obtained from ANSI A58.1 (1982).

Let the total wind load, L, be represented by the product q•A where A is the area over which the wind pressure is acting. Then, the wind speed needed to cause failure can be calculated by setting the structural resisting moment equal to the wind load moment. Therefore, at failure

$$R \cdot d \leq L \cdot e \tag{2.7a}$$

where d and e represent respective moment arms. Substituting Equations (2.5) and (2.6),

$$R_n MFPd \leq cAGC_p V^2 e \tag{2.7b}$$

It is important to recognize that the terms on the left hand side of Equation (2.7b) are a function of the resistance of the structure, and the terms on the right side are the function of the wind load. Solving for the failure wind speed

$$V^2 = \frac{R_n MFPd}{cAGC_p e} \tag{2.7c}$$

In order to establish confidence limits on the failure wind speed, the uncertainties in the terms on the right side of Equation (2.7c) must be known.

2.3 Binary Operations

The coefficient of variation or degree of uncertainty of a random variable X with mean μ_X and standard deviation σ_X is defined as

$$V_x = \frac{\sigma_x}{\mu_x} \tag{2.8}$$

which is simply the ratio of the standard deviation divided by the mean. The magnitude represents the degree of dispersion from the mean.

When combining two or more probability distributions, the resultant coefficient of variation can be determined by using the equations of binary operations. Haugen (1968) summarizes the binary operations for means which can be used for combining independent random variables (Table 1). For our purposes, it is most convenient to express the standard deviation in terms of the coefficient of variation. From Table 1, the standard deviation for the product of two distributions is

$$\sigma_{xy} = \sqrt{\mu_x^2\sigma_y^2 + \mu_y^2\sigma_x^2 + \sigma_x^2\sigma_y^2} \tag{2.9}$$

Square both sides and divide by $\mu_x^2\mu_y^2$.

$$\frac{\sigma_{xy}^2}{\mu_x^2\mu_y^2} = \frac{\mu_x^2\sigma_y^2}{\mu_x^2\mu_y^2} + \frac{\mu_y^2\sigma_x^2}{\mu_x^2\mu_y^2} + \frac{\sigma_x^2\sigma_y^2}{\mu_x^2\mu_y^2} \tag{2.10}$$

Simplify and using Equation (2.8),

$$V_{xy}^2 = V_x^2 + V_y^2 + V_x^2V_y^2 \tag{2.11}$$

For small V_x and V_y (below about 0.2), $V_x^2V_y^2 \ll V_x^2 + V_y^2$, thus

$$V_{xy}^2 \approx V_x^2 + V_y^2 \tag{2.12}$$

For multivariate quantities, this can be expressed as

$$V_t^2 = \sum_{i=1}^{n} V_i^2 \quad \text{or} \quad V_t = \sqrt{\sum_{i=1}^{n} V_i^2} \tag{2.13}$$

Next, consider the standard deviation for the quotient of two independent random variables. We can find an expression for the combined

TABLE 1

SUMMARY OF BINARY OPERATIONS FOR COMBINING TWO NORMAL PROBABILITY DISTRIBUTIONS

(after Haugen, 1968)

Addition	$\mu_{x+y} = \mu_x + \mu_y$ $\sigma_{x+y} = \sqrt{\sigma_x^2 + \sigma_y^2}$
Subtraction	$\mu_{x-y} = \mu_x - \mu_y$ $\sigma_{x-y} = \sqrt{\sigma_x^2 + \sigma_y^2}$
Multiplication	$\mu_{xy} = \mu_x \mu_y$ $\sigma_{xy} = \sqrt{\mu_x^2 \sigma_y^2 + \mu_y^2 \sigma_x^2 + \sigma_x^2 \sigma_y^2}$
Division	$\mu_{x/y} = \mu_x / \mu_y$ $\sigma_{x/y} = \frac{1}{\mu_y} \left[\frac{\mu_x^2 \sigma_y^2 + \mu_y^2 \sigma_x^2}{\mu_y^2 + \sigma_y^2} \right]^{1/2}$
Second order	$\mu_z = \mu_x^2$ $\sigma_z = \sigma_x^2 = \sqrt{4\mu_x^2 \sigma_x^2 + 2\sigma_x^4}$

coefficient of variation. From Table 1,

$$\sigma_{x/y}^2 = \frac{1}{\mu_y^2}\left[\frac{\mu_x^2\sigma_y^2 + \mu_y^2\sigma_x^2}{\mu_y^2 + \sigma_y^2}\right] \tag{2.14}$$

Substitute $\sigma_y^2 = \mu_y^2 V_y^2$.

$$\sigma_{x/y}^2 = \frac{1}{\mu_y^2}\left[\frac{\mu_x^2\mu_y^2 V_y^2 + \mu_y^2\sigma_x^2}{\mu_y^2(1 + V_y^2)}\right] \tag{2.15}$$

Substitute $\sigma_x^2 = \mu_x^2 V_x^2$ and simplify.

$$\sigma_{x/y}^2 = \frac{1}{\mu_y^2}\left[\frac{\mu_x^2 V_y^2 + \mu_x^2 V_x^2}{1 + V_y^2}\right] \tag{2.16}$$

Let $\mu_{x/y}^2 = \mu_x^2/\mu_y^2$ and $V_{x/y}^2 = \sigma_{x/y}^2/\mu_{x/y}^2$ thus,

$$V_{x/y}^2 = \frac{V_y^2 + V_x^2}{1 + V_y^2} \tag{2.17}$$

For small V_y,

$$V_{x/y}^2 \approx V_x^2 + V_y^2 \tag{2.18}$$

For multivariate quantities,

$$V_t^2 = \sum_{i=1}^{n} V_i^2 \quad \text{or} \quad V_t = \sqrt{\sum_{i=1}^{n} V_i^2} \tag{2.19}$$

It is interesting to note that the coefficient of variation for combined Normal independent distributions is the same whether the distributions are multiplied or divided. The binary operations for products and quotients now can be used to express the coefficient of variation of the failure wind speed as a function of the coefficient of variation of the load and resistance terms.

Recalling Equation (2.5) resistance of a structural member was shown to be

$$R = R_n\ M\ F\ P \tag{2.5}$$

Using Equation (2.13), the coefficient of variation of the resistance can be expressed as

$$V_r = \sqrt{V_m^2 + V_f^2 + V_p^2} \tag{2.20}$$

where the subscripts r, m, f, and p denote the coefficient of variation of structural resistance, material, fabrication, and professional terms respectively.

The coefficient of variation of the calculated wind speed in the wind load equation is more difficult to compute because of the presence of the second order speed term. Recalling Equation (2.7c),

$$V^2 = \frac{R_n MFPd}{cAGC_p e} \tag{2.7c}$$

We must first consider the presence of the second order wind speed term by using the second order binary operation equation in Table 1. Let us define a first order variable Z in terms of the wind speed with mean $\mu_z = \mu_w^2$, standard deviation $\sigma_z = \sigma_w^2$ and coefficient of variation $V_z = V_w^2$. From Table 1,

$$\sigma_z = \sqrt{4\mu_w^2\sigma_w^2 + 2\sigma_w^4} \tag{2.21}$$

where μ_w is the calculated wind speed, σ_w the standard deviation of the wind speed and σ_z is the standard deviation of the square of the wind speed.

Substituting $\sigma_w = \mu_w V_w$, the standard deviation is

$$\begin{aligned} \sigma_z &= \sqrt{4\mu_w^4 V_w^2 + 2\mu_w^4 V_w^4} \\ &= \mu_w^2 \sqrt{4V_w^2 + 2V_w^4} \end{aligned} \tag{2.22}$$

Now $\mu_w^2 = \mu_z$ and assume the coefficient of variation of the fourth order term is small enough to be insignificant. Thus,

$$V_z = 2 V_w \tag{2.23}$$

It is now possible to determine the coefficient of variation of the calculated wind speed in terms of the variables on the right side of Equation (2.7c). If we take the variation in the geometry of the structure to be small such that there is little discrepancy between construction plan dimensions and the actual dimensions of the structure, then the uncertainties in d, e, and A will be insignificant. Using Equation (2.19), the coefficient of variation of the calculated wind speed can be expressed as

$$V_z = 2V_w = \sqrt{V_c^2 + V_{GC_p}^2 + V_m^2 + V_f^2 + V_p^2} \tag{2.24}$$

Substituting Equation (2.20) and solving for V_w then

$$V_w = \tfrac{1}{2} \sqrt{V_c^2 + V_{GC_p}^2 + V_r^2} \tag{2.25}$$

This equation expresses the coefficient of variation of the wind speed as one half the sum of the square of the coefficient of variation of the air density term, gust response factor, pressure coefficient, and structural resistance terms.

2.4 Confidence Levels

A desired degree of confidence can be made on the calculated wind speed if its coefficient of variation is known. Ghiocel et al. (1975) have shown that, for a Normal distribution, the upper and lower bounds of the calculated wind speed can be expressed as

$$WS = V (1 \pm KV_w) \tag{2.26}$$

where K represents the numbers of standard deviations from the mean which are selected. The values of K for a Normal distribution are as

follows:

K	% Confidence
1	68.3
2	95.5
3	99.7

Probability distributions other than Normal can be approximated by the Normal distribution by employing the Central Limit Theorem (Ellingwood et al., 1980). The Central Limit Theorem states that, for a random sample from any probability distribution with finite mean and standard deviation, the sampling distribution approaches Normal as the sample size becomes large.

CHAPTER III
STRUCTURAL RESISTANCE STATISTICS

Equation (2.5) shows that the resistance of a structural member is dependent upon the nominal strength of the material multiplied by ratios which represent the mean material, fabrication, and professional terms. The next step is to quantify these terms for materials used in construction. A summary of strength data for steel, concrete, masonry, timber, and glass was assembled from various sources in the literature and is presented in this chapter.

3.1 Steel

Structural steel is widely used in engineered, pre-engineered, and marginally engineered buildings (Mehta et al., 1981). Wind effects on such structures have been extensively investigated by R. Minor et al. (1971) and J. Minor et al. (1979). From their investigations of damage to steel structures, they have concluded that the collapse of all or part of the structure usually results from an initial localized failure of a component or cladding. Resulting openings allow wind to enter the building and exert additional outward wind pressures on the building interior which can lead to progressive collapse of other components. The most common types of damage initiation are loss of sheet metal roofing or siding, buckling of purlins or girts, buckling of end frames and failure of overhead door systems. Failure mechanisms of the entire steel frame resulted from yielding of primary steel members or connection failures. In order to obtain wind speed estimates, strength statistics of steel sections and connections must be known.

3.1.1 Steel Sections

The strength of steel is dependent upon the chemical composition of the alloys and on the methods of manufacture and testing. Implementation of strict quality control standards in the steel mill insure a small variability in the material strength of the final product. For this reason, Ellingwood et al. (1980) suggested coefficients of variation of 0.10 and 0.05 for the material and fabrication terms respectively

for steel resistance.

Factors which influence the strength of steel are listed in Table 2. Of primary importance is the rate and duration of load. Strength data in the literature are usually expressed in terms of the static yield stress. The static yield stress is defined by Galambos et al. (1978) as the value of ultimate stress after straining is stopped when the stress-strain curve reaches a plastic plateau. They state that this adjustment is made since mill tests are performed at higher strain rates than normally experienced in a structure. In addition, they mention that mill test samples are taken directly from the web coupon and do not reflect the weighted contribution of the flange stress. Therefore, the average mill strength for A36 steel is reduced about 10 percent from 44 ksi to 40 ksi. In this study, 40 ksi will be used as the mean strength of A36 steel.

In the literature reviewed, the strength of steel closely fits a log-normal distribution since strict quality control practices "weed out" members of lower than specified strength. Thus, the log-normal probability distribution is used herein to describe steel strength.

3.1.2 Bending Resistance

Steel beams can fail by lateral-torsional buckling, local buckling of the compression flange, or web buckling. Lateral-torsional buckling is the most common failure under compressive loading (van Kuren et al., 1964). Failure may occur with the initiation of buckling over some portion of the beam when the cross section is either in the elastic, inelastic, or plastic range. Yura et al. (1978) determined the variability of bending resistance for steel beams in all three ranges. Values of 0.12, 0.14, and 0.13 were obtained for the coefficient of variation of steel resistance for the elastic, inelastic, and plastic ranges respectively. These values are different because of the influence of residual stresses on the yield strength (V_p varies from 0.05 to 0.11). Residual stresses affect the stress-strain relationship by reaching the proportional limit sooner and causing a non-linear relationship between the elastic and fully plastic region. Therefore, the largest residual

TABLE 2

FACTORS WHICH AFFECT THE STRENGTH OF STEEL

I. Material considerations
   a) Carbon content
   b) Residual stresses

II. Fabrication
   a) Size and shape of the member

III. Testing procedures
   a) Rate and duration of load

stresses and coefficient of variation in strength occurs in the inelastic region. A summary of the resistance statistics for steel as assembled by Ellingwood et al. (1980) is shown in Table 3. Cold formed members have a higher variability in strength because of the large residual stresses which are incurred in the rolling process.

3.1.3 Steel Connections

In general, connections are stronger than the components being joined. However, unanticipated uplift pressures on pre-engineered and marginally engineered structures have caused failures in roof connections and column anchorages (Minor et al., 1972). Roof connections include attachment of open web joists or purlins to beams or walls and beam-to-column connections. Column anchorages involve anchor bolts and column-base plate details. In some instances, optimization in the competitive metal building industry has led to a smaller margin of safety between components and connections. In these cases, a connection failure is more likely to lead to a progressive failure of other building components or to total collapse of the structure.

Fillet welds are primarily used for joining structural members. The strength of fillet welds subjected to shear have been tested by Fisher et al. (1978). Statistical results show that the mean tensile stress of the weld is dependent on the size of the electrode used. Fisher et al. determined that the overall coefficient of variation in strength for all size fillet welds is 18 percent. They concluded that there are no uncertainties present in the professional factor since the lower bound theorem of plasticity is valid for ductile members in tension ($V_p = 0$). Fisher et al. state that uncertainties in the fabrication of the weld are highly dependent on the quality of workmanship. They determined that the variation of weld length and throat thickness from the actual design is 15 percent ($V_f = 0.15$). Therefore, the uncertainty in fabrication has the greatest effect on weld strength.

Bolted connections are becoming more common because they are economical and easy to install. Primary members are usually attached by high strength bolts. Fisher et al. (1978) assembled statistical information on the strength of A325 and A490 bolts. Variations in the

TABLE 3

SUMMARY OF RESISTANCE STATISTICS FOR STEEL
(after Ellingwood et al., 1980)

Mean material strength	
Static yield stress, web	1.1 F_y
Tensile stength of steel	1.1 F_u
Tensile strength of welds	1.05 F_{EXX}
Tensile strength of A325 bolts	1.2 F_u
Tensile strength of A490 bolts	1.07 F_u

Coefficient of variation	V_r
A490 bolts, tension	.05
A325 bolts, tension	.09
Tension member	.11
Elastic beam, LTB	.12
Plastic Beam, LTB	.13
Inelastic beam, LTB	.14
Cold formed steel	.17
Fillet welds	.18

F_y: Specified yield stress

F_u: Specified tensile strength

F_{EXX}: Specified tensile strength of weld

LTB: Lateral-torsional buckling

strength of bolts are low because of the use of high quality material and good quality control practices in fabrication. The overall coefficient of variation in strength of A325 and A490 bolts was found to be 0.09 and 0.05 respectively assuming V_m = 0.07 and 0.02, respectively, V_f =0.05 and V_p = 0.

3.2 Concrete

The strength of concrete is much more variable than steel because of the nonhomogeneous mix. There are five different types of cements and varous sizes and types of aggregates used in manufacturing concrete.

The most common type of concrete used in construction is made with Type 1 portland cement, stone-type aggregate and has a unit weight of about 150 pounds per cubic foot. It can be cast-in-place or pre-cast, prestressed or post-tensioned. Cast-in-place concrete involves pouring fresh concrete into a form to obtain a desired shape. Pre-cast concrete is poured into forms in a plant after applying a tensile force to the pre-stressing strands. The finished product is then shipped to the job site. Post-tensioned concrete has the tension applied to the steel tendons after the concrete has cured.

Factors which influence the strength of concrete are listed in Table 4. Most sources in the literature agree that the quality of workmanship and water-cement ratio are the primary factors which govern the strength of concrete. Studies by Mirza et al. (1979) on the statistical nature of concrete strength showed that variations in the quality of workmanship can affect concrete strength by 20 percent. The lowest variability in strength attributed to workmanship was pre-cast concrete whereas the highest was cast-in-place. Also, variations in the water-cement ratio can affect concrete strength by more than 50 percent. Good quality control practices are very important in regulating how much water should be added to the mix. Mirza et al. mention that the amount of water necessary for good workability is always more than needed for hydration.

Another important question is whether the variability in strength of concrete within a structure under field conditions is actually the same as the strength of concrete in test cylinders under laboratory

TABLE 4

FACTORS WHICH AFFECT THE STRENGTH OF CONCRETE

I. Concrete mix
   a) Water/cement ratio
   b) Moisture content of aggregate
   c) Grade and shape of aggregate
   d) Air content in the cement
   e) Admixtures
   f) Type of portland cement
   g) Retempering
   h) Volume of concrete poured

II. Testing procedures
   a) Age-time strength change
   b) Curing conditions- humidity
   c) Temperature
   d) Rate and duration of load
   e) Size of test specimens- cube,cylinder,core

III. Quality of workmanship
   a) Proportioning
   b) Mixing
   c) Transporting
   d) Placement

controlled conditions. Ellingwood et al. (1980) assembled strength data on concrete cylinders and determined an empirical expression which relates the coefficient of variation of cylinder strength tests to actual in situ concrete. The expression

$$V_{concrete} = \left[V^2_{cylinder} + .0084 \right]^{1/2} \qquad (3.1)$$

approximates the coefficient of variation of in situ concrete under the conditions of a slow loading rate, twenty-eight day strength, and average workmanship. The results of Ellingwood's work are summarized in Table 5. For reinforced concrete, it appears that $V_f = 0.05$, $V_p = 0.05$, such that V_r ranges from .08 to .14 depending on the type of reinforcing steel used.

3.1 Masonry

The failure of a masonry wall from lateral wind forces can result when the bond between the mortar and the masonry unit is broken (Sahlin, 1971). The bond failure of the mortar joint is a tensile failure which occurs in the weakest portion of the wall. As a result, the failures of unreinforced masonry walls have been documented at relatively low wind speeds (Minor et al., 1977).

The strength of masonry under wind loading is governed by three primary factors: a) the tensile bond strength of the mortar, b) the strength properties of the masonry unit and, c) the quality of workmanship used in assembling the masonry structure. Table 6 lists the primary and secondary factors which can affect the strength of masonry under a lateral load. These factors are assembled from various sources in the literature. Test results on the effect of primary factors on masonry strength have recently appeared in the literature.

3.3.1 Tensile Bond Strength

The tensile bond strength of mortar depends on the amount of cement in the mix. There are four basic types of mortar used in masonry construction which are classified according to their cement content. These are Types M, S, N, and O in order of decreasing amounts of

TABLE 5

SUMMARY OF RESISTANCE STATISTICS FOR CONCRETE
(after Ellingwood *et al.*, 1980)

Concrete in flexure	V_r
Reinforced	.14
Pretensioned	.08
Postensioned	.10

TABLE 6

FACTORS WHICH AFFECT THE STRENGTH OF MASONRY WALLS

I. Tensile bond strength of mortar
   a) Proportions of the mix, water-cement ratio
   b) Type of mortar
   c) Thickness of mortar joint
   d) Elapsed time mortar is exposed to air
   e) Water retentivity
   f) Retempering
   g) Air content in the mortar
   h) Curing conditions- humidity

II. Strength properties of masonry units
   a) Size of the unit, hollow or solid
   b) Type of aggregate used
   c) Height of the masonry wall
   d) Previous loading history
   e) Water absorption rate- suction
   f) Surface texture
   g) Pattern of the wall
   h) Age of the wall-weathering
   i) Testing procedures- 3 point or uniform load

III. Quality of workmanship
   a) Inspected or uninspected
   b) Initial pressure applied to the mortar joint
   c) Amount of tapping on unit after placement

cement content. Types N and S are most common for above grade use in masonry construction. Hedstrom (1961) published test results on the strength of laterally loaded masonry on full-size walls. From his results, the average strength of Types N and S mortars appears to be 20 and 30 psi, respectively.

3.3.2 Strength Properties of Masonry

Hundreds of masonry strength tests have been conducted during the last fifty years. However, most of the test results are not consistent because of the large variations in testing procedures used. O'Conner (1967) indicated that variations in masonry strength can be as much as 100 percent depending on which test method is used. He states that, for a laterally loaded wall, the three point load method is typically used. Test results from his experiments on masonry walls show that the modulus of rupture for the three point load method averaged 22.9 psi, whereas the modulus of rupture for the applied uniform load averaged 45.6 psi.

Variations in masonry strength also depend on the size of the test specimens. Full-size masonry wall tests are rare because of large material costs and small number of tests which can be conducted. Most of the strength tests surveyed in the literature use a small-size test specimen such as a brick couplet or wallette. This enables a large number of tests to be conducted. However, the question remains whether or not the results of the strength tests actually simulate the strength of full-size masonry walls.

Large variabilities in masonry strength have occurred in brick couplet and wallette-size tests. Neis and Chow (1980) showed coefficients of variation between 22 and 62 percent for concrete block couplets. In addition, Hendry (1976) showed coefficients of variation between 32 and 44 percent for brick wallettes. Ellingwood (1981b) mentions that these values may be the result of the smaller test specimens being more susceptible to variation in workmanship. Therefore, he assembled masonry strength data only for full-size walls with good workmanship. A summary of the resistance statistics which he determined is presented

in Table 7. The coefficient of variation in fabrication, V_f ranges from 0.1 to 0.15 depending on the quality of workmanship. V_m was determined to be 0.14 for brick masonry and 0.15 for concrete block masonry and V_p =0.05.

Hendry (1976) tested the effects of the quality of workmanship and environmental conditions on the strength of masonry. He concluded that the strength of masonry can decrease as much as 60 percent from good workmanship under laboratory controlled conditions to poor workmanship in field conditions.

3.4 Wood

For structural purposes, wood is cut into nominal sizes called dimension lumber or is assembled as glulam lumber. Dimension lumber is primarily used for light-frame construction. Glulam lumber is made by bonding layers of dimension lumber together with an adhesive so that the grain directions of all laminations are essentially parallel. The final product is stronger than the individual pieces of lumber and the variability in strength is lower since the bonded layers act as a unit.

Though there are many advantages in using wood, there are also several disadvantages such as its variability in strength. Wood is an anisotropic material because of its cellular structure. Thus, the strength of wood varies along the radial, tangential, and longitudinal directions. The longitudinal direction is the strongest since the tensile stress is parallel to the grain. Other factors which influence the strength of wood are listed in Table 8. The amount of influence that each factor has on the overall strength of wood has yet to be quantified since few test results have appeared in the literature.

Ellingwood (1981c) assembled the most current information on the strength of wood and these data are summarized in Table 9. These data represent variations in the modulus of rupture of Douglas fir and southern pine for both glulam and dimension lumber. Statistical tests performed by Ellingwood show no significance, at the 95 percent confidence level, between the variabilities in the modulus of rupture for various species of trees. V_m ranges from 0.09 to 0.18 for glulam

TABLE 7

SUMMARY OF RESISTANCE STATISTICS FOR MASONRY
(after Ellingwood, 1981b)

Mean strength of mortar	
Type N	20 psi
Type S	30 psi
Variability in strength of full-size masonry walls	V_r
Inspected brick	.18
Uninspected brick	.21
Inspected concrete block	.19
Uninspected concrete block	.21

TABLE 8

FACTORS WHICH AFFECT THE STRENGTH OF WOOD

Material Considerations

a) Direction of the grain

b) Position of growth rings- age

c) Moisture content

d) Specific gravity

e) Size and distribution of imperfections such as knots, cross grain, shakes and checks

f) Rate and duration of load

g) Air or kiln dried

h) Cut dimension

TABLE 9

SUMMARY OF RESISTANCE STATISTICS FOR WOOD
(after Ellingwood, 1981c)

	V_r
Glulam Lumber (all species)	
Compression	.14
Bending	.18
Tension	.21
Dimension Lumber (all species)	
Compression	.24
Bending	.39
Tension	.45

lumber and from 0.22 to 0.44 for dimension lumber depending on the type of load. In addition, an eight percent variation in loading rate and a seven percent variation in the size of the lumber is included.

3.4.1 Nailed Connections

Nails are commonly used in light frame and residential construction. Two types of connections are primarily used: straight and toenailed. Toenailing is the process of driving a nail at an angle into a joint; e.g., wood roof joists are usually toenailed to the top of a wall. Two or more nails are typically used in a given connection.

Wind induced failures of roof and wall sections are usually the result of connection failures. As the wind flows over a structure, local outward acting pressures develop over the roof, eave, or corner. These forces are transferred to the connections and, under a strong wind, the connections can fail in tension. In the case of a nailed connection, the nails can be pulled out.

Information on the strength of nailed connections was not readily available in the literature. Therefore, the author conducted four series of tension tests on various nailed connections. Each series of tests included 30 nailed specimens. The specimens consisted of a pair of 8d or 16d nails which were driven straight or toenailed joining two 2 x 4 sections of white pine lumber. Then each connection was pulled apart using a Riehle testing machine and the ultimate strength was recorded. The test results appear in Appendix I and are summarized in Table 10. It is interesting to note that the coefficient of variation in strength of toenailed connections decreases with increasing nail sizes but remains essentially the same for straight nailed connections.

3.5 Window Glass

The resistance of window glass to lateral wind loads is an important problem since the utilization of window glass on building facades has increased dramatically over the past decade. Use of large-size panes as well as taller structures have led engineers to become more concerned with the effects of wind on glass.

TABLE 10

SUMMARY OF RESISTANCE STATISTICS FOR NAILED CONNECTIONS

Type of Connection	Mean strength (lbs.)	V_r
2-8d toenailed	206	.36
2-16d toenailed	298	.23
2-8d straight	69	.36
2-16d straight	235	.38

The failure of window glass in windstorms allows the wind to enter the building which can result in further structural damage by contributing to additional internal wind pressures. For example, if a windward pane fails, additional outward pressures would be caused on the roof, side walls, and leeward wall (See Minor et al., 1977). Breach of containment of the building can also lead to damage of the contents. Documentation of window glass failures in windstorms by Minor (1974) has led to the recognition of two damaging mechanisms: wind pressure and small missile impact. The resistance of window glass to these loads is a function of glass strength and type.

3.5.1 Types of Window Glass

There are two categories of manufactured glass: annealed and heat treated. Annealed glass is typically used in non-engineered structures. Heat treated glass is annealed glass which has been reheated to a temperature near its softening point and then cooled rapidly. This process induces additional compressive stresses on the surface of the glass which need to be overcome when laterally loaded. Thus, heat treated glass is more resistant to wind pressure effects and small missile impact. Engineered buildings such as schools and hospitals usually contain heat treated glass in doors and windows.

3.5.2 Window Glass Strength

The strength of window glass is a highly variable quantity which depends on material considerations, workmanship, and environmental factors (Table 11). Tests on individual glass panes indicate that the primary factor affecting strength is the surface conditions of the glass and rate of loading (Stanworth, 1950). Quantification of the variability in strength due to the quality of workmanship and environmental factors still needs further research.

Studies on window glass failures have been performed by Abiassi (1981), who studied lateral pressure on weathered window glass, and by Minor (1974), who studied missile impact on new window glass. From these data, an average coefficient of variation in strength for laterally loaded weathered window glass is 0.25 and for missile impact on

TABLE 11

FACTORS WHICH AFFECT THE STRENGTH OF WINDOW GLASS

I. Material Considerations
   a) Type of glass- annealed or heat treated
   b) Type of load- pressure or missile
   c) Duration of load
   d) Number and size of surface flaws
   e) Plate geometry- aspect ratio
   f) Edge conditions
   g) History of loading

II. Quality of Workmanship
   a) Manufacturing method
   b) Testing procedures
   c) Degree of handling and shipping

III. Environment
   a) Temperature changes
   b) Humidity changes
   c) Age- degree of weathering , cleaning

glass is 0.22. Actual values of glass strength information can be readily obtained from the manufacturer.

A comparison of test data from Minor (1978) between the resistance of tempered glass to annealed glass shows that the coefficient of variation is nearly the same, though tempered glass appears more resistant to missile impact. In contrast, the coefficient of variation in strength is primarily dependent on the type of window glass for wind pressure. Values of the coefficient of variation used by Robertson (1967) are 0.25 for heat strengthened and 0.15 for fully tempered glass. These values are also consistant with the test results by Minor (1981) and Abiassi (1981).

A summary of strength statistics for glass is presented in Table 12. Variations in the fabrication between glass industries are assumed to be small. Thus, the term $V_f = 0$ in the resistance equation is reasonable. Also, uncertainties in design assumptions are taken to be zero ($V_p = 0$). Therefore, the variability in material strength is assumed to represent the overall resistance of the glass. In all the above references, the strength of glass closely fits a Normal distribution.

TABLE 12

SUMMARY OF RESISTANCE STATISTICS FOR WINDOW GLASS

Load	Type of Glass	V_r
Wind pressure	Annealed	.25
	Heat Strengthened	.20
	Fully Tempered	.15
Missile impact	All types	.22

CHAPTER IV
WIND LOAD STATISTICS

4.1 Wind Load Variables

Now that structural resistance statistics have been quantified, the next step is to determine the statistics of wind load variables in order to compute wind speeds. These wind load parameters involve the terms in Equation (2.6) which include air density, gust response factor, and the pressure coefficient. Uncertainties of each term are examined for use in obtaining confidence levels in the wind speed calculations.

4.1.1 The Air Density Term

The mean value of the air density term is tabulated in ANSI-A58.1 (1982) for a given altitude. Air density is dependent on the air pressure and temperature through the equation of state for an ideal gas. The degree of uncertainty in this term is relatively small since changes in air pressure and temperature remain small during the time a structure is under a wind load. A typical value for the coefficient of variation in the air density term is five percent (Ellingwood et al., 1980). Uncertainty in the density term can also be realized under a tornadic wind load where variations in air density occur.

4.1.2 Pressure Coefficients

There are three basic types of pressure coefficients used in wind speed calculations: net, internal, and external. Net pressure coefficients are used for structures such as chimneys or towers, internal pressure coefficients are used on the walls and roofs of buildings with openings, and external pressure coefficients are used on the exterior portions of enclosed buildings.

The gust response factor accounts for the fluctuating nature of the wind and its interaction with the building interface. For building components and cladding, the gust response factor is combined with the external pressure coefficient (ANSI-A58.1, 1982).

The mean and coefficient of variation of the pressure coefficient

are highly dependent on the variables which influence the wind flow. Since the wind speed fluctuates greatly with time, so does the pressure coefficient. Therefore, several issues must be addressed when using pressure coefficients to compute wind speeds.

First, let us define the types of variables which influence the pressure coefficient. Wind tunnel studies on low-rise buildings conducted by Davenport (1977) show that pressure coefficients are highly dependent on the degree of turbulence in the wind flow, the orientation of the building, the tributary area and model parameters such as scale, height, length, and roof slope.

Stathopoulos (1980,1981) showed that the most important factor influencing peak pressure coefficients is the degree of turbulence in the wind flow. In his study on flat roof, low-rise buildings, he determined the values of local pressure coefficients in open country and built-up terrain. The types of terrain correspond to exposures C and B respectively in ANSI-A58.1 (1982). From his results, mean local pressure coefficients increased about 30 percent over the entire roof from exposure C to exposure B. Regardless of the exposure, the largest negative pressures occurred near the windward edge of the roof and decreased toward the interior of the roof. The most severe upward pressures were encountered on the roof when the wind flow was 45 degrees to the windward wall. The coefficient of variation of the local pressure coefficients ranged from 0.1 to 0.4 for interior roof sections and from 0.3 to 0.7 for eave sections in exposures C and B respectively. The variability in the pressure coefficient was a maximum near the windward edge of the roof-wall interface and gradually decreased downstream. It is important to recognize that these test results are point pressures and that the peak pressures effecting a tributary area of the roof or walls are less.

Ravindra et al. (1978) suggest that the mean wind pressure be increased by 25 percent to account for the non-uniform nature of the wind. This, in turn, would increase the wind speed by about 12 percent. Crowe (1974) suggested that pressure coefficients can be twice as much as values in the 1982 ANSI-A58.1 standard if the wind flow is turbulent and

approaches the building from an oblique angle. This conclusion is primarily based on experience with wind tunnel modeling.

Secondly, questions arise as to whether the wind tunnel pressure coefficients really simulate actual ambient pressure coefficients on a full scale structure. The introduction of a turbulent boundary layer has made vast improvements in pressure coefficient data as compared to previous uniform, stead-flow conditions (Davenport et al., 1977). Modern boundary layer flow simulations in the wind tunnel have indeed led to satisfactory agreements with full scale measurements (Stathopoulos, 1981).

The third question is whether a static wind load assumption is reasonable for tornadic wind fields. Previous wind speed calculations on structures in tornadic winds have used a static wind load approach (Mehta et al., 1976; Minor et al., 1977). The contribution of the acceleration of the wind to wind loading has been justified to be small since most wind speed calculations involve structural components in rigid or semi-rigid structures with relatively high natural frequencies.

Lastly, the type of probability distribution of pressure coefficients must be determined. Stathopoulos (1980) has researched the probability distribution of local pressure coefficients on low-rise structures. He states that the Normal distribution for local negative pressures is skewed toward the negative side and can be more accurately modeled by a Weibull distribution. He adds that, as the tributary area increases, the negative pressures are distributed more normally, as a consequence of the Central Limit Theorem.

In summary, it appears that the mean and coefficient of variation of the wind pressure are highly dependent on the degree of turbulence and tend to distribute normally for area loads.

4.1.3 Pressure Coefficient Reduction

In ANSI-A58.1 (1982), the external pressure coefficients for loads on building components and cladding, GC_p, are peak values based on a fastest mile wind speed for smooth terrain (exposure C). From evidence presented in the previous section, the direct use of these values would be inappropriate for a turbulent tornadic wind field since the average

values of pressure coefficients tend to increase with increasing turbulence. Therefore, the external pressure coefficients given in the ANSI standard need to be modified. In this study, a mean pressure coefficient describing a turbulent environment for a three second gust is selected to simulate a tornadic wind field.

First, the standard value of GC_p is converted from a fastest mile value to an equivalent mean hourly value.

$$\text{Mean Hourly } GC_p = 1.69\ GC_p \text{ (fastest mile)} \qquad (4.1)$$

Next, the mean hourly value is converted to a three second gust value using a graph developed by Durst (1960). If the three second external pressure coefficient is denoted as GC_{p3}, then

$$GC_{p3} = 0.44 \times \text{Mean Hourly } GC_p \qquad (4.2)$$

Substituting into Equation (4.1), the relation between a three second external pressure coefficient and an equivalent fastest mile value is

$$GC_{p3} = 0.74\ GC_p \text{ (fastest mile)} \qquad (4.3)$$

Stathopoulos (1981) demonstrated that a peak pressure coefficient exceeds the mean value by two or three standard deviations. He also stated that a mean pressure coefficient for smooth wind flow increases two or three standard deviations in a turbulent wind flow. Thus, it is reasonable that a mean pressure coefficient in a turbulent wind flow adequately describes a peak pressure coefficient in a smooth wind flow; therefore, the above conversion need not be modified further. A summary of GC_{p3} values for roof and wall sections is contained in Figure 2. It is important to emphasize that the external pressure coefficients for the main wind force resisting system are uneffected by this conversion since they are basically time invariant. This is true because the load is distributed over a large area.

From the information presented in the last section, it is apparent that the coefficient of variation also depends upon the degree of

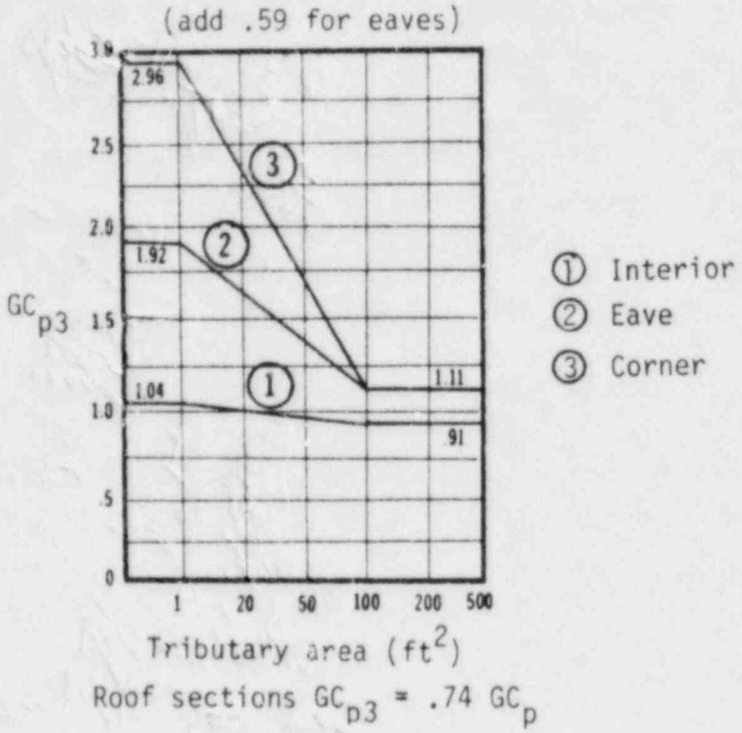

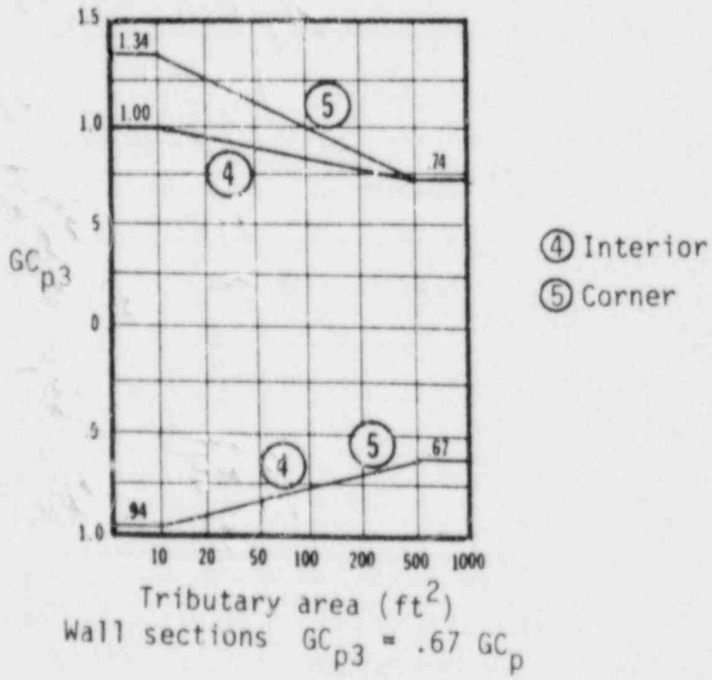

Figure 2 Mean GC_{p3} values for flat roof and wall sections.

turbulence in the wind flow, the tributary area, and the location on the structure. At present, values of the coefficient of variation have not been fully quantified. Idealized values have been assembled by Ellingwood (1981a) based on experience with wind tunnel data. A summary of the statistical properties of wind load variables is presented in Table 13. In the absence of additional research, these values will be used herein for wind speed calculations.

4.2 Summary of Load and Resistance Statistics

The statistical properties of structural resistance and wind load variables are now quantified. Utilizing this information, wind speed estimates can be obtained from a damaged structure. It is desirable to organize all the statistical information on a single page for use in wind speed computation. Table 14 lists the coefficient of variation for structural resistance and wind load variables. This information has been put into three categories which denote credence levels in a wind speed assessment.

Credence levels were developed by Mehta (1976) as a first attempt to categorize the uncertainties inherent in wind speed calculations. Categories entitled good, acceptable, and questionable reflect the degree of confidence in the wind speed calculation. Since statistical data are now available, coefficients of variation were assembled into each credence level according to their magnitude. Construction materials in the good credence level category are most reliable for wind speed calculations. These consist of steel and precast concrete products which have coefficients of variation in resistance less than 0.13. Under wind loading, these materials will yield wind speed estimates with small confidence bands. Most construction materials have coefficients of variation in resistance between 0.14 and 0.21 and appear in the acceptable credence level category. These materials consist of glulam timber, masonry, cast-in-place concrete, and heat treated window glass. Finally, wide confidence bands in wind speed calculations will occur for construction materials in the questionable credence level. These materials consist of annealed glass, dimension timber, and all types of nailed connections.

TABLE 13

SUMMARY OF WIND LOAD VARIABLE STATISTICS

Mean

External pressure coefficients for a three second gust for:

Components and cladding	$GC_{p3} = .74\ GC_p$	(ANSI-1982)
Main resisting system	$C_{p3} = C_p$	(ANSI-1982)

Coefficient of variation

Components and cladding	$V_{GC_p} = .17$
Main resisting system	$V_{C_p} = .12$
Gust response factor	$V_G = .11$
Exposure coefficient	$V_{K_z} = .16$
Density term	$V_c = .05$

TABLE 14

CREDENCE LEVELS FOR WIND SPEED CALCULATIONS
BASED ON VARIABILITY

Designation	GOOD			ACCEPTABLE			QUESTIONABLE		
	Variable	V_r	PD	Variable	V_r	PD	Variable	V_r	PD
Strength of Materials	A490 bolts,T	.05	LN	Reinforced concrete,F	.14	N	All glass-missiles	.22	N
	Concrete,pretensioned,T	.08	N	Steel beam,inelastic,LTB	.14	LN	Annealed glass	.25	N
	A325 bolts,T	.09	LN	Glulam Timber,			Dimension Timber,		
	Concrete,postensioned,T	.10	N	-Compression	.14	W	-Compression	.25	W
	Hot rolled steel,T	.11	LN	-Bending	.18	W	-Bending	.40	W
	Steel beams,elastic,LTB	.12	LN	-Tension	.21	W	-Tension	.46	W
	Steel beams,plastic,LTB	.13	LN	Cold formed steel,F	.17	LN	Nailed connections,T		
				Fillet welds,T	.18	LN	-16d toenailed	.23	N
				Brick masonry	.21	LN	-10d toenailed	.30	N
				-If inspected	.19	LN	-8d toenailed	.36	N
				Concrete masonry	.21	LN	-8-16d straight	.36	N
				-If inspected	.18	LN			
				Fully tempered glass	.15	N			
				Heat strengthened glass	.20	N			
AMSI,1982 coefficents and other pressure coefficents	Density constant,	.05	N	Gust response factor	.11	N	Local pressure coefficents for low-rise buildings		
	Net pressure coefficent	.05	N	External/Internal pressure coefficent	.12	N	-smooth terrain	.30	N
				Velocity Pressure exposure coefficent	.16	N	-rough terrian	.70	N
				External pressure coef. for components and cladding	.17	N	for high-rise buildings		
							-smooth terrain	.20	N
							-rough terrain	.50	N

Definition of variables

V_r = coefficent of variation
T^r = tension members
F = fexural members
LTB= lateral torsional buckling

PD = probability distribution
N = normal
LN = log-normal
W = weibull

Variability formulas

$$V_r = \sqrt{V_m^2 + V_p^2 + V_f^2}$$

$$V_{wind} = \tfrac{1}{2}\sqrt{V_r^2 + V_{C_p}^2 + V_c^2}$$

Credence levels for pressure coefficients primarily depend on the size of the tributary area. Wind speed calculations based on the external pressure coefficient for the main wind resisting system would be acceptable since fluctuations in the pressure coefficient are averaged over an area. However, wind speed calculations based on point pressures would be questionable because of highly fluctuating peak pressures.

The statistical properties given in Table 14 also can be used to determine the smallest confidence band in wind speed as a function of the mean wind speed and the type of construction material. Table 15 describes the limits in accuracy in wind speed calculations for selected materials with 95 percent confidence. An example using A490 bolts with a mean calculated wind speed of 100 mph is included to show how these values were obtained.

From Equation (2.25), the variability of the wind speed is

$$V_W = \tfrac{1}{2} \sqrt{V_r^2 + V_{GC_p}^2 + V_C^2}$$

Using the values of coefficient of variation from Table 14, the coefficient of variation of the wind speed becomes

$$V_W = \tfrac{1}{2} \sqrt{(.05)^2 + (.12)^2 + (.05)^2} = .14$$

From Equation (2.26), confidence limits can be obtained on the wind speed. Choosing a 95 percent confidence, K=2,

$$WS = 100\ (1 \pm 2\ V_W)$$
$$= 100 \pm 14 \text{ mph}$$

This table can be used as an initial lower bound estimate of wind speed confidence in lieu of more detailed calculations.

4.3 Load and Resistance Wind Speed Compared to F-Scale

The F-scale is the most frequently used method for assessing the intensity of damage to structures (Fujita, 1971). F-scale ratings are

TABLE 15

LIMITS IN ACCURACY IN WIND SPEED

FOR VARIOUS MATERIALS*

Type of material	Maximum Wind Speed 100 mph	150 mph	200 mph	250 mph
Steel-				
A490 bolts	± 14	± 21	± [illegible]	± 35
A325 bolts	± 16	± 24	± 32	± 40
A36 steel,tension	± 17	± 26	± 34	± 43
A36 steel,flexure	± 18	± 28	± 37	± 46
Fillet welds	± 22	± 33	± 44	± 55
Concrete-				
Reinforced	± 19	± 29	± 38	± 48
Masonry-Brick or block				
Uninspected	± 25	± 37	± 49	± 62
Inspected	± 22	± 33	± 44	± 55
Timber-				
Glulam,flexure	± 22	± 33	± 44	± 55
Dimension,flexure	± 41	± 62	± 82	± 103

* 95% confidence for main-wind force resisting systems

assigned to a structure according to one of six damage intensity classifications ranging from F-0 to F-5 with increasing amounts of damage. The F-scale is a subjective, visual interpretation of the damage. The methodology is easy to use and readily accepted by the National Weather Service and others in the scientific community. However, since knowledge of the load and resistance properties of structures and types of construction practices used are not considered, shortcomings arise in using the F-scale (Table 16).

The first shortcoming which is important to recognize is that wind speeds associated with the F-scale have been determined without regard to the load and resistance behavior of structures. Variations in the strength of materials and degree of engineering attention determine the resistance of structures to wind loading. Mehta et al. (1981) have shown that the degree of engineering attention during the design stage of structures has a marked effect on overall wind resistance. From their investigation of damage caused by Hurricane Frederic, fully engineered structures performed better than marginally engineered or non-engineered structures at the same wind speed.

Secondly, the F-scale assumes each building is homogeneously constructed when, actually, vast differences in construction practices occur from rural to city locations and across the country. Minor et al. (1977) state that these differences are attributable to variations in traditional methods of construction and differences among building codes.

Finally, the type of damage analysis conducted will effect the F-scale rating. As an example, different F-scale ratings can be assigned to a structure depending on whether a ground or aerial damage survey was conducted. If a residence is not anchored to its foundation, it has little resistance to lateral wind forces. A ground survey of the damage may indicate the lack of anchoraging and a low F-scale rating will be assigned. On the other hand, an aerial survey of the same structure may lead to an excessive F-scale rating since the lack of anchoring may not be recognized from aerial photographs. In addition, aerial surveys can lead to overrated tornadoes simply by considering a single "poorly" constructed structure in the tornado path. This can occur since the F-scale methodology rates the overall tornado intensity

TABLE 16

FACTORS WHICH CAN INFLUENCE THE F-SCALE RATING

Load and Resistance properties

Type of construction material used
Degree of engineering attention

Construction practices

Traditional methods used
Building code used
Extent and type of anchoraging to foundation used
Orientation of eaves and/or garage door
Type of roof geometry
Extent and type of roof-wall connections

Damage analysis

Type of survey- ground, aerial or both
Documentation of missiles
Effect of shielding by trees, other buildings, etc.

by the worst damage at a point in the tornado path.

Proper knowledge of load and resistance properties, acquisition of construction plans and techniques of damage analysis can be used to better define the failure wind speed of a given structure. If an accurate damage analysis is conducted and the information on the construction plans is accurate, the variation in wind speed will be a function of the variation in load and resistance properties only.

Using Equation (2.5) and the information available in Table 14, wind speed bounds are calculated for selected coefficients of variation of structural resistance. The calculated load and resistance wind speed bounds and the F-scale wind speed bounds are shown in Table 17 for comparative purposes. There are two important points which must be recognized from the tabulated wind speed values in Table 17:

1) A range of overlapping wind speeds occurs for calculated load and resistance wind speeds. This results from the inherent variabilities in structural resistance and wind load variables. Therefore, the damage intensity of a structure may lie in more than one F-scale category. Note that the range of failure wind speeds necessary to cause damage to a structure becomes wider as the calculated wind speed increases.
2) The wind speed bounds become wider as the coefficient of variation of structural resistance becomes larger. The coefficient of variation of structural resistance is also influenced by the degree of engineering attention in the design of the structure. Therefore, the range in failure wind speeds will be larger for residential buildings than for public and more permanent structures.

A sample calculation of the load and resistance wind speed values in Table 17 is shown for $V_r = 0.1$.

From Equation (2.5),

$$V_w = \tfrac{1}{2} \sqrt{V_r^2 + V_{C_p}^2 + V_c^2} \qquad (2.5)$$

TABLE 17

COMPARISON OF F-SCALE WIND SPEED TO
LOAD AND RESISTANCE WIND SPEED

F-scale (after Fujita, 1971)			Load and Resistance Wind Speed *		
F-scale	Wind Speed Range	Mean	V_r = .1	V_r = .2	V_r = .3
0	40-72 mph	56 mph	47-65 mph	43-69 mph	38-74 mph
1	73-112	92	77-107	70-114	62-122
2	113-157	135	113-157	103-167	91-179
3	158-206	182	152-212	139-225	132-232
4	207-260	233	195-271	177-289	157-309
5	261-318	289	242-336	220-358	195-383

*95% confidence limits

$$= \tfrac{1}{2} \sqrt{(0.1)^2 (0.12)^2 + (0.05)^2}$$
$$= 0.082$$

For an F-0 rating, the mean wind speed is 56 mph. Using Equation (2.26) and selecting 95 percent confidence

$$WS = V (1 \pm 2V_w) \qquad (2.26)$$
$$= 56 \pm 9 \text{ mph}$$

Minor et al. (1977) also derived wind speed ranges based on the performance of housing in windstorms. They compared their results with the F-scale wind speeds and concluded that there is good agreement between the two damage versus wind speed relationships at lower wind speeds but, above 125 mph, the F-scale associates much higher wind speeds with the observed damage. They suggest that this difference is attributable, in part, to the variation in housing construction materials and practices. A comparison between the load and resistance wind speed and the wind speed scale for the performance of housing is shown in Table 18. For well constructed residences, the coefficient of variation in structural resistance would most likely be between 0.2 and 0.3. Thus, a calculated wind speed of 150 mph with $V_r = 0.2$ could result in an F-scale rating of F-2, F-3, or F-4.

In this chapter, wind load statistics were presented. This information along with structural resistance statistics can be used to determine the coefficient of variation for a calculated wind speed. Pressure coefficients were modified to account for the increase in turbulence in a tornadic wind field and comparisons of the load and resistance wind speeds to the F-scale and performance of housing wind speeds were shown.

TABLE 18

COMPARISON OF THE PERFORMANCE OF HOUSING WIND SPEED
TO LOAD AND RESISTANCE WIND SPEED

Performance of Housing (after Minor et al., 1977)			Load and Resistance Wind Speed *	
F-scale	Wind Speed Range	Mean	V_r = .2	V_r = .3
0	40-75 mph	57 mph	44-71 mph	38-76 mph
1	75-110	92	70-114	62-122
2	110-140	125	95-155	84-166
3	140-170	155	118-192	104-206
4	170-200	185	141-229	125-245
5	200-240	220	168-272	148-292

*95% confidence limits

CHAPTER V
WIND SPEED CALCULATIONS USING LOAD AND RESISTANCE STATISTICS

Wind speed calculations are presented on four structures which were damaged by a tornado which struck the Altus Air Force Base in Oklahoma on 11 May 1982. Construction plans were obtained for the Parachute Drying Tower, Dining Hall, Recreation Center, and Communications building. From these plans, a mean wind speed and confidence limits are calculated. Lower bound wind speeds were obtained for those sections of the structure which were damaged whereas upper bound wind speeds were obtained from undamaged sections.

5.1 Altus Tornado Damage Path

The tornado first touched down on the east side of the city of Altus and traveled for three miles in a northeastward direction through the Altus Air Force Base. On the following day, a team of windstorm investigators, including the author, was sent to the disaster scene. The purpose of the investigation was to define the tornado damage path and to assess the damage to structures on the base.

Our initial survey revealed that the damage path extended from the main gate, across the center of the base and ended just east of the runway (Figure 3). Gradations of damage were visually determined using the F-scale (Fujita, 1971). Buildings which sustained F-1 intensity damage or greater are shaded. Six buildings were heavily damaged (F-3), eleven had moderate damage (F-2), and seven had light damage (F-1). From analysis of fallen trees and debris trajectories, the center line of the tornado appeared to be parallel to the northern periphery of the F-3 intensity damage track. Characteristics of the damage path are shown in Table 19.

5.2 Parachute Drying Tower Wind Speed Calculation

The parachute drying tower was located on the right side of the tornado path approximately 650 feet from the tornado center (Figure 4).

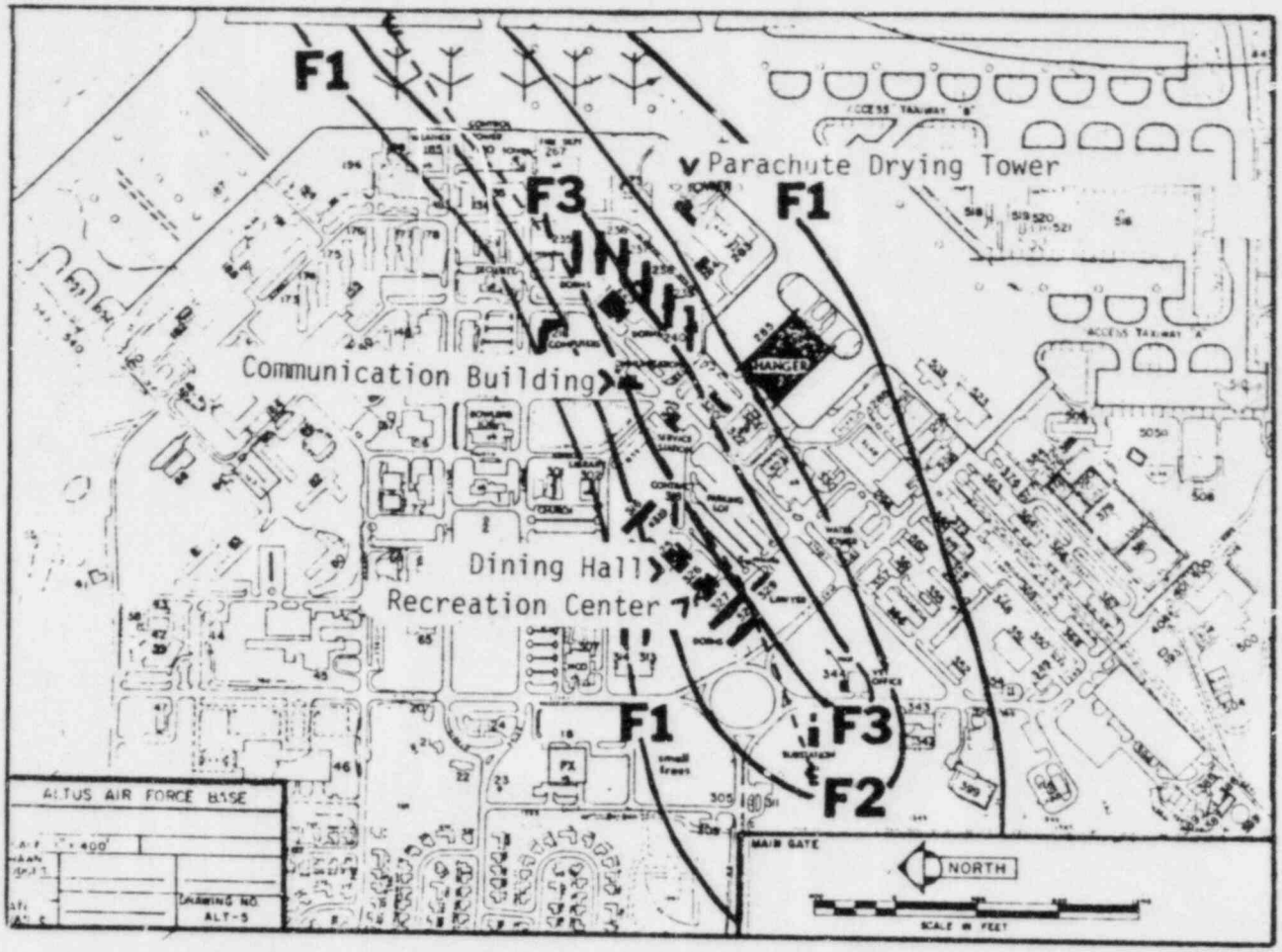

Figure 3 Tornado damage path through the Altus Air Force Base. Gradations of damage is shown by F-scale.

TABLE 19

CHARACTERISTICS OF THE ALTUS TORNADO

Tornado sequence (LDT)	
Observed funnel touchdown	5:48 pm
Tornado entered Air Base	5:51 pm
Tornado over weather station	5:55 pm
Tornado dissipated	6:00 pm
Path length	
Total	3.5 mi.
Damage of F-3 intensity	1.0 mi.
Path width	
Average F-1 intensity	1500 ft.
Average F-2 intensity	900 ft.
Average F-3 intensity	300 ft.
Sense of rotation	counterclockwise
Direction of travel	east-northeast
Average translational speed	5-15 mph
Tornado circulation	single-cell

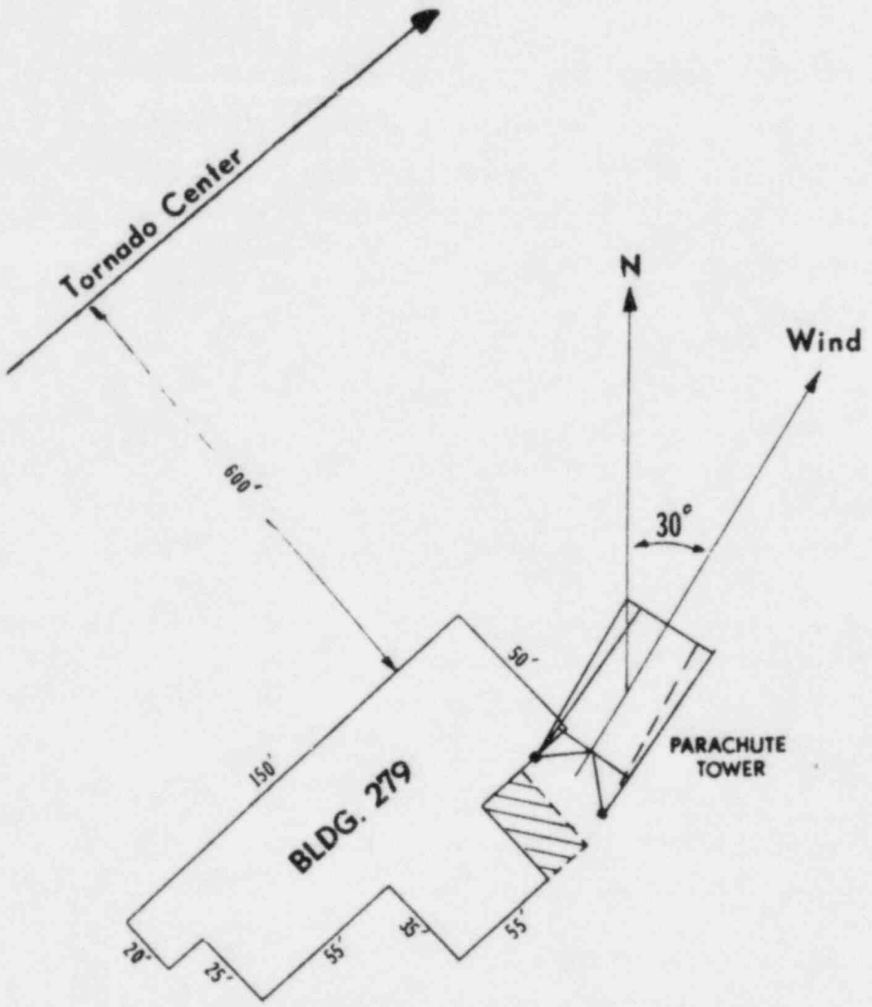

Figure 4 Plan view of the Parachute Drying Tower and Building 279.

Apparently, as the tornado passed, the 62-foot high tower overturned falling toward the northeast, pivoting about a line through the two supporting columns on the leeward side of the structure. It appeared that the longest side of the tower was normal to the strongest tornadic winds. Anchor bolts, which secured the tower to its foundation, failed in tension.

Two sheets of construction drawings were obtained from the Civil Engineering Section of the Air Base which enabled verification of the dimensions and weight of the structure. A wind speed estimate was determined based on information from the plans and using the following conditions and assumptions:

1) The wind pressure was essentially constant over the 62-foot height of the tower.
2) The static wind load acted normal to the longest side.
3) The strength of A307 bolts is distributed normally. This assumption is needed for ease in combining the coefficient of variation with other normally distributed factors.
4) Mean wind pressure calculations are based on the ANSI-A58.1 (1982) standard.
5) Internal pressure had a negligible effect on the overturning of the structure.
6) Pressure coefficients have a coefficient of variation of 12 percent (see Table 14). Values as given in the ANSI-A58.1 (1982) standard are:

Windward wall	$C_p = 0.8$ for all values of L/B
Leeward wall	$C_p = 0.5$ for L/B = 0.54
Roof	$C_p = 0.7$ for θ = zero degrees and H/L = 4

where θ is the roof angle, H is the height, B is the width, and L is the length normal to the wind direction.

7) Total weight of the structure obtained from construction plans was 67,107 lbs.

5.2.1 Overall Wind Loading

1. Mean tensile strength of the bolts: from Ellingwood et al. (1980), the mean tensile strength of bolts is approximated by

$$\overline{F}_u = 1.2\ F_u$$

where F_u is the minimum guaranteed tensile strength of the bolts. For A307 bolts, F_u is 60 ksi. Thus $\overline{F}_u$ = 72 ksi. (AISCM, 1980).

2. Net tensile area of the bolt: from Salmon and Johnson (1980), the proof load of a bolt is obtained by multiplying the stress value by the tensile area given as

$$A_S = .7854 \left(D - \frac{.9743}{n}\right)^2$$

where A_S is the stress area in square inches, D is the nominal diameter of the bolts and n is the number of threads per inch. For 5/8 inch diameter bolts, D = .625 and n = 11. Thus, $A_S = .226$ in^2.

3. Mean resistance of the bolts:

$$\bar{R} = N A_S \bar{F}_u$$

where N is the number of bolts resisting tension, A_S is the tensile area in square inches and $\bar{F}_u$ is the mean tensile strength. For this example, N = 8 so the resistance of the bolts is $\bar{R}$ = 130 kips.

4. Mean resisting moment:

$$\bar{M}_r = \bar{R}\, d + \text{Weight (arm)}$$
$$= 130\ (15.5) + 67.1\ (7.75)$$

where $\bar{R}$ is the mean resistance of all the bolts and d is a moment arm. Thus, $\bar{M}_r$ = 2535 ft kips.

5. Overturning moment produced by the wind load:

$$\bar{M}_u = e\ q\ A\ C_p$$

where e is a moment arm, q is the mean wind pressure, A is the area of the face considered and C_p is the mean pressure coefficient. Summing the overturning moments from Figure 5:

$$\bar{M}_u = [.8\ (49.25 \times 29.2)\ (37.6) + .5\ (62.25 \times 29.2)\ (31.13) +$$
$$.7\ (16.2 \times 29.2)\ (15.51)]\ q$$
$$= 74{,}106\ q \text{ ft lbs or } 74.2\ q \text{ ft kips}$$

6. Equate $\bar{M}_r$ and $\bar{M}_u$ and solve for q:

$$\bar{M}_r = \bar{M}_u$$
$$2535 = 74.2\ q$$
$$q = 34.16 \text{ psf}$$

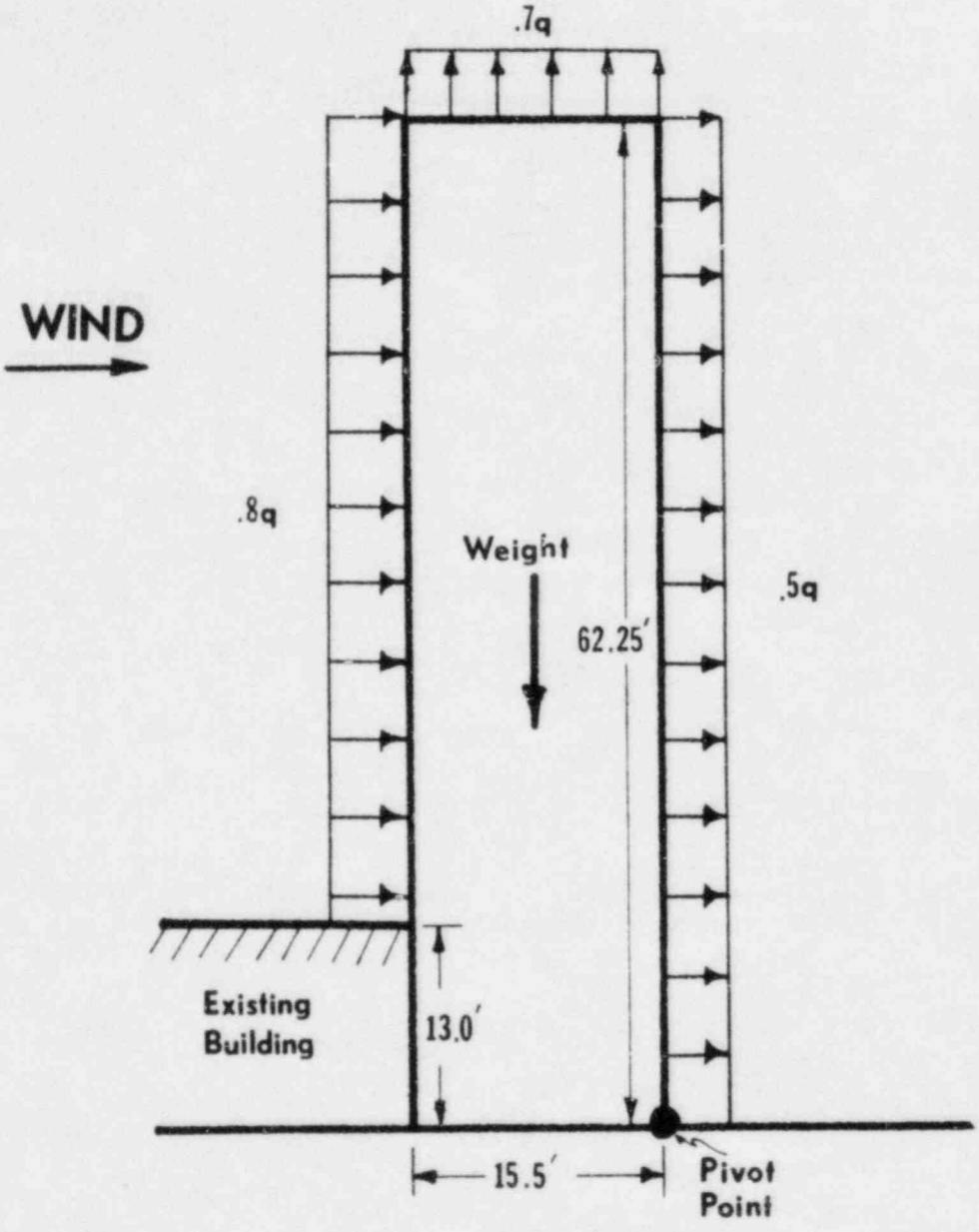

Figure 5 Wind loading on the Parachure Drying Tower at Altus Air Force Base.

7. Determine the combined coefficient of variation of the resisting moment. From Table 14, $V_r = 0.09$ for bolts in tension and the variability in the dead load is 0.1. Thus,

$$\sigma_r = \sqrt{\sum \sigma_i^2} = \sqrt{(2015 \times .9)^2 + (520 \times .1)^2} = 188.6 \text{ lbs.}$$

$$\text{Thus } V_r = \frac{\sigma_r}{\bar{M}_r} = .0744$$

8. Average three second gust:

$$V = \sqrt{\frac{q}{.00256}} \cong 116 \text{ mph}$$

9. Coefficient of variation of the wind speed: from Equation (2.25),

$$V_w = \tfrac{1}{2} \sqrt{V_r^2 + V_{GC_p}^{\ 2} + V_c^2}$$

$$= \tfrac{1}{2} \sqrt{(.0744)^2 + (.12)^2 + (.05)^2} \cong .08$$

10. Establish a degree of confidence in the wind speed calculation. A 95 percent confidence level is chosen, K=2. From Equation (2.26),

$$WS = \bar{V} (1 \pm 2 V_w)$$

$$= 116 \pm 19 \text{ mph}$$

Therefore, with 95 percent confidence, the three second gust necessary to overturn the tower is 116 ± 19 mph. This value appears to be consistent with other damage in the area. Building 279, which is adjacent to the parachute drying tower, remained free of damage including facia and window glass. It is anticipated that wind speeds higher than the calculated value would have led to additional damage to the structure as well.

5.3 Dining Hall Wind Speed Calculation

The dining hall was located to the left of the tornado damage path and was within 200 feet of the tornado center (refer to Figure 3). The

damaging winds came from the northwest; thus, the rear wall of the building was the windward wall. Roof damage was observed along the entire length of the windward wall (Figure 6). The roof consisted of 2 x 10 wooden joists spaced 12 inches on center and were perpendicular to the windward wall. The joists were secured with 10d nails which were toenailed to a wood plate at the top of the windward wall. A cross section of the windward wall is shown in Figure 7. It was anticipated that, as the tornado passed, the nails pulled out as the roof was uplifted. Wind speed calculations were determined for three roof sections of the building in order to obtain upper and lower wind speed bounds. These roof sections are located over the cafeteria, offices, and interior sections.

The following assumptions are made regarding the wind speed calculations:

1) The wind pressure was essentially constant over the height of the structure.
2) The static wind load acted normal to the longest side of the structure.
3) Mean wind pressure calculations are based on the ANSI-A58.1 (1982) standard.
4) Wood joists were toenailed to the top of the wall using 10d nails which have a mean resistance of 250 lbs/pair. The strength of nails in wood is distributed normally.
5) Interior wind pressure effects were negligible because of the lack of openings in the windward wall.
6) The coefficient of variation for mean pressure coefficients is 17 percent (Ellingwood, 1981a).

5.3.1 Cafeteria Roof

1. Tributary area of the cafeteria roof (Figure 8):

Roof area = 20 (36.67) + 9.66 (2) =	752.7 ft^2
Eave area = 22 (2) + (36.67) (2) + 12.33 (2) =	142.0 ft^2
Tributary area =	894.7 ft^2

2. Dead load of the roof and eave sections: unit weights of construction materials were obtained from AISCM (1980).

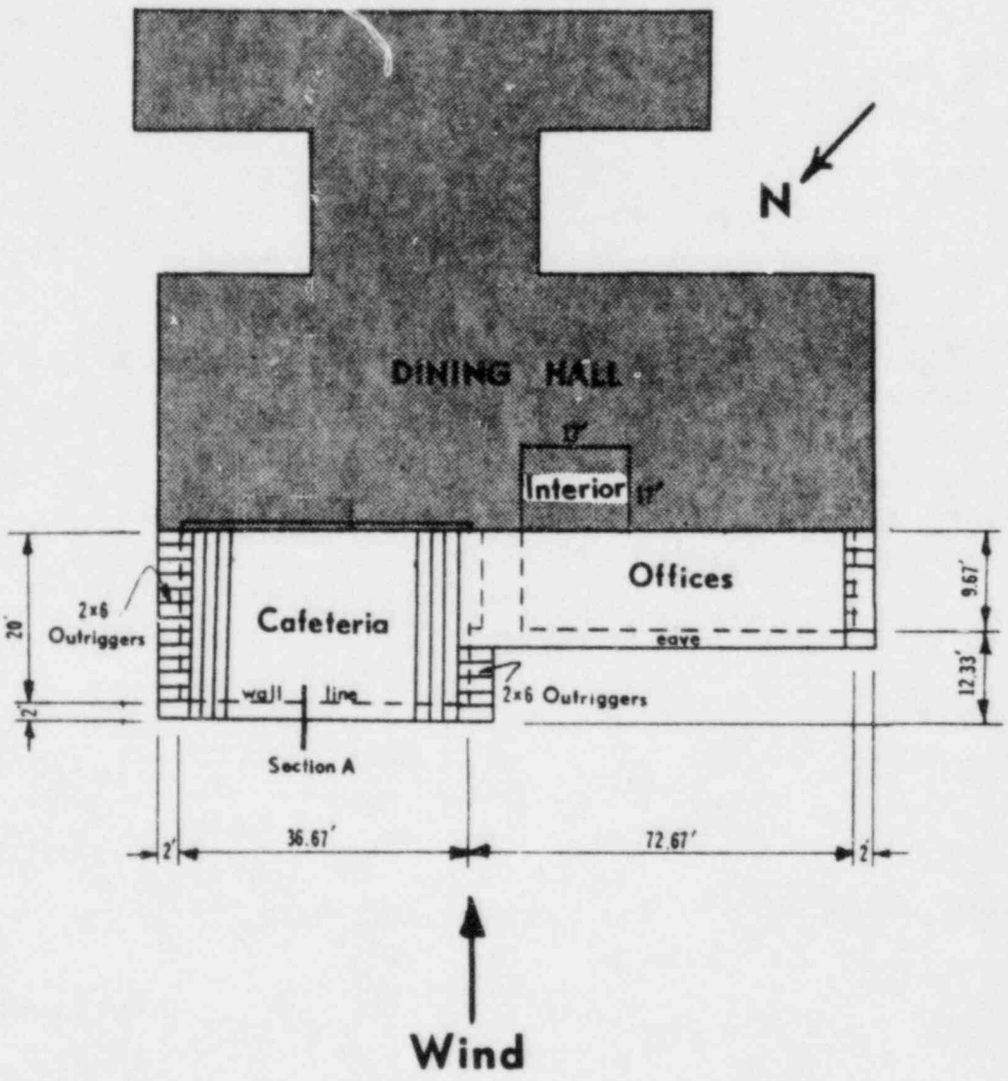

Figure 6 Plan view of Dining Hall showing windward roof damage (unshaded portion).

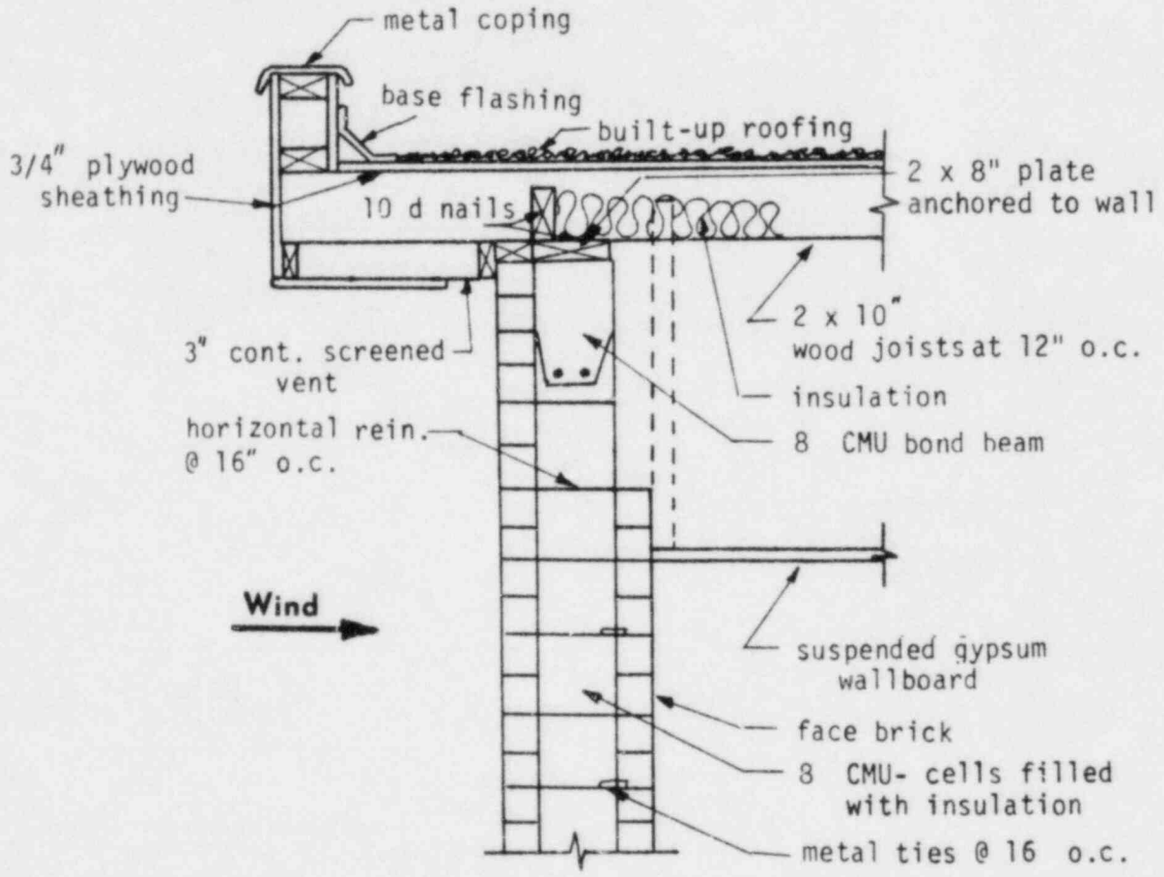

Figure 7 Windward roof-wall detail of the Dining Hall at Section A.

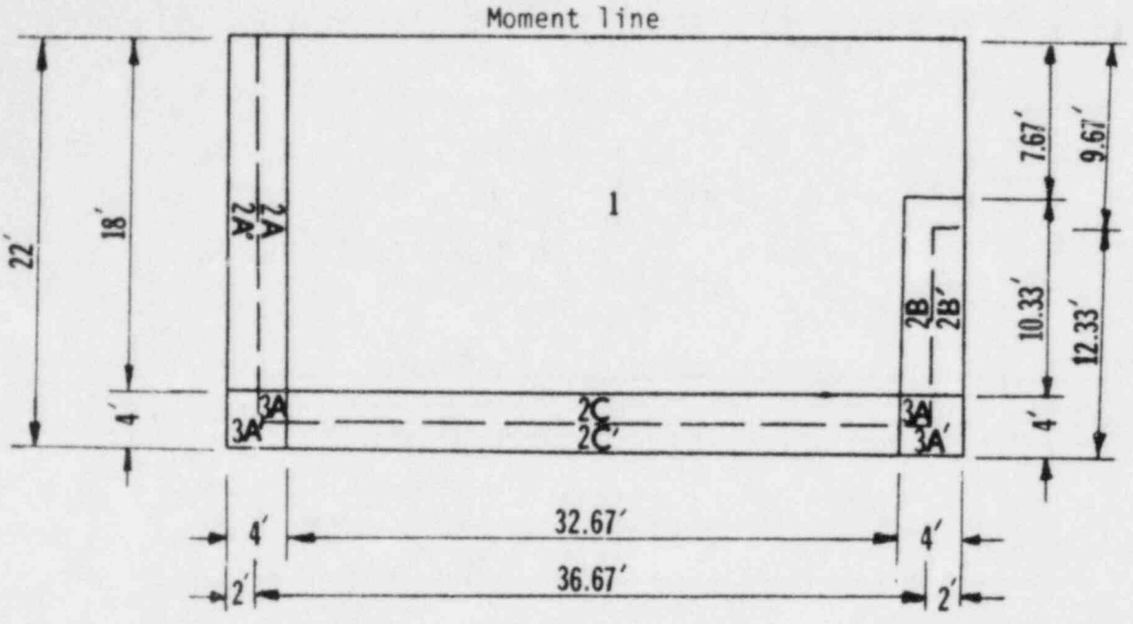

(A)

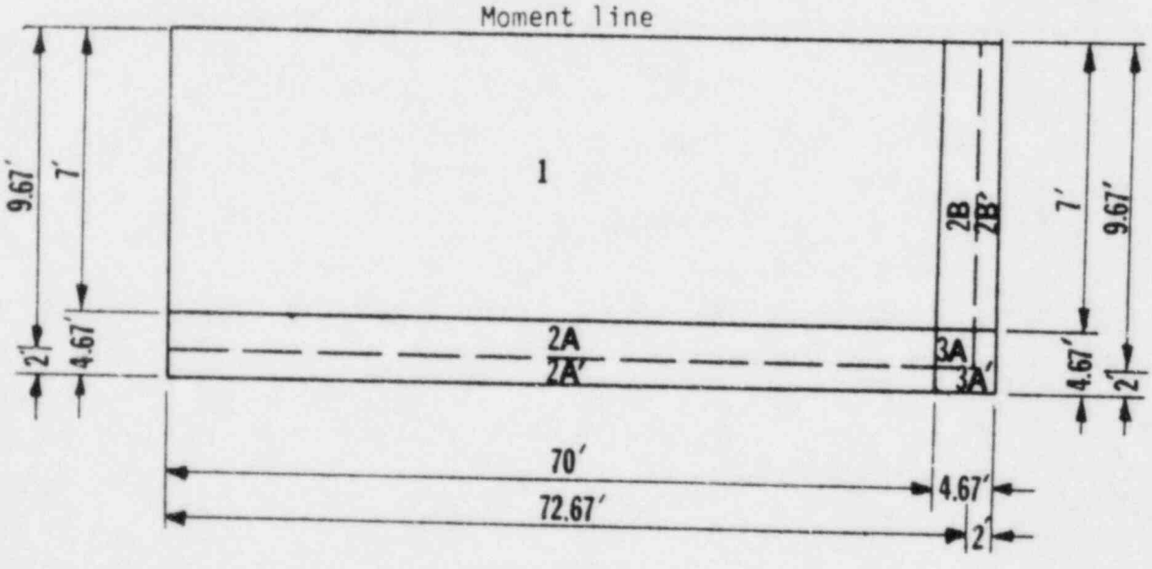

(B)

Figure 8 Plan view of the roof sections of the Dining Hall over a) cafeteria and b) offices as divided into ANSI-A58.1 1982 wind regimes.

Roof section dead load	psf
2 x 10 roof joists @ 12 inches o.c.	4
4 inch insulation	2
3/4 inch plywood sheathing	3
2 x 8 suspended ceiling	3
5 ply felt gravel roof	6
ductwork and electrical	2
gypsum wallboard	2
	22 psf

Eave section dead load without suspended ceiling, wallboard and insulation = 15 psf.

3. Total weight of the roof:

Roof section = 752.7 (22) = 16,560 lbs.
Eave section = 142.0 (15) = 2,130 lbs.

Total weight of roof 18,690 lbs.

4. Resisting moment of the roof due to the combination of roof anchorage and dead load: from Table 14,

Anchorage- 33 - 2 x 10 joists spaced 12 inches o.c. with 10d toenailed connections at 250 lbs each

Resistance = 33 (250) = 8,250 lbs.

15 - 2 x 6 outriggers spaced 16 inches o.c. with 10d toenailed connections at 250 lbs. each

Resistance = 15 (250) = 3,750 lbs.

5 - 6 x 6 outriggers spaced 16 inches o.c. with 10d toenailed connections at 250 lbs. each

Resistance = 5 (250) = 1,250 lbs.

Resisting moment

$\bar{M}_r$ = 18,690 (11) + 8,250 (20) + 3,750 (10) + 1,250 (14.83)

= 426,600 ft lbs.

5. Coefficient of variation of the resisting moment: from Table 14, the variation in strength of nailed connections is 0.3 and dead load is 0.1

$$\sigma_r = \sqrt{\sum_{i=1}^{n} \sigma_i^2}$$

$$\sigma_r = \sqrt{(205{,}590 \times 0.1)^2 + (165{,}000 \times 0.3)^2 + (37{,}500 \times 0.3)^2 + (18{,}540 \times 0.3)^2}$$

= 55,049 lbs.

$$\text{Thus, } V_r = \frac{\sigma_r}{\bar{M}_r} = .129$$

6. Compute the overturning moment based on Figure 8a. From Equation (4.3) and ANSI-A58.1 (1982), the mean values of GC_p for three second gust can be obtained. The value of "a" is computed from ANSI-A58.1 (1982) to be 4 ft.

Region	Area (ft^2)	Moment arm (ft)	GC_{p3}
1	619	9	.89
2A	36	9	1.11
2A'	36	9	1.70
2B	25	12.8	1.11
2B'	17	13.8	1.70
2C	65	19	1.11
2C'	65	21	1.70
3A	8	19	1.11
3A'	24	21	1.70
	895		

$$\bar{M}_u = [\ .89(619)9 + 1.11(36)9 + 1.7(36)9 + 1.11(25)12.8 + 1.70(17)13.8 + 1.11(65)19 + 1.7(65)21 + 1.11(8)19 + 1.7(24)21]\ q$$

$$= 11{,}340\ q \text{ ft lbs.}$$

7. Equate $\bar{M}_r$ and $\bar{M}_u$ and solve for the mean wind pressure.

$$q = 37.62 \text{ psf}$$

8. Average three second gust:

$$\bar{V} = \sqrt{\frac{q}{.00256}} \cong 121 \text{ mph}$$

9. Coefficient of variation of the wind speed:

$$V_w = \tfrac{1}{2}\sqrt{V_r^2 + V_{GC_p}^2 + V_C^2}$$

$$= \tfrac{1}{2}\sqrt{(0.129)^2 + (0.17)^2 + (0.05)^2}$$

$$= 0.11$$

10. Establish a degree of confidence in the computed wind speed. For 95 percent confidence:

$$WS = \overline{V} (1 \pm 2V_w) = 121 \pm 27 \text{ mph}$$

Thus, with 95 percent confidence, the three second gust necessary to uplift the cafeteria roof is 121 ± 27 mph. If anchorage of nailed connections is neglected, using the similar procedure would give a mean wind speed of 85 mph.

5.3.2 Roof Over Offices

1. Tributary area of the roof section (Figure 8b):

Roof area = 72.67 (9.67) =	702.4 ft^2
Eave area = 2 (74.67) + 2 (9.67) =	168.6 ft^2
Tributary area =	871 ft^2

2. Dead load for roof and eave sections are the same as the previous problem.

3. Total weight of the roof:

Roof section = 702.4 (22) =	15,453 lbs.
Eave section = 168.1 (15) =	2,529 lbs.
	17,982 lbs.

4. Resisting moment of the roof due to the combination of roof anchorage and dead load:

Anchorage- 70 - 2 x 10 joists spaced 12 inches o.c. with 10d toenailed connections at 250 lbs. each

Resistance = 70 (250) = 17,500 lbs.

7 - 2 x 6 outriggers spaced 16 inches o.c. with 10d toenailed connections at 250 lbs. each

Resistance = 7 (250) = 1,750 lbs.

Resisting moment-

$\overline{M}_r$ = 17,982 (4.83) + 17,500 (9.67) + 1,750 (4.83)

= 264,478 ft lbs.

5. Coefficient of variation of the resisting moment as shown by the method in the previous problem:

$$V_r = .195$$

Overturning moment based on Figure 8b: from Equation (4.3) and ANSI-A58.1 (1982) values of GC_{p3} can be obtained. The value of "a" is computed to be 4.67 ft.

Region	Area (ft^2)	Moment arm (ft)	GC_{p3}
1	490	3.5	.89
2A	186.5	8.33	1.11
2A'	140	10.67	1.70
2B	18.6	3.5	1.11
2B'	14	3.5	1.70
3A	7.1	8.33	1.11
3A'	14.6	9.67	1.70
	871		

$$\bar{M}_u = [0.89(490)3.5 + 1.11(186.6)8.33 + 1.7(140)10.67 + 1.11(18.6)3.5 + 1.7(14)3.5 + 1.11(7.1)8.33 + 1.7(14.6)9.67]\, q$$

$$= 6{,}254\ q \text{ ft lbs.}$$

7. Equate $\bar{M}_r$ and $\bar{M}_u$ and solve for the mean wind pressure.

$$q = 42.29 \text{ psf}$$

8. Average three second gust:

$$\bar{V} = \sqrt{\frac{q}{.00256}} \cong 129 \text{ mph}$$

9. Coefficient of variation of the wind speed:

$$V_w = \tfrac{1}{2}\sqrt{(.195)^2 + (.17)^2 + (.05)^2}$$

$$= .13$$

10. Establish a degree of confidence in the computed wind speed. For 95 percent confidence:

$$WS = \bar{V}\,(1 \pm 2V_w) = 129 \pm 34 \text{ mph}$$

Thus, with 95 percent confidence, the three second gust necessary to uplift the cafeteria roof is 129 ± 34 mph. If anchorage of nailed connections is neglected, using the similar procedure would give a mean wind speed of 74 mph.

5.3.3 Interior Roof Section

Since this section of the roof was not uplifted, these calculations will yield an upper bound on the wind speed.

1. Tributary area of the interior roof section:

   Roof area = $(17)^2 = 289\ ft^2$

2. Dead load for the roof is the same as the previous section.
3. Total weight of the roof:

   Roof section = 289 (22) = 6,358 lbs.

4. Resisting moment computation:

   Anchorage- 17-2 x 10 joists spaced at 12 inches o.c. with 10d toenailed connections at 250 lbs. each

   Resistance = 17 (250) = 4,250 lbs.

   Resisting moment-

   $\bar{M}_r = 6,358\ (8.5) + 4,250\ (17) = 126,293$ ft lbs.

5. Coefficient of variation of the resisting moment:

   $$V_r = .177$$

6. Overturning moment of the square roof section:

   $$\bar{M}_u = .89q(289)8.5 = 2,186\ q \text{ ft lbs.}$$

7. Equate $\bar{M}_r$ and $\bar{M}_u$ and solve for the mean wind pressure.

   $$q = 57.77 \text{ psf}$$

8. Average three second gust:

   $$\bar{V} = 150 \text{ mph}$$

9. Coefficient of variation of the wind speed:

   $$V_w = \tfrac{1}{2}\sqrt{(.177)^2 + (.17)^2 + (.05)^2} = .125$$

10. With 95 percent confidence, the three second gust needed to uplift the roof is 150 ± 38 mph.

The wind speed calculations of the above roof sections show that the observed damage was probably caused by wind speeds which did not exceed 150 mph.

5.4 Recreation Building Wind Speed Calculation

The recreation building is adjacent to the dining hall. Roof damage was confined to the windward corner facing west (Figure 9). The roof consisted of 2 x 8 wooden joists spaced at 16 inches on center and extended twenty inches over the wall as an eave. The roof experienced the same failure mode as the previous problem. As the tornado passed, the nailed connections were pulled out.

A cross section of the windward wall is presented in Figure 10. The construction of the roof was similar to that of the dining hall; however, the wall cross sections varied considerably. The wooden roof joists were supported on posts rather than CMU blocks.

Wind speed calculations are shown for the windward roof corner and windward roof section.

The same assumptions hold true for this building as the dining hall.

5.5.1 Windward Roof Corner

1. Tributary area of the windward roof corner (Figure 11):

Roof area = 16 x 12	192.0 ft^2
Eave area = 17.67(1.67) + 12(1.67) =	49.4 ft^2
Tributary area	241.4 ft^2

2. Dead load of the roof and eave sections: values for the dead loads of various construction materials were obtained from AISCM (1980).

Roof section	psf
2 x 8 roof joists @ 16 inches o.c.	3
1 inch insulation board	2
3/4 inch gypsum wallboard	2
4 ply built-up roofing	6
duct and electrical	2
3/4 inch plywood sheathing	3
	18 psf

Eave section dead load = Roof section dead load - weight of insulation and wallboard

= 14 psf

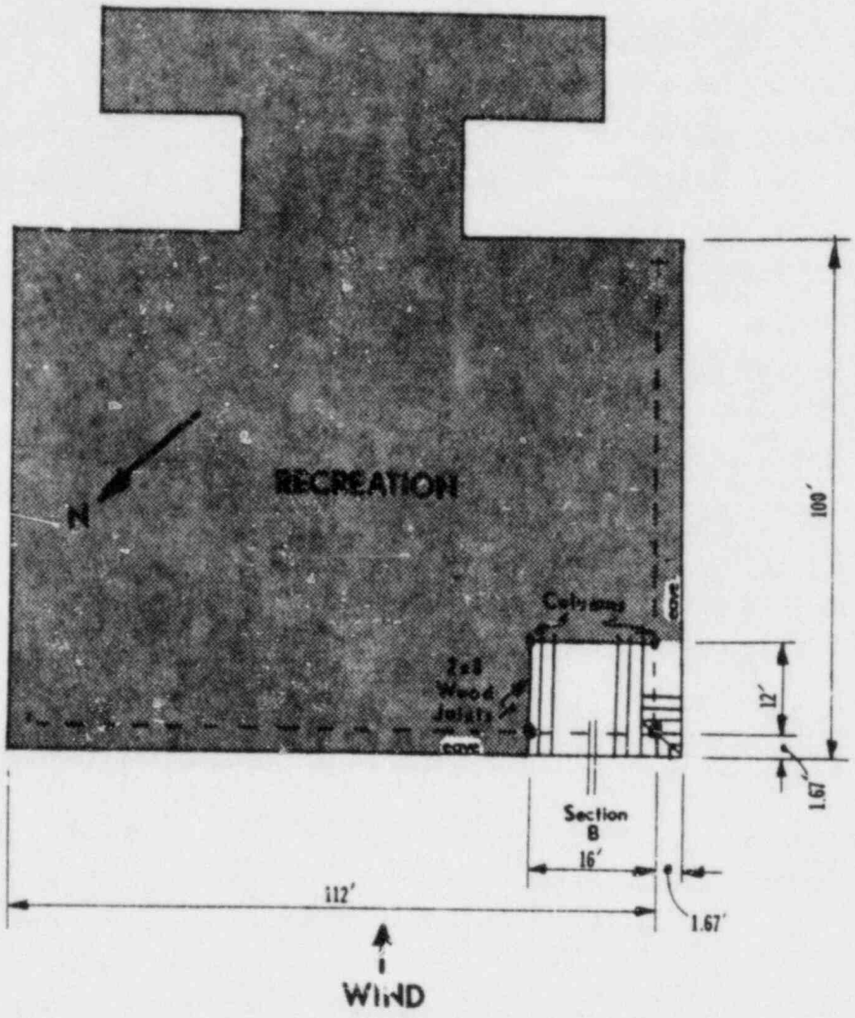

Figure 9 Plan view of the Recreation Building showing windward corner roof damage (unshaded portion).

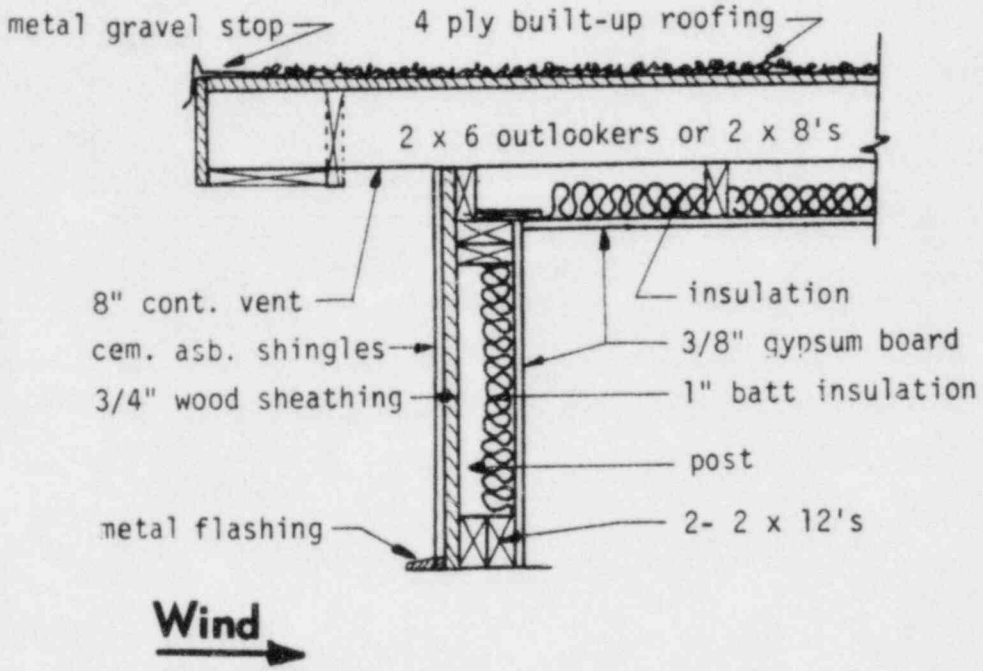

Figure 10 Windward roof-wall detail of the Recreation Building at section B.

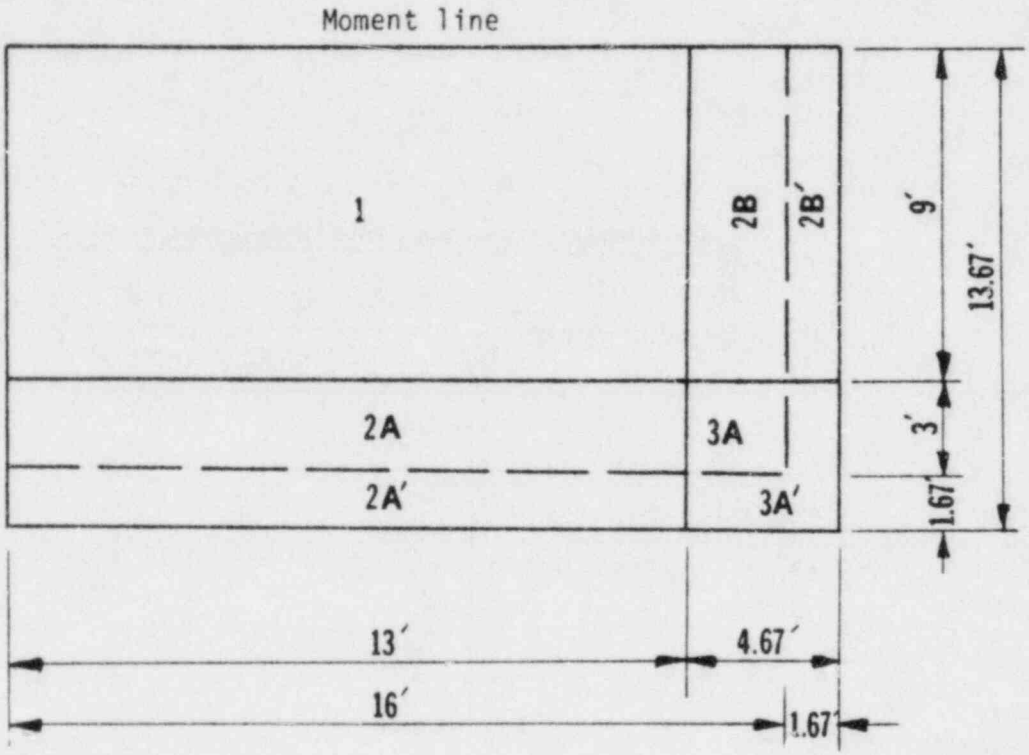

Figure 11 Plan view of the failed roof section of the Recreation Building as divided into ANSI-A58.1 1982 wind regimes.

3. Total weight of the roof:

Roof section = 192 (18) = 3,456 lbs.
Eave section = 49.4 (14)= 692 lbs.

Total weight 4,148 lbs.

4. Resisting moment of the roof due to the combination of the roof anchorage and dead load:

Anchorage- 12 - 2 x 8 joists spaced at 16 inches o.c. with 10d toenailed connections at 250 lbs. each

Resistance = 12 (250) = 3,000 lbs.

9 - 2 x 6 outriggers spaced at 16 inches o.c. with 10d toenailed connections at 250 lbs. each

Resistance = 9 (250) = 2,250 lbs.

Resisting moment-

$\overline{M}_r$ = 4,148(6) + 3,000(12) + 2,250(6)

= 74,388 ft lbs.

5. Coefficient of variation of the resisting moment:

V_r = .159

6. Overturning moment based on Figure 11: the value of "a" is 4.67 ft.

Region	Area (ft^2)	Moment arm (ft)	GC_{p3}
1	117	4.5	.89
2A	39	10.5	1.11
2A'	21.7	12.8	1.70
2B	27	4.5	1.11
2B'	15	4.5	1.70
3A	9	10.5	1.11
3A'	12.8	12	1.70
	241		

$\overline{M}_u$ = [.89(117)4.5 + 1.11(39)10.5 + 1.7(21.7)12.8 + 1.11(27)4.5 + 1.7(15)4.5 + 1.11(9)10.5 + 1.7(12.8)12] q

= 2,010 q ft lbs.

7. Equate $\overline{M}_r$ and $\overline{M}_u$ and solve for the mean wind pressure.

q = 37 psf

8. Average 3 second gust:

$\overline{V}$ = 120 mph

9. Coefficient of variation of the wind speed:

$$V_w = \tfrac{1}{2}\sqrt{V_r^2 + V_{GC_p}^2 + V_c^2} = .12$$

Thus, with 95 percent confidence, the average three second gust necessary to uplift the corner section of the roof is 120 ± 29 mph. If anchorage of nailed connections is neglected, using the similar procedure would give 68 mph.

5.4.2 Windward Roof Section

Since this section of the roof was not uplifted, these calculations will yield an upper bound on the wind speed.

1. Tributary area of the windward roof section:

   Roof area = 16 (12) = 192 ft^2

2. Dead load for the roof is the same as the previous problem.
3. Total weight of the roof:

   Roof section = 192 ft^2 (18 psf) = 3,456 lbs.

4. Resisting moment:

   Anchorage- 12 - 2 x 8 joists spaced at 16 inches o.c. with 10d toenailed connections at 250 lbs. each

   Resistance = 12 (250) = 3,000 lbs.

   Resisting moment-

   $\bar{M}_r$ = 3,456(6) + 3,000(12) = 56,736 ft lbs.

5. Coefficient of variation of the resisting moment:

   $V_r = .194$

6. Overturning moment:

   $\bar{M}_u = .89\ q(192)6 = 1,025\ q$ ft lbs.

7. Solve for the mean wind pressure.

   $q = 55.34$ psf

8. Average three second gust : $\bar{V}$ = 147 mph
9. Coefficient of variation of the wind speed:

$$V_w = \tfrac{1}{2}\sqrt{V_r^2 + V_{GC_p}^2 + V_c^2} = .13$$

10. With 95 percent confidence, the average three second gust needed to uplift the interior sections of the roof is 147 ± 38 mph.

The wind speed calculations on the above roof sections show that the damaging wind speeds at the recreation hall were probably lower than 150 mph; otherwise, further damage would have been expected.

5.5 Communication Building Wind Speed Calculation

The communication building has a long, rectangular shape oriented in a north-south direction (Figure 12). As the tornado passed, roof sections on the southernmost portion of the roof were uplifted and moved eastward. However, the roof sections near the center portion were moved westward.

The northernmost portion of the building remained relatively free from damage suggesting lower wind speeds. It appeared that the center of the tornado passed directly over the building (refer to Figure 3).

Two different regions of the building were selected for wind speed calculations a) the windward roof and b) the windward wall. The roof consisted of a 2 inch perlite (lightweight) concrete slab poured over a fabric-backed wire mesh. The mesh was divided into 8 foot wide sections and lightly secured to the top of the steel joists by twisted galvanized wire. Open web steel joists were spaced at 30 inches on center and secured to a bond beam with two one-half inch diameter bolts. The composite nature of the roof was the result of the building being designed to resist blast. However, as the tornado passed, the twisted galvanized wire failed and the 2 inch perlite slab "rolled" off the roof in 8 foot sections. The open web steel joists remained in place.

The windward wall is 11 feet high and consists of loadbearing clay tile units which support the steel joists and perlite roof (Figure 13). Horizontal reinforcement was placed in the mortar joint at alternate courses, but there was no vertical reinforcement. The wind speed calculation on the wall followed a procedure similar to the one described by McDonald et al. (1981).

The assumptions are the same as in previous sections. In addition,

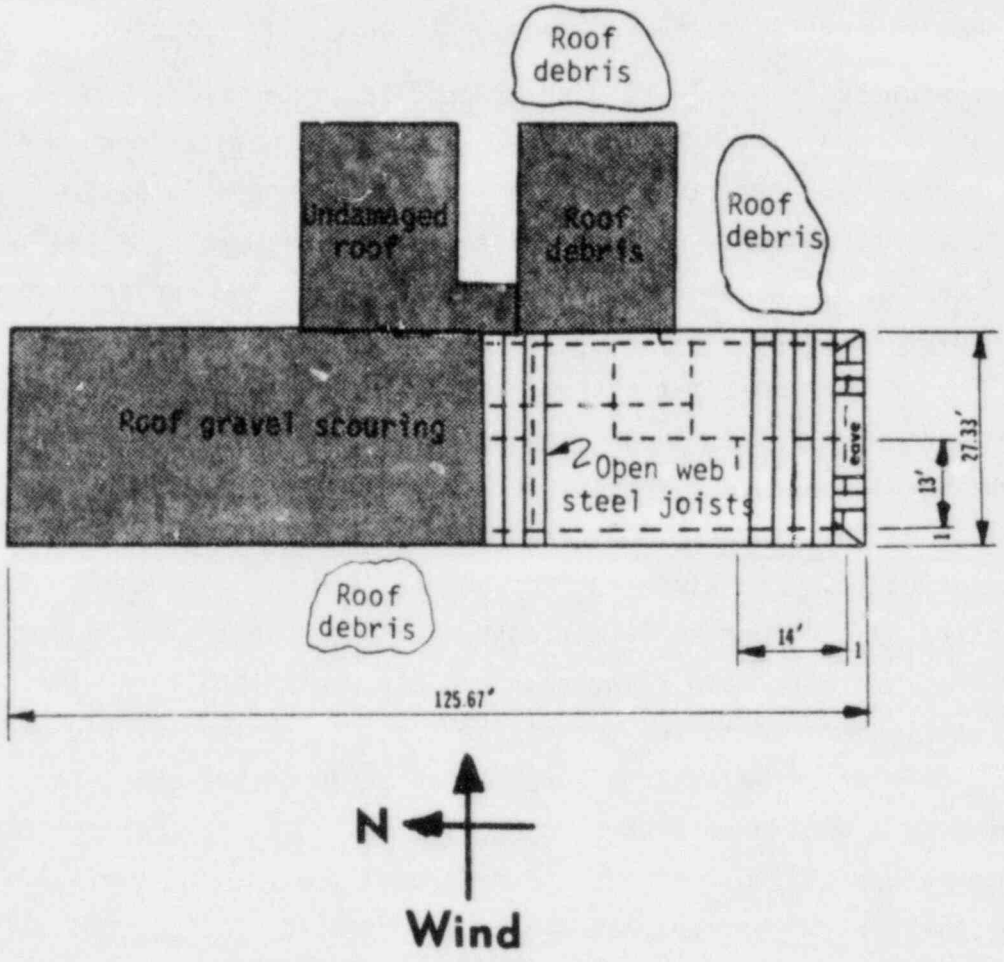

Figure 12 Plan view of the Communications Building showing windward roof damage (unshaded portion).

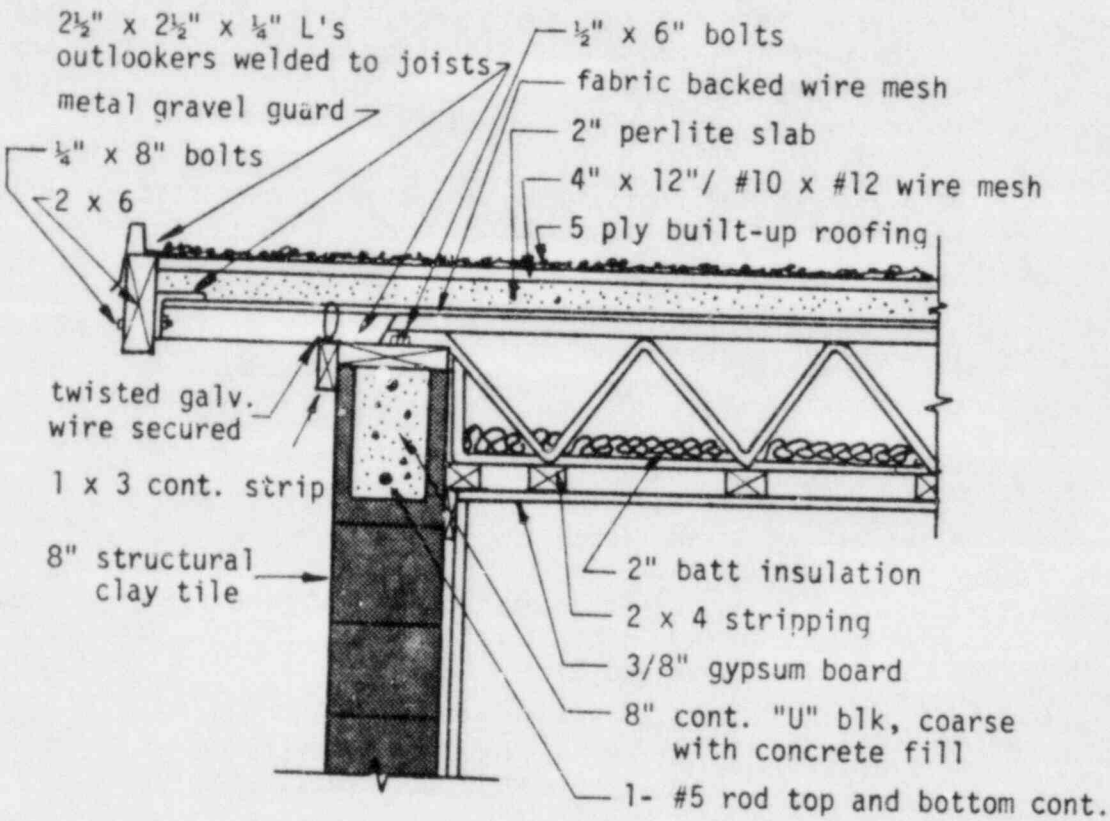

Figure 13 Windward roof-wall detail of the Communications Building.

Type N mortar will be assumed for the wall having a mean strength of 20 psi and coefficient of variation of 0.21 (refer to Table 14). The resistance of galvanized wire as well as the number and spacing are unknown. Therefore, three conditions of anchorage were selected: no resistance, 300 lb. resistance, and 600 lb. resistance.

5.5.1 Windward Roof

1. Tributary area of the windward roof: eight foot wide sections of the roof are used and construction materials are the same over the roof and eave.

   Total roof area = 8 (14) = 112 ft^2

2. Dead load of the roof: unit weights of construction materials were obtained from AISC (1980).

2 inch perlite slab	8 psf
5 ply built-up roof	6 psf
fabric-backed wire mesh	2 psf
Roof weight uplifted	16 psf

3. Total weight of the roof:

   Total weight = 112 (16 psf) = 1,792 lbs.

4. Resisting moment of the roof from the combination of the roof anchorage and dead load: three conditions of anchorage for the twisted galvanized wire were selected:

   Case 1 No resistance
   Case 2 300 lb. ea. resistance
   Case 3 600 lb. ea. resistance

   By comparison, 300 lb. resistance is equal to a 16d toenailed connection. Since there are three steel joists supporting the roof deck, it is assumed that at least three wire twists were present.

   Resisting moment-

   Case 1 $\bar{M}_r$ = 1,792 (7) = 12,544 lbs.

   Case 2 $\bar{M}_r$ = 1,792 (7) + 3(300) (13) = 24,244 ft lbs.

   Case 3 $\bar{M}_r$ = 1,792 (7) + 3(600) (13) = 35,944 ft lbs.

5. Coefficient of variation of the resisting moment:

   Case 1 V_r = .10

   Case 2 V_r = .153

Case 3 V_r = .198

6. Overturning moment based on Figure 14a: the value of "a" is 2.58 ft.

Region	Area(ft^2)	Moment arm (ft)	GC_{p3}
1	91.3	5.7	.89
2A	12.7	12.2	1.11
2A'	8.0	13.5	1.70
	112.0		

$\overline{M}_u$ = [.89(91.3)5.7 + 1.11(12.7)12.2 + 1.7(8)13.5] q

= 819 q ft lbs.

7 Solve for the wind pressures.

Case 1 15.32 psf

Case 2 29.6 psf

Case 3 43.89 psf

8. Determine the average three second gust using ANSI-A58.1 (1982).

Case 1 77 mph

Case 2 108 mph

Case 3 131 mph

9. Coefficient of variation of the wind speed:

Case 1 0.10

Case 2 0.12

Case 3 0.13

10. Establish 95 percent confidence limits on the three second gust according to the anchorage assumptions.

Case 1	no resistance	V = 77 $\pm$ 15 mph
Case 2	300 lb. wire resistance	V = 108 $\pm$ 26 mph
Case 3	600 lb. wire resistance	V = 131 $\pm$ 34 mph

Clearly, a second estimate is needed in order to better define the wind speed. Since the windward wall remained intact, an upper bound wind speed can be calculated.

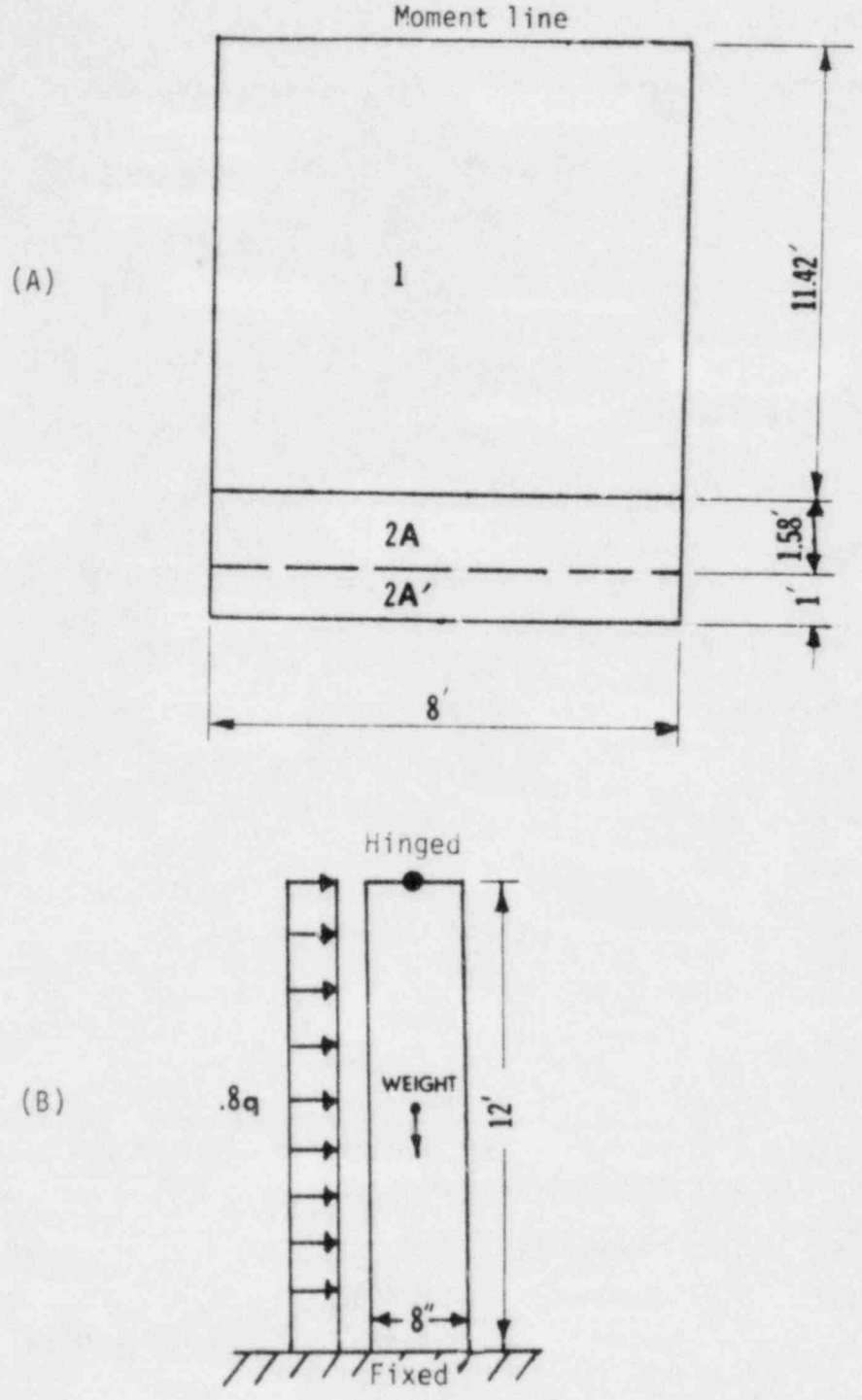

Figure 14 Sections of the Communications Building used to determine wind speed calculations a) roof as divided into ANSI-A58.1 1982 wind regimes and b) windward wall.

5.5.2 Windward Wall

Since this section of the wall did not fail, the wind speed calculation will represent an upper bound value.

1. Dead load of the roof and wall:

Roof weight remaining	psf
open web steel joists at 30 inch spacing	5
2 inch batt insulation	1
3/8 inch gypsum wallboard	2
2 x 4 wooden rafters at 16 inches spacing	3
duct and electrical	2
	13 psf

Wall weight	
15 - loadbearing clay tile units at 33 psf each	495 lbs.
1 - grouted CMU bond beam at 55 psf	55 lbs.
	550 lbs/ft

2. Axial load on the wall which includes the weight of the wall and roof:

$$P = 550 + 13 \text{ psf } (27.3/2) = 727 \text{ lbs/ft}$$

3. Bending moment produced by the wind: the wall is assumed to be hinged at the top and fixed at the bottom (Figure 14b). From NCMA (1970), a reduction of 10 percent can be taken in the bending moment as a small portion will be distributed to the intersecting vertical walls. This reduction is valid for a span-to-height ratio of 1:4.

$$M = .00256\ V^2\ (.8q)\ (10)^2\ (12)\ (.9)\ /\ 8$$
$$= .276\ V^2$$

4. Tensile stress produced by the combined axial load and bending moment should not exceed the modulus of rupture of the mortar. Thus,

$$MOR = -\frac{P}{A} + \frac{M}{S}$$

Geometric properties of the 8 x 8 x 12 clay tile units were obtained from Schneider (1980).

$$20 \text{ psi} = -\frac{727}{38} + \frac{.276\ V^2}{80}$$

Term A Term B Term C

Solving for the threshold wind speed, $\overline{V}$ = 107 mph.

5. Coefficient of variation as a weighted average for the three terms above: from Table 14, the coefficients of variation are 0.21, 0.12, 0.1 and 0.5 for the modulus of rupture of the mortar, pressure coefficient, dead load, and density constant, respectively.

$$V_{A+B} = \frac{\sqrt{(19.13 \times .1)^2 + (20 \times .21)^2}}{39.13} = .12$$

$$V_w = \tfrac{1}{2} \sqrt{(V_{A+B})^2 + (V_c)^2} = .065$$

With 95 percent confidence, the three second gust necessary to topple the wall is 107 $\pm$ 14 mph. Since the wall did not fail, this value represents an upper bound on the wind speed. Therefore, Case 1 to 2 seems reasonable for wind speeds on the Communications building roof.

5.6 Summary

After visual inspection of the damage at Altus Air Force Base, the intensity of the damage was rated F-3, (158-206 mph). Further investigation of the construction plans revealed that wind speeds which caused the observed damage were between 85 and 135 mph. Overall wind speeds probably did not exceed 150 mph; otherwise, additional damage to exterior walls and interior roof sections would have been caused.

A summary of wind speed calculations for each building is shown in Table 20. In all of the wind speed calculations presented, the primary cause of failure initiated where the structure was anchored. The Parachute drying tower overturned as the result of the anchor bolts failing in tension. The roof failures at the Dining hall and Recreation building resulted from uplift of the toenailed connections between the wooden joists and the nail strip at the top of the wall. The roof failure at the Communications building resulted from uplift on the galvanized wire twists. It should be emphasized that the F-scale wind speeds overestimated the wind speed necessary to cause the observed damage, especially in the case of the Communications building. Though each building had considerable differences in construction details, the wind speeds calculated were quite consistent.

TABLE 20

SUMMARY OF WIND SPEED ESTIMATES IN THE ALTUS TORNADO

Building	Failure origin	Distance from tornado center	F-scale rating	Failure wind speed*	No failure wind speed*
Parachute Drying Tower	Anchor bolt connection	650 ft right	F1	116 ± 19 mph	--
Dining Hall	Toenailed roof connection	200 ft left	F2	121 ± 27 mph 129 ± 34 mph	150 ± 38 mph
Recreation Hall	Toenailed roof connection	100 ft left	F2	120 ± 29 mph	147 ± 38 mph
Communications building	Twisted wire connection	0 ft	F3	--	107 ± 14 mph

* Three second gust with 95% confidence limits

CHAPTER VI
CONCLUSIONS

6.1 General Conclusions

Knowledge of load and resistance statistics of the components of a structure can be utilized in the design process to resist a load or to determine the load needed to cause failure. This study has addressed the latter in the context of determining wind speed estimates for structures damage by a tornado which struck the Altus Air Force Base on 11 May 1982. In order to derive wind speed estimates, statistical data were collected from the literature on the structural resistance of various construction materials and on wind load variables. The probabilistic approach shown herein makes use of the uncertainties in the structural resistance and wind load variables in order to place upper and lower bound wind speeds with a certain degree of confidence. This approach improves the quality of a wind speed estimate by treating each variable as a statistical random variable in contrast to a discrete value.

Wind speed estimates using the load and resistance approach were shown for the Parachute Drying Tower, Dining Hall, Recreation Building, and the Communications Building. The calculated wind speeds were consistent among the structures and reasonable for the type of damage observed. In this study, a mean pressure coefficient describing a turbulent environment for a three second duration was selected to simulate a tornadic wind field.

The application of load and resistance statistics to obtain wind speed estimates raises two important points. First, a range of overlapping wind speeds will result because of the inherent uncertainties in structural resistance and the wind load. Therefore, the damage intensity of a structure may actually lie in more than one F-scale category. Second, as the uncertainties in structural resistance and load effects increase, the confidence bands in the calculated wind speed widen. Therefore, a failure wind speed for a residential structure will have a wider confidence band than for public and more per-

manent structures.

Meaningful wind speed estimates can only be obtained by thorough damage documentation and the acquisition of construction plans. From this, accurate details on the size of the connection and components of the structure as well as the type of construction materials used can be determined.

6.2 Future Research

The probabilistic approach in the design of structures to resist loads is a relatively recent one. Most of the advancements in this subject have been made within the past eight years. In most cases, the theory is more advanced than the knowledge of structural resistance statistics. In this study, the most recent data on load and resistance statistics were used. In the future, improved testing and modeling in the performance of structures under wind loads will yield additional load and resistance data. As a result, wind speed estimates can become more improved.

Additional variability exists in the gust sensitivity of the structure, in the orientation of the structure to the wind, and in the assumptions made herein to obtain the wind speed estimate. Also, variability exists in using the structural resistance of a single member to describe the strength and performance of an entire structural system. The additional uncertainties can be included in Equation (2.25) as data become available. Thus,

$$V_w = \tfrac{1}{2}\sqrt{V_r^2 + V_{C_p}^2 + V_c^2 + \sum_{i=1}^{n} V_i^2}$$

where V_i describes the additional uncertainties. Studying the variables which influence structural resistance and wind load will provide the meteorologist and engineer with better insight to obtain more accurate wind speed estimates.

LIST OF REFERENCES

Abiassi, J., 1981: The strength of weathered window glass using surface characteristics. M.S. Thesis, Dept. of Civil Engineering, Texas Tech University, Lubbock, TX, 110 pp.

AISCM, 1980: Specifications for the design, fabrication and erection of steel buildings. American Institute of Steel Construction, Eighth Edition, Chicago, IL, 778 pp.

ANSI A58.1, 1982: American national standard building code requirements for minimum design loads in buildings and other structures. American National Standards Institute, New York, NY, 100 pp.

Crowe, C., 1974: Are the codes safe for wind pressures? J. Struct. Div., ASCE, 100, ST8, 1745-1747.

Davenport, A.G., D. Surry, and T. Stathopoulos, 1977: Wind loads on low-rise buildings: Final report of phases I and II. BLWT SS8-1977, University of Western Ontario, Ontario, Canada, 38 pp.

Durst, C.S., 1960: Wind speeds over short periods of time. Meteor. Mag., 89, 181-186.

Ellingwood, B., 1981a: Wind and snow load statistics for probabilistic design. J. Struct. Div., ASCE, 107, ST7, Technical notes, 1345-1350.

_____, 1981b: Analysis of reliability for masonry structures. J. Struct. Div., ASCE, 107, ST5, Proc. Paper 15253, 757-773.

_____, 1981c: Reliability of wood structural elements. J. Struct. Div., ASCE, 107, ST1, Proc. Paper 15964, 73-87.

_____, T.V. Galambos, J.G. MacGregor, and C.A. Cornell, 1980: Development of a probability based load criterion for American National Standard A58, National Bureau of Standards, Publication 577, 222 pp.

Fisher, J.W., T.V. Galambos, G.C. Kulak, and M.K. Ravindra, 1978: Load and resistance factor design criteria for connectors. J. Struct. Div., ASCE, 104, ST9, Proc. Paper 14017, 1427-1441.

Fujita, T.T., 1971: Proposed characterization of tornadoes and hurricanes by area and intensity. SMRP Research Report 91, University of Chicago, 15 pp.

Galambos, T.V., and M.K. Ravindra, 1978: Properties of steel for use in LRFD. J. Struct. Div., ASCE, 104, ST9, Proc. Paper 14009, 1459-1468.

Ghiocel, D., and D. Lungu, 1975: Wind, Snow and Temperature Effects on Structures Based on Probability. Abacus Press, Turnbridge Wells, Kent, 411 pp.

Haugen, E.B., 1968: Probabilistic Approaches to Design. John Wiley and Sons, New York, NY, 323 pp.

Hedstrom, R.O., 1961: Load tests of patterned concrete masonry walls. J. Amer. Concrete Inst., 57. 1265-1268.

Hendry, A.W., 1976: The effect of site factors on masonry performance. First Canadian Masonry Symposium, Calgary, Alberta, Canada, 182-194.

McDonald, J.R., K.C. Mehta, and J.E. Minor, 1981: Wind loads: standards of practice. Institute for Disaster Research, Texas Tech University, Lubbock, TX, 184 pp.

Mehta, K.C., J.E. Minor, and J.R. McDonald, 1976: Wind speed analyses of April 3-4 1974 tornadoes. J. Struct. Div., ASCE, 102, ST9, Proc. Paper 12429, 1709-1724.

_____, J.E. Minor, and T.A. Reinhold, 1981: Wind speed damage correlation in Hurricane Frederic, J. Struct. Eng., ASCE, 109, No. 1, Proc. Paper 17626, 37-49.

Minor, R.R., and A.J. Sanger, 1971: Observations of the response of metal building systems to the Lubbock Tornado. Institute for Disaster Research doc. 4D, Texas Tech University, Lubbock, TX, 110 pp.

Minor, J.E., 1974: Window glass in windstorms. Civil Eng. Report CE74-01, Texas Tech University, Lubbock, TX, 168 pp.

_____, 1981: Window glass design practices: a review. J. Struct. Div., ASCE, 107, ST1, Proc. Paper 15966, 1-12.

_____, K.C. Mehta, and J.R. McDonald, 1972: Failures of structures due to extreme winds. J. Struct. Div., ASCE, 98, ST11, Proc. Paper 9324, 2455-2471.

_____, J.R. McDonald, and K.C. Mehta, 1977: The tornado: an engineering oriented perspective. NSSL Tech. Memo., ERL-NSSL-82, 195 pp.

_____, W.L. Beason, and P.L. Harris, 1978: Design for windborne missiles in urban areas. J. Struct. Div., ASCE, 104, ST11, Proc. Paper 14143, 1749-1759.

_____, and K.C. Mehta, 1979: Wind damage observations and implications. J. Struct. Div., ASCE, 105, ST11, Proc. Paper 14980, 2279-2291.

Mirza, S.A., M. Hatzinibolas, and J.G. MacGregor, 1979: Statistical descriptions of the strength of concrete. J. Struct. Div., ASCE, 105, ST6, Proc. Paper 14628, 1021-1035.

NCMA, 1970: Engineered concrete masonry-wind loads. Information Series 24, National Concrete Masonry Association, 4 pp.

Neis, V.V., and D.Y. Chow, 1980: Tensile bond testing of structural masonry units. Second Canadian Masonry Symposium, Ottawa, Ontario, Canada, 381-395.

O'Conner, J.P., 1967: NCMA tests on flexural strength of concrete masonry walls. Seminar on High-Rise Load Bearing Concrete Masonry, 47th Annual Convention of the National Concrete Masonry Association, San Francisco, CA, 17 pp.

Ravindra, M., and T.V. Galambos, 1978: Load and resistance factor design for steel. J. Struct. Div., ASCE, 104, ST9, 1337-1353.

Robertson, L.E., 1967: Engineering approach to designing glass for wind. Architectural Record, 2, 163-166.

Sahlin, S., 1971: Structural Masonry, Prentice Hall, Englewood Cliffs, NJ, 290 pp.

Salmon, C.G., and J.G. Johnson, 1980: Steel Structure Design and Behavior. Harper and Row, New York, NY, 1007 pp.

Schneider, R., and W. Dickey, 1980: Reinforced Masonry Design. Prentice Hall, Englewood Cliffs, NJ, 619 pp.

Segner, E.P., 1960: Estimates of minimum wind forces causing structural response to natural wind. Proceedings: Wind Effects on Buildings and Structures, University of Toronto Press, 1, 595-630.

Stanworth, J.E., 1950: Physical Properties of Glass. Clarendon Press, Oxford, England, 218 pp.

Stathopoulos, T., 1980: PDF of wind pressures on low-rise buildings. J. Struct. Div., ASCE, 106, ST5, Proc. Paper 15409, 973-990.

_____, D. Surry, and A.G. Davenport, 1981: Effective wind loads on flat roofs. J. Struct. Div., ASCE, 107, ST2, Proc. Paper 16039, 281-297.

Van Kuren, R.C., and T.V. Galambos, 1964: Beam-Column experiments. J. Struct. Div., ASCE, 90, ST2, Proc. Paper 3876, 223-251

Yura, J.A., and T.V. Galambos, 1978: The bending resistance of steel beams. J. Struct. Div., ASCE, 104, ST9, Proc. Paper 14015, 1355-1370.

APPENDIX I
NAILED CONNECTION STRENGTH TEST

A common method of roof-to-wall or wall-to-floor connection is to use nails. Strong winds can induce outward acting forces which can pull the nailed connections apart. Therefore, the resistance of nailed connections must be known if an accurate wind speed assessment is to be made. Though some pull out strength data can be found in the literature, toenailed strength data are virtually non-existent.

Therefore, the author conducted a series of 120 strength tests on toenailed and straight connections using 8d and 16d nails. The series of tests included 30 pairs of nailed connections which were 8d straight, 8d toenailed, 16d staight, and 16d toenailed driven into grade two, 2x4, white pine lumber. Figure 15 depicts the types of nailed connections which were used in the experiment. At least half of the length of the nails were driven in at angles between 45 and 60 degrees for the toenailed connections.

A Reihle tension machine was used to test the nailed connections. Each specimen was secured to the machine at the top by treaded grips and at the bottom using C-clamps as shown in Figure 16. Then each connection was pulled apart at a rate of about 1000 lbs per minute and the ultimate strength was recorded. The test results appear in Tables 21 and 22. These data were ranked and the mean and coefficient of variation were determined. For 8d nailed connections straight pull and toenailed, the mean strength was 69 and 206 respectively with both having a coefficient of variation of 0.35. For 16d nailed connections straight pull and toenailed, the mean strenght was 235 and 298 lbs respectively with coefficients of variation of 0.37 and 0.21 respectively. As anticipated, the strength required to pull the nailed connections apart increased with increasing nail sizes. The coefficient of variation which appears in Tables 21 and 22, is a combination of the raw values and includes a 10 percent variation in workmanship. Thus,

$$V_r = \sqrt{V_m^2 + (.1)^2}$$

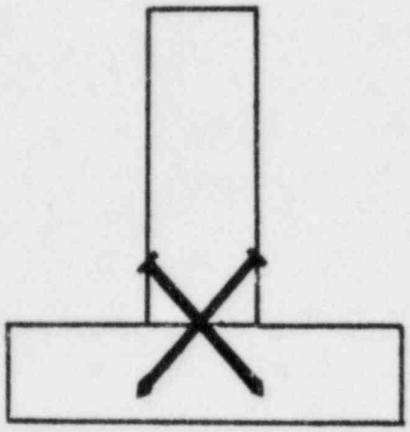

a)

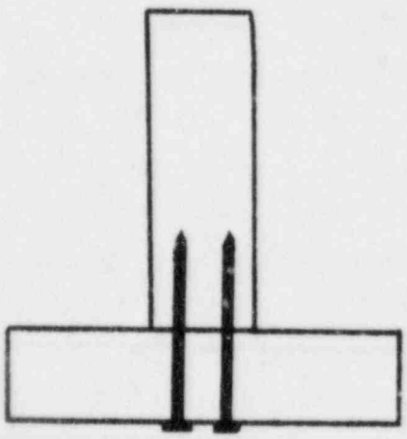

b)

Figure 15 The types of nailed connections used in the tensile tests a) toenailed and b) straight. Nails were driven into grade two, 2 x 4, white pine lumber.

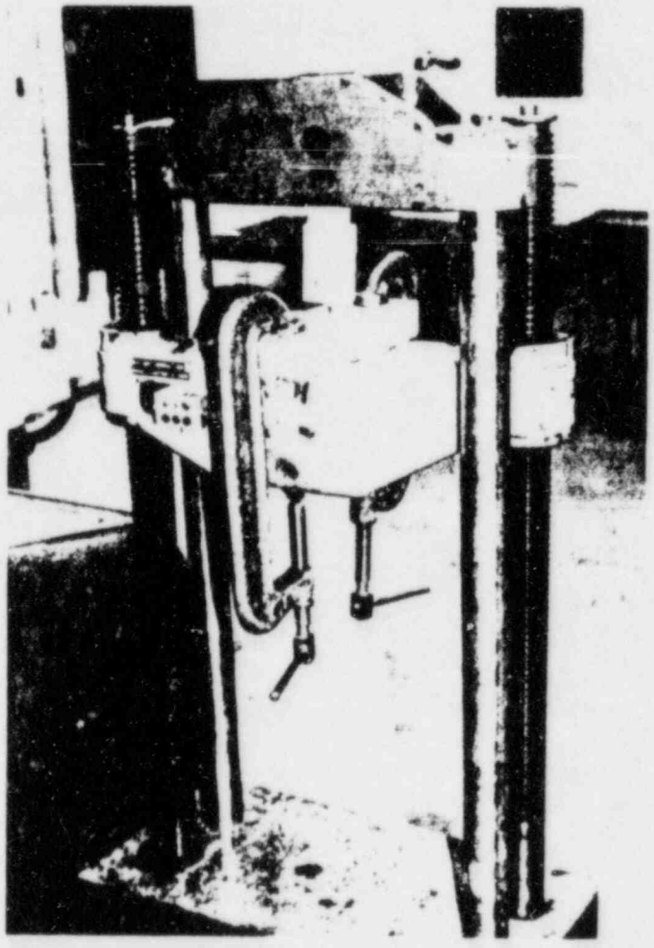

Figure 16 View of the Reihle testing machine used to pull apart the nailed connections.

TABLE 21

SUMMARY OF STRENGTH DATA FOR 8d NAILED CONNECTIONS

Straight Pull

Rank	Force (lbs)	Rank	Force (lbs)
1	35	16	60
2	40	17	65
3	45	18	65
4	45	19	70
5	45	20	70
6	45	21	80
7	50	22	80
8	50	23	85
9	55	24	85
10	55	25	95
11	60	26	95
12	60	27	105
13	60	28	115
14	60	29	120
15	60	30	125

Mean: 69.3 Median: 60 Mode: 60
C.O.V. .36

Toenailed

Rank	Force (lbs)	Rank	Force (lbs)
1	125	16	185
2	125	17	200
3	125	18	205
4	130	19	240
5	130	20	245
6	135	21	250
7	140	22	255
8	140	23	270
9	140	24	270
10	145	25	280
11	160	26	295
12	165	27	300
13	175	28	300
14	175	29	335
15	180	30	360

Mean: 206 Meadian: 180 Mode: 140
C.O.V. .36

TABLE 22

SUMMARY OF STRENGTH DATA FOR 16d NAILED CONNECTIONS

Straight Pull

Rank	Force (lbs)	Rank	Force (lbs)
1	130	16	220
2	130	17	250
3	140	18	255
4	150	19	260
5	155	20	260
6	160	21	260
7	165	22	260
8	175	23	270
9	175	24	270
10	180	25	270
11	190	26	280
12	200	27	300
13	200	28	360
14	200	29	450
15	220	30	500

Mean: 234.5 Median: 220 Mode: 260
c.o.v. .38

Toenailed

Rank	Force (lbs)	Rank	Force (lbs)
1	215	16	295
2	215	17	300
3	220	18	300
4	225	19	300
5	240	20	320
6	240	21	325
7	240	22	330
8	245	23	330
9	245	24	345
10	255	25	350
11	265	26	350
12	270	27	380
13	285	28	400
14	290	29	405
15	295	30	455

Mean: 297.6 Median: 295 Mode: 300
c.o.v. .23

NRC FORM 335 (11-81)

U.S. NUCLEAR REGULATORY COMMISSION

BIBLIOGRAPHIC DATA SHEET

1. REPORT NUMBER (Assigned by DDC)
NUREG/CR-3874

4. TITLE AND SUBTITLE (Add Volume No., if appropriate)
NEAR-GROUND TORNADO WIND FIELDS

2. (Leave blank)

3. RECIPIENT'S ACCESSION NO.

7. AUTHOR(S)
James R. McDonald

5. DATE REPORT COMPLETED
MONTH: May YEAR: 1984

9. PERFORMING ORGANIZATION NAME AND MAILING ADDRESS (Include Zip Code)
Institute for Disaster Research
Texas Tech University
Post Office Box 4089
Lubbock, Texas 79409

DATE REPORT ISSUED
MONTH: July YEAR: 1984

6. (Leave blank)

8. (Leave blank)

12. SPONSORING ORGANIZATION NAME AND MAILING ADDRESS (Include Zip Code)
Division of Radiation Programs & Earth Sciences
Office of Nuclear Regulatory Research
U.S. Nuclear Regulatory Commission
Washington, D.C. 20555

10. PROJECT/TASK/WORK UNIT NO.

11. FIN NO.
B8099

13. TYPE OF REPORT
Technical

PERIOD COVERED (Inclusive dates)

15. SUPPLEMENTARY NOTES

14. (Leave blank)

16. ABSTRACT (200 words or less)

This report is written as a general treatise on near-ground tornado wind fields. In Section II an engineering perspective on tornadoes is stated. Section III describes the data available for the study of near-ground tornado wind fields. Section IV discusses tornado wind speeds and briefly describes a new method for making more rational estimates of tornado wind speeds from damaged structures. Section V describes the damage indicators that are present in the wake of a tornado event and discusses other factors that affect the appearance of damage. A perspective on tornado-generated missiles is presented in Section VI. Conclusions and recommendations for further study are contained in the last section of the report.

17. KEY WORDS AND DOCUMENT ANALYSIS

17a. DESCRIPTORS

17b. IDENTIFIERS/OPEN-ENDED TERMS

18. AVAILABILITY STATEMENT
Unlimited

19. SECURITY CLASS (This report)
Unclassified

21. NO. OF PAGES

20. SECURITY CLASS (This page)

22. PRICE
$

UNITED STATES
NUCLEAR REGULATORY COMMISSION
WASHINGTON, D.C. 20555

120555078877 1 1ANIRB
US NRC
ADM-DIV OF TIDC
POLICY & PUB MGT BR-PDR NUREG
W-501
WASHINGTON DC 20555